The University Of Sheffield.

The impacts of forest conversion and degradation on climate resilience in the tropics

By:

Rebecca Anne Senior

A thesis submitted in partial fulfilment of the requirements for the degree of Doctor of Philosophy

The University of Sheffield

Faculty of Science

Department of Animal and Plant Sciences

August 2018

Contents

List of Tables

List of Figures

Abstract

Most terrestrial biodiversity is found in tropical forests. Conservation of these forests is therefore a global priority, which must be reconciled with ongoing land-use and climate change. Tropical species are among the most sensitive to climate change; their persistence in the long-term is dependent on their ability to adapt *in situ* or move. A crucial unknown is the extent to which these strategies are impeded by land-use change. In this thesis, I first assess how tropical forest conversion and degradation impacts local climate. Using site-level (m-ha) temperature data, I show that tropical forest conversion to farmland results in local warming of 1.6-13.6°C, but this is avoided in degraded forests and below-ground. I then explore the conservation value of degraded forests by considering temperature at finer spatial scales (mm-m), where thermal variation can allow species to avoid suboptimal temperatures. I develop an R package to automate processing of images from FLIR thermal cameras and to calculate metrics of thermal heterogeneity for gridded temperature data. Combining this approach with data from temperature loggers, I compare thermal buffering capacity in the understorey of selectively logged and unlogged forests on Borneo. I find that 9-12 years after intensive selective logging the potential for thermal buffering is similar in logged and unlogged forests. Finally, I consider that even where thermal buffering is feasible, range shifts may be necessary for long-term persistence. Combining global forest cover and climate datasets, I find that 62% of global tropical forest area fails to connect to analogous future climates. In 12 years, connectivity to future climate analogues decreased in 27% of tropical forest area, with losses accelerating as the area of forest loss increased. Put together, my findings suggest that degraded forests can buffer species from climate change, but thermal buffering is severely compromised with conversion to non-forest habitats. To enhance climate resilience of tropical forests there is a need to protect remaining tropical forests and to strategically plan reforestation and forest restoration with climate gradients and connectivity in mind.

Acknowledgements

A huge thanks first of all to both of my supervisors: Dr David Edwards and Prof Jane Hill. Your guidance throughout has been invaluable.

Thanks to the Natural Environment Research Council for funding this project, and to the ACCE (Adapting to the Challenges of a Changing Environment) Doctoral Training Partnership for providing so many great opportunities. A particular thanks to Dr Venelina Koleva for dealing with all my awkward requests.

Thanks to my local collaborator, Dr Suzan Benedick, for supporting my work in the field. Thanks to Sabah Biodiversity Council, Danum Valley Wildlife Management Committee, the South East Asia Rainforest Research Partnership, Yayasan Sabah and the Sabah Wildlife Department for permitting me to work in Sabah and the Danum Valley Conservation Area. For facilitating my fieldwork I thank all the staff at Danum Valley Research Centre, particularly the logistical support of Adrian Karolus and Datuk Dr Glen Reynolds. For field assistance I thank: Azlin Bin Sailim, Ahmad Bin Jelling, Deddy Nurdin, Jessica Olid and Chloe Walker-Trivett.

Throughout my PhD I was humbled to receive data, advice and code freely from various different researchers (named in the relevant chapters). Numerous people within my Universities of Sheffield and York provided helpful discussions and feedback: my project supporter, Prof Rob Freckleton, the J2 lab, and everyone from Conservation Bites. Felix Lim and Simon Mills must get a special mention for joining me on various rambling thought processes.

Many people (and some animals!) supported me on a personal level, without which I would have probably been in a perpetual, chocolate-laden slump. Thanks to the Mynas for listening to my rants and keeping the snack table topped up. Thanks to Cindy Cosset and Chloe Walker-Trivett for general laughs and amazing food. Thanks to my brother, Thomas, for being a source of entertainment and for helping me with mathsy stuff, and to my Grandparents – Charles and Marylyn Marchington – for remaining interested in the strange activities of your wayward granddaughter.

For unconditional love and the best cuddles a human could ask for, I am grateful to my beautiful doggies: Ruby (left) and Teddy (right).

To my Mum – where to start! Thanks for always being there, for always being supportive, and for being a total inspiration. Whenever I think I can't do something, I think of you. Not just your words of encouragement, but the example you live by every day: turning your hand to anything and never giving up.

To Kieran – you've been an anchor throughout my PhD and I can't really do that justice here. I'm so grateful for everything: the pep talks, the silliness, the enforced relaxing, the emergency mug cakes…so many things! Now it's your turn, and I hope I can return the favour. Noms, fol and abductions.

I dedicate my PhD to Dr Aisha Coggan. I wish you were here to finish this with me.

Author's declaration

The research presented in this thesis is my own. This thesis has not been submitted for any other award at this or any other institution. In addition to myself (R.A.S.) there were several collaborators in this research: David Edwards (D.P.E.), Jane Hill (J.K.H.), Pamela González del Pliego (P.G.), Laurel Goode (L.K.G.) and Suzan Benedick (S.B.).

Chapter 2

This chapter has been published as:

Senior RA, Hill JK, González del Pliego P, Goode LK, Edwards DP. A pantropical analysis of the impacts of forest degradation and conversion on local temperature. Ecology and Evolution. 2017;7:7897–7908.

The manuscript is reproduced in full in this thesis, with minor formatting alterations. The overall contribution of authors was as follows: R.A.S., D.P.E., and J.K.H conceived the study. R.A.S., P.G. and L.K.G. collated the data. R.A.S. performed statistical analyses. R.A.S. wrote the manuscript, with contributions from D.P.E. and J.K.H.

Chapter 3

This chapter is currently in preparation for submission to *Ecography* as:

Senior RA, Hill JK, Edwards DP. A framework for quantifying fine-scale thermal heterogeneity using thermography.

The manuscript is reproduced in full in this thesis, with minor formatting alterations. The overall contribution of authors was as follows: R.A.S. conceived the study. R.A.S., D.P.E., and J.K.H developed the methods. R.A.S. wrote the R package and performed statistical analyses. R.A.S. wrote the first draft of the manuscript, with contributions from D.P.E. and J.K.H.

Chapter 4

This chapter has been published as:

Senior RA, Hill JK, Benedick S, Edwards DP. Tropical forests are thermally buffered despite intensive selective logging. Global Change Biology. 2018;24:1267–1278.

The manuscript is reproduced in full in this thesis, with minor formatting alterations. The overall contribution of authors was as follows: R.A.S., D.P.E., and J.K.H conceived the study. R.A.S. collected the data, with S.B. providing logistical support. R.A.S. performed all statistical analyses and wrote the manuscript, with contributions from D.P.E. and J.K.H.

Chapter 5

This chapter is currently in preparation for submission to *Nature* as:

Senior RA, Hill JK, Edwards DP. Global loss of climate connectivity in tropical forests.

The manuscript is reproduced in full in this thesis, with minor formatting alterations. The overall contribution of authors was as follows: R.A.S. and D.P.E conceived the study. R.A.S., D.P.E., and J.K.H developed the methods, with R.A.S. writing scripts to calculate climate connectivity and performing statistical analyses. R.A.S. wrote the first draft of the manuscript, with contributions from D.P.E. and J.K.H.

Chapter 1

General Introduction

Sunshine through rainforest canopy in Danum Valley.

1.1 The global extinction crisis

Recent rates of species extinction are between 100 and 1,000 times greater than pre-human levels (Pimm et al., 1995). It is estimated that if all species currently classified as Critically Endangered were to go extinct, the Earth would enter its sixth mass extinction event (Barnosky et al., 2011). Awareness and mitigating action has increased accordingly in recent years, but the loss of biodiversity has not slowed (Butchart et al., 2010).

The key drivers of biodiversity loss are land-use change, climate change, pollution, over-exploitation (including hunting and wildlife trade) and invasive species (Hirsch and Secretariat of the Convention on Biological Diversity, 2010). These drivers have varying importance depending on location and taxonomic group (Baillie et al., 2004). The greatest overall threat to terrestrial systems is currently land-use change, with climate change becoming increasingly important as the century progresses (Sala et al., 2000).

Tackling the extinction crisis is a monumental undertaking, which raises the question – why is it necessary? The importance of biodiversity can be broken down broadly into intrinsic and extrinsic value. Intrinsic value underpins much of traditional conservation thinking, and is based on the notion that all life has inherent value and the right to exist (Millennium Ecosystem Assessment, 2005). Extrinsic value encompasses ecosystem products and services, recognising the tangible benefits that humans derive from nature (Balmford et al., 2002; Costanza et al., 1997). Another consideration is that conserving maximum biodiversity is likely to maintain redundancy in the planetary system as a whole. Crudely, the more genes, traits and species that exist, the less likely that loss through natural or anthropogenic disturbance causes whole processes and ecosystems to collapse (Oliver et al., 2015). Ecosystem resilience is important at local and regional scales, where its absence may be felt most tangibly by humans, but without global resilience we are likely to exceed planetary boundaries with severe negative consequences for all life on Earth (Rockström et al., 2009).

With limited resources, conservation must prioritise places that are most imperilled and convey the most benefits for people and for biodiversity. Most of the world's biodiversity is found in the tropics (Barlow et al., 2018; Jenkins et al., 2013), including species yet to be discovered (Joppa et al., 2011; Scheffers et al., 2012) and thus with unknown benefits. The tropics also includes some of the world's only remaining wilderness areas (Mittermeier et al., 2003; Watson et al., 2016), which are irreplaceable within any time-scale that matters to humans. Tropical forests play a key role in the global carbon cycle and atmospheric circulation (Barlow et al., 2018; Foley et al., 2005), and accrue local benefits to some of the world's most deprived people and countries (Agrawal et al., 2013; Barlow et al., 2018). Simultaneously, the tropics are disproportionately threatened by ongoing disturbance by humans, the drivers of

which may negatively interact to exacerbate the consequences for biodiversity.

1.2 Land-use change in the tropics

The tropics are undergoing a huge amount of land-use change, particularly through loss or degradation of tropical forest. Land-use change has already driven extensive and severe losses of biodiversity across the planet (Newbold et al., 2015), so there is a clear need to understand what underpins these losses and how they can be mitigated.

1.2.1 Forest conversion

Globally, there is increasing demand for agricultural land to feed a growing and developing human population (Godfray et al., 2010; Foley et al., 2011; Tilman et al., 2011). The primary source of new agricultural land is tropical forests (Gibbs et al., 2010), because temperate regions have already undergone severe land-use change and because demand for food is increasing most rapidly in developing countries, which are mostly found in the tropics (United Nations Development Programme, 2018). The result has been a devastating loss of habitat (particularly in Southeast Asia and the Amazon), with a total of ~150 million hectares converted between 1980 and 2012 (Gibbs et al., 2010; Hansen et al., 2013).

With forest loss comes biodiversity loss (Brook et al., 2003; Newbold et al., 2015; Sodhi et al., 2004). Under current rates of forest loss, Betts et al. (2017) predict that 121-219 species will become threatened in the next 30 years in the high-risk regions of Borneo, the central Amazon and the Congo Basin. Forest loss has numerous secondary impacts, such as opening up remaining forest to exploitation for timber or hunting, and delineating forests into small fragments with associated edge effects and hazards from road traffic (Ewers and Banks-Leite, 2013; Laurance et al., 2009; Murcia, 1995; Pfeifer et al., 2017). Deforestation is also a major contributor to greenhouse gas emissions (Foley et al., 2005; IPCC, 2013), compounding impacts for global biodiversity by driving climate change.

1.2.2 Forest degradation

Forest degradation refers to negative, anthropogenic changes to forest that do not cause complete loss of forest cover. Degradation includes the secondary impacts of nearby deforestation as described above (e.g. fragmentation and poaching), as well as direct degradation through selective logging and fire (Barlow et al., 2016). While the impacts of

deforestation may be more extreme locally than forest degradation, wholesale conversion affected only 1.4% of the humid tropical biome from 2000 to 2005, compared to 20% that was designated for selective logging in the same period (Asner et al., 2009; Hansen et al., 2008). The term 'selective' refers to the targeting of particular species and stems (usually above a minimum trunk diameter; Edwards et al., 2014c), however these targets are typically the largest, oldest trees, the removal of which reduces canopy height and canopy density (Kumar and Shahabuddin, 2005; Okuda et al., 2003), fragments the forest canopy, and opens up large gaps that are often invaded by non-tree species, such as climbers and bamboo (Edwards et al., 2014c). Commercial selective logging also causes collateral damage – particularly where trees are connected by climbers (Schnitzer et al., 2004) – and requires roads and skid trails that bring further challenges for wildlife (Brodie et al., 2015; Laurance et al., 2014), as well as heavy machinery that causes soil compaction (Putz et al., 2008).

Degraded tropical forests are significant for global conservation because a greater proportion of primary forest species are found there than in converted habitat, and it is often these species that are of high conservation concern (Edwards et al., 2011; Edwards and Laurance, 2013; Gibson et al., 2011). A meta-analysis by Putz et al. (2012) found that 85-100% of mammals, birds, invertebrates and plants persist 1-100 years after a single round of selective logging, and indeed Edwards et al. (2011) observed that only 1-8 years after a second round of logging, 75% of bird and dung beetle species found in unlogged, primary forests were still present in the twice-logged forest, including many globally threatened bird species. Logged forests retain a substantial proportion of above-ground live carbon (~76% in once-logged forest; Putz et al., 2012), and can facilitate movement between intact forests (Gillies and Clair, 2008), thereby supporting metapopulation processes (Edwards et al., 2014c).

1.3 Climate change in the tropics

While land-use change is the biggest current driver of biodiversity loss, and will certainly continue to be a major threat to tropical species (Gibbs et al., 2010), conservation must also seek to bolster species against additional threats that are likely to negatively interact with land-use change, particularly climate change (Maxwell et al., 2016). There is some debate about the vulnerability of tropical species to climate change relative to species at higher latitudes, which has led climate research to be neglected in this region until recently (Corlett, 2012).

Vulnerability to climate change depends on exposure (extrinsic factors) and species' sensitivity (intrinsic factors; Williams et al., 2008). Exposure and sensitivity interact to determine whether species *need* to resist or recover from climate perturbations, as well

as their *ability* to do so. In terms of absolute changes in climate, exposure will be less in the tropics than elsewhere (IPCC, 2013). Relative change, however, will be greatest in the tropics because of long periods of climatic stability (Mora et al., 2013). Temperature in the tropics also varies very little within the year or with latitude (Colwell et al., 2008), predisposing tropical species to high thermal sensitivity because of narrow thermal limits (Deutsch et al., 2008; Khaliq et al., 2014; Tewksbury et al., 2008) that many species are already operating near the upper end of (Deutsch et al., 2008; Khaliq et al., 2014; Tewksbury et al., 2008).

Land-use change can directly influence species' exposure to climate change by changing vegetation structure. Evidence from global General Circulation Models (Davin and de Noblet-Ducoudré, 2010; Findell et al., 2007; Pielke et al., 2011) and observational studies in Brazil (Loarie et al., 2009), Malaysia (Luskin and Potts, 2011) and Indonesia (Ramdani et al., 2014) demonstrate that loss of vegetation cover increases local daytime temperature by reducing direct absorption and reflection of incident solar radiation (Oke, 1987; Murcia, 1995; Snyder et al., 2004), and by reducing the amount of thermal energy dissipated through evapotranspiration (Findell et al., 2007; Lawrence and Vandecar, 2015; Oke, 1987). However, studies that rely on coarse-scale (~1 km) weather station data have limited relevance for the majority of terrestrial species (Frenne and Verheyen, 2016), which experience temperature at mm to m, within a few cm of the ground surface and usually with overhead vegetation and variation in topography (Gillingham, 2010; Suggitt et al., 2011; Wiens and Bachelet, 2010). Local observational studies are able to account for these factors, but are difficult to generalise across regions, land-use types, times of year (e.g. dry versus wet season) and habitat strata (e.g. above-ground versus below-ground). In Chapter 2, I combine the advantages of both approaches by using site-level temperature data from across the tropics in a mixed-effects modelling framework, to ask how land-use change impacts local temperature in different land-use types, seasons and above-ground versus below-ground (also see Senior et al., 2017).

Assuming tropical species are exposed to climate change and do need to respond, a key unknown is the extent to which land-use change affects the ability of species to adaptively respond to climate change. There are several ways that species can respond to climate change, broadly divided into adapting *in situ* or moving elsewhere (Corlett, 2011).

1.3.1 *In situ* adaptation

1.3.1.1 Genetic adaptation

As yet there is limited evidence for evolutionary responses to climate change, in the tropics or elsewhere (Corlett, 2011; Parmesan, 2006). It could be that there has not yet been sufficient time or selection pressure to drive such change, although evidence is also lacking in the fossil record despite climate change of much greater magnitude during events such as the Pleistocene glaciation event (Parmesan, 2006). Genetic adaptation is less intuitive and harder to document than ecological responses (O'Connor et al., 2012), and is less likely in tropical species of high conservation concern because these species are highly specialised, and specialisation tends to reduce variation in heritable traits and thus decrease potential for genetic adaptation (Williams et al., 2008). Thermal tolerance, especially upper thermal limits, appear to be highly constrained in the species that have been assessed (Hoffmann et al., 2013). Evidence from temperate regions suggests a more common phenomenon is evolution in traits that underlie other adaptive responses to climate change. For example, Dutch great tits that have greater plasticity in their timing of reproduction are better able to match egg-laying to food availability – the peak of which has advanced as a result of climate change – and thus achieve greater fitness (Nussey et al., 2005). Meanwhile, some British insects have evolved improved flight capacity, which is thought to assist dispersal to track shifting climates (Hill et al., 1999; Thomas et al., 2001).

1.3.1.2 Physiological plasticity

Similar to genetic adaptation, direct acclimation of thermal tolerance appears to be limited (Hoffmann et al., 2013; Parmesan, 2006), but there is ample evidence for phenological changes. Again, most evidence derives from temperate regions of the Northern hemisphere, where seasonality is the overarching determinant of species' phenology, and is itself dramatically altered by climate change (Bradshaw and Holzapfel, 2006). Specifically, spring has advanced and the growing season has lengthened. Organism responses include earlier breeding in animals such as birds and butterflies, earlier arrival of migratory birds, and earlier flowering in plants (Walther et al., 2002). Recent evidence also suggests that shifts in phenology may affect both the need and opportunity for other responses to climate change, such as range shifts, by stabilising temperature during critical and thermally sensitive life events like nesting (Socolar et al., 2017). Similar changes in phenology are less clear in the tropics, where seasonality is less marked and less directly associated with climate change, and where long-term phenological monitoring is lacking (Corlett, 2011). Changes in rainy seasons and the timing of El Niño events may be interesting avenues for further research in

this area.

1.3.1.3 Dispersal and movement

Over short time-scales, arguably the easiest and most effective response to unsuitable climatic conditions at coarse spatial scales is for species to move towards suitable climatic conditions that manifest at finer spatial scales: 'microrefugia' (Hannah et al., 2014; Maclean et al., 2017). At this scale (mm to m), microrefugia provide a 'microclimate' that deviates from the climate at the level of the whole habitat (m to ha; meso- or local scale). Heterogeneity at the micro- scale is related to variation in slope and aspect (Suggitt et al., 2011; Maclean et al., 2017), as well as the presence of vegetation (Oke, 1987) and features such as rocks, leaf litter and tree holes, commonly referred to as 'microhabitats' (Scheffers et al., 2014b).

Paleoecological evidence suggests that refugia at various spatial scales have been instrumental in allowing species to persist through global and regional shifts in climate, and are important for explaining modern day species distributions (Hannah et al., 2014; Stewart et al., 2010). Mobile species commonly utilise microclimates within generations, through thermoregulatory behaviour of individuals. For example, possums in tropical Australia choose the coolest tree hollows in which to den (Isaac et al., 2008), and herpetofauna of Singapore occupy microrefugia that both warm more slowly and more rarely exceed thermal limits than the wider macroclimate (Scheffers et al., 2014b). Immobile species utilise microclimates indirectly, according to differences in fitness between generations (Maclean et al., 2015). Microrefugia are unlikely to support species indefinitely within areas that become climatically unsuitable at coarser scales, but the disconnect between climate at coarse and fine spatial scales means that microrefugia can buffer species from change (Maclean et al., 2017; Scheffers et al., 2014b), allowing more time for other responses to manifest, such as genetic adaptation or physiological plasticity. In England, this buffering effect reduces extinction risk of temperature-sensitive species by up to 22% for plants and 9% for insects (Suggitt et al., 2018).

Until the recent 'revolution' in climate-change biology, microclimate research had been somewhat neglected (Hannah et al., 2014). A substantial limiting factor was the ability to measure climate both at fine resolution and with broad coverage (Potter et al., 2013), which is now made possible with the advent of affordable dataloggers, Unmanned Aerial Vehicles and thermal imaging cameras (Faye et al., 2016; Scheffers et al., 2017a). There remains a great deal of untapped potential for thermography in ecology, in part because there is little guidance on how to process the images and what metrics are of primary interest for thermal biology (Faye et al., 2016). In Chapter 3, I present an R package, `ThermStats`,

which simplifies the processing of images from FLIR thermal cameras, and calculates a variety of biologically relevant metrics from any gridded temperature data (Senior et al., in prep 2018a).

Whether microclimates allow species to persist through climate change in local refugia, or simply give more time for other responses to manifest, the influence of land-use change is a critical unknown. Changes in vegetation structure through land-use change are likely to affect not only the average temperature (Chapter 2; Senior et al., 2017), but also the availability and distribution of microclimates. For example, overall structural simplification and loss of microhabitats associated with large, old trees (e.g. deadwood and tree holes; Ball et al., 1999; Blakely and Didham, 2008) could decrease the number and buffering potential of cool microclimates. This topic is addressed in Chapter 4. Using fine-scale temperature and microhabitat data collected in intensively logged and unlogged forests on Borneo, I tested the hypothesis that selective logging decreases thermal buffering potential, with associated consequences for conservation under future climate change (also see Senior et al., 2018).

1.3.2 Range shifts

We have already seen that movement operates at fine spatial scales to allow species to persist in habitats that are considered to be unsuitable at coarser scales. Eventually, however, meso-scale climate change will be felt even within microclimates, and for some species *in situ* adaptation will become insufficient. To avoid extinction, the only remaining option is for species' to shift their ranges to track favourable climates. Range shifts are largely thought to occur through net population extinctions at the trailing edge, and/or net population colonisations at the leading edge (Parmesan et al., 1999). Range shifts within a generation could also occur via individual dispersal in highly mobile species. In temperate regions there is evidence for both latitudinal and altitudinal shifts in response to rising temperatures (Hill et al., 2002; Parmesan et al., 1999; Thomas and Lennon, 1999), while the latter is much more frequently observed in the tropics owing to shallow latitudinal temperature gradients (Colwell et al., 2008; Parmesan, 2006). On Borneo's Mount Kinabalu, for example, moth species moved upwards by an average of 67 m over 42 years (Chen et al., 2009). For a given area of habitat, tropical rainforests also offer a diverse and expansive amount of vertical habitat (Scheffers et al., 2013, 2017b; Scheffers and Williams, 2018), which may prove to be an additional and significant temperature gradient for range-shifting tropical species.

Facilitating climate-driven range shifts is increasingly acknowledged as important for enhancing climate resilience. There are several factors that influence whether range shifts will work for a given species:

1. Availability of analogous climate – is there available habitat with a similar climate to that of the species' current distribution?
2. Accessibility of analogous climate – is there a feasible route to habitat with analogous climate?
3. Traits of the focal species – can the species of interest actually utilise available routes to reach habitat with analogous climate, and does it need to?

Previous studies have tended to use Species Distribution Models to answer the first of these, using the relationship between climate (and other environmental variables) and species' current distribution to predict which areas will be climatically suitable under future climate change (Hijmans and Graham, 2006; Willis et al., 2015). Several studies consider the connectedness of suitable habitat without considering whether that habitat will remain climatically suitable (Cosgrove et al., 2018; Tucker et al., 2018). Increasingly, studies are beginning to combine approaches to ask whether habitat is sufficiently connected along climate gradients to facilitate range shifts, hereafter referred to as 'climate connectivity' (Bagchi et al., 2018; Lawler et al., 2013; Littlefield et al., 2017; McGuire et al., 2016). In Chapter 5, I combine global tree cover and temperature data to quantify climate connectivity across the whole of the tropics, and to assess how climate connectivity has changed with recent deforestation (Senior et al., in prep 2018b).

1.4 Thesis aims and rationale

The main aims of this thesis are to determine how land-use change in the tropics impacts: (1) exposure to local warming, and the feasibility of both (2) microclimates and of (3) range shifts as mechanisms by which species can avoid extinction under global climate change. I begin by collating data from the literature to compare local, site-level temperature data for different land-use types across the tropics. I then develop metrics and software to assess microclimates in the field using thermal images, which – in combination with dataloggers and microhabitat measurements – I use to compare the thermal buffering potential of selectively logged and primary forests on Borneo. Finally, I use pantropical forest cover and climate datasets to consider how recent forest loss has impacted species' ability to track climate change by shifting their distribution. In the General Discussion I synthesise all results to provide an overall picture of how land-use change in the tropics impacts species responses to climate change, and provide recommendations for action and further research. The specific objectives of the main data chapters are outlined below:

Chapter 2 – A pantropical analysis of the impacts of forest degradation and conversion on local temperature

The recent surge in studies assessing impacts of climate warming on biodiversity hints at the importance of temperature for species' ecology. We recognise land-use change as the main driver of biodiversity loss, mediated in a large part by changes to vegetation structure that also governs climate at a local scale (< 1 ha). Considering interactions with climate change, previous studies tend to focus on greenhouse gas emissions from forest conversion, or on barriers to range shifts. This chapter instead considers how land-use change directly causes local warming, thereby increasing the baseline temperature onto which climate change is projected. By comparing site-level data from the literature, the main objectives of this chapter were to: (1) compare local temperature in different land-use types across the tropics; and (2) assess whether results were consistent between wet and dry seasons and above-ground compared to below-ground.

Chapter 3 – A framework for quantifying fine-scale thermal heterogeneity using thermography

Most terrestrial biodiversity experiences temperature at much finer spatial scales and much nearer to the ground than is represented by coarse-scale climate research (> 1 km). Microclimate research is gaining traction, but has in part been neglected because of technological limitations in measuring temperature at a fine spatial scale (mm to m). Thermal cameras are an increasingly affordable and practical means to measure microclimates, but the technology and data remain underutilised. The objectives of this chapter were to: (1) provide a simple R package to streamline the processing of thermal images from FLIR thermal cameras; and (2) to suggest and facilitate the calculation of key metrics of thermal heterogeneity, for any gridded temperature data.

Chapter 4 – Tropical forests are thermally buffered despite intensive selective logging

Temperature variation at a fine spatial scale allows species to cope with suboptimal temperatures that manifest at a coarser scale, leading many to suggest that microclimates will be increasingly important under climate change. Simultaneously, selective logging affects a huge area of the tropics, particularly in Southeast Asia, but we do not know how land-use change impacts microclimates. Combining microhabitat assessments with temperature data from dataloggers and thermal images, this chapter compares various

components of thermal buffering between intensively logged and unlogged forests on Borneo. The main objectives were to: (1) assess the impact of commercial selective logging on the difference between temperature at coarse (m to ha) and fine scales (mm to m); and (2) investigate whether selectively logged and unlogged forests differ in the thermal stability and availability of microclimates.

Chapter 5 – Global loss of climate connectivity in tropical forests

In addition to *in situ* adaptation, or where such adaptation is insufficient, species may shift their ranges at coarse scale in response to climate change. Range shifting is well-documented in both modern times and paleoecological records, but its feasibility across the tropics as a means to prevent species from extinction under climate change depends on species being able to reach suitable habitat with a suitable climate. No study to date has assessed the global connectivity of tropical forests to future climate analogues, nor investigated how this connectivity is affected by ongoing deforestation. This chapter utilises global climate and forest cover data to determine: (1) the extent to which current forest cover in the tropics facilitates species movement to analogous future climate; and (2) how this has been impacted by recent changes in forest cover.

Chapter 2

A pantropical analysis of the impacts of forest degradation and conversion on local temperature

Bornean horned frog (*Megophrys nasuta*).

This chapter has been published as:

Senior RA, Hill JK, González del Pliego P, Goode LK, Edwards DP. A pantropical analysis of the impacts of forest degradation and conversion on local temperature. Ecology and Evolution. 2017;7:7897-7908.

2.1 Abstract

Temperature is a core component of a species' fundamental niche. At the fine scale over which most organisms experience climate (mm to ha), temperature depends upon the amount of radiation reaching the Earth's surface, which is principally governed by vegetation. Tropical regions have undergone widespread and extreme changes to vegetation, particularly through the degradation and conversion of rainforests. Since most terrestrial biodiversity is in the tropics, and many of these species possess narrow thermal limits, it is important to identify local thermal impacts of rainforest degradation and conversion. We collected pantropical, site-level (< 1 ha) temperature data from the literature to quantify impacts of land-use change on local temperatures, and to examine whether this relationship differed above-ground relative to below-ground and between wet and dry seasons. We found that local temperature in our sample sites was higher than primary forest in all human-impacted land-use types (n = 113,894 day-time temperature measurements from 25 studies). Warming was pronounced following conversion of forest to agricultural land (minimum +1.6°C, maximum +13.6°C), but minimal and non-significant when compared to forest degradation (e.g. by selective logging; minimum +1°C, maximum +1.1°C). The effect was buffered below-ground (minimum buffering 0°C, maximum buffering 11.4°C), whereas seasonality had minimal impact (maximum buffering 1.9°C). We conclude that forest-dependent species that persist following conversion of rainforest have experienced substantial local warming. Deforestation pushes these species closer to their thermal limits, making it more likely that compounding effects of future perturbations, such as severe droughts and global warming, will exceed species' tolerances. By contrast, degraded forests and below-ground habitats may provide important refugia for thermally-restricted species in landscapes dominated by agricultural land.

2.2 Introduction

It is well established that temperature is important in ecology, for everything from biochemistry, to physiology, to biogeography (Kearney et al., 2009; Kingsolver, 2009; Puurtinen et al., 2016; Thomas et al., 2004). Temperature is a key explanatory variable in species distribution models that predict the likely impacts of projected global climate change on biodiversity (e.g. Thomas et al., 2004). However, the majority of organisms experience temperature at much finer spatial scale (Gillingham, 2010; Suggitt et al., 2011) than assumed in species distribution models (often > 100 km^2), and at local scales temperature is more dependent on local factors (Suggitt et al., 2011) than on regional or global atmospheric circulation (Davin and de Noblet-Ducoudré, 2010; Oke, 1987; Wiens and Bachelet, 2010;

Pielke et al., 2011). One such local factor is vegetation cover, which influences temperature through direct absorption and reflection of incident solar radiation (Murcia, 1995; Oke, 1987; Snyder et al., 2004) and through evapotranspiration, by determining the amount of thermal energy dissipated through the evaporation of water as opposed to a change in temperature (Findell et al., 2007; Lawrence and Vandecar, 2015; Oke, 1987).

Land-use change can profoundly influence vegetation cover. Current and future land-use change is concentrated in the tropics, where > 150 million hectares of forest was converted between 1980 and 2012 (Gibbs et al., 2010; Hansen et al., 2013) and 20% of the humid tropical biome was selectively logged from 2000 to 2005 (Asner et al., 2009). Previous studies, from a range of disciplines, demonstrate that land-use change in the tropics tends to increase temperature (Davin and de Noblet-Ducoudré, 2010; Findell et al., 2007; Lawrence and Vandecar, 2015; Loarie et al., 2009; Luskin and Potts, 2011; Pielke et al., 2011; Ramdani et al., 2014). This suggests severe consequences for global terrestrial biodiversity, most of which is found in tropical rainforests (Myers et al., 2000) and is thought to be especially sensitive to temperature change, owing to narrow thermal limits (Deutsch et al., 2008; Kingsolver, 2009; Tewksbury et al., 2008).

Additionally, while absolute warming from global climate change will be highest at the poles (IPCC, 2013), it is the tropics where relative warming will be greatest, with historically unprecedented temperatures occurring by 2050 (Mora et al., 2013). It is frequently stated that habitat fragmentation from land-use change will make it increasingly difficult for tropical species to track climate (Brook et al., 2008; Scriven et al., 2015), hampered by the poor dispersal ability of many tropical species (Van Houtan et al., 2007) and shallow latitudinal temperature gradients (Colwell et al., 2008). However, it is less commonly discussed that the baseline temperature onto which global climate predictions are projected might itself be dramatically higher in altered land-use types (Foster et al., 2011; Tuff et al., 2016).

To understand current and future consequences for tropical biodiversity from land-use change and climate change it is vital to understand thermal change at the scale at which temperature is experienced by organisms (Gillingham, 2010; Suggitt et al., 2011; Wiens and Bachelet, 2010). Prior evidence for local warming in the tropics as a result of land-use change originates from global General Circulation Models (Davin and de Noblet-Ducoudré, 2010; Findell et al., 2007; Pielke et al., 2011) and observational studies focused on particular locations, such as Brazil (Loarie et al., 2009), Malaysia (Luskin and Potts, 2011) and Indonesia (Ramdani et al., 2014). While General Circulation Models are limited in biological relevance by their coarse spatial resolution, observational studies are limited in generality by the site-specificity required to achieve their fine spatial resolution (Li et al., 2015). Any studies that utilise meteorological station data have limited biological relevance because stations

are specifically positioned to minimise the influence of the very same local characteristics that are important to local biota, such as vegetation cover, slope and aspect (Frenne and Verheyen, 2016).

There are several conditions under which local warming due to land-use change might be ameliorated, which have yet to be explicitly tested. We hypothesise that low intensity forest degradation, including commercial selective logging, fragmentation and forest regrowth (Lewis et al., 2015), will correspond to relatively little net change in vegetation, and hence a smaller difference in temperature. Any warming effects of land-use change are likely reversed at night, as habitats with relatively low vegetation cover will radiate heat back to the atmosphere more freely (Chen et al., 1995; Oke, 1987). Water availability is fundamental in determining how much thermal energy can be dissipated through evaporation, and so we also expect that warming would be less during the wet season given the high water availability (and more cloudy weather) relative to dry season, and below-ground relative to above-ground. In the latter case, even when water availability is very low, soil buffers external temperature change (Scheffers et al., 2014a) because soil has a higher specific heat capacity than air, and thus requires a greater change in thermal energy to achieve the same change in temperature (Oke, 1987).

In the present study, we carry out analyses of published data to test the effect of land-use change on local temperature across the tropics. We collected local, *in situ* temperature data from the literature for paired sites (< 1ha) that differed in land-use type. Categories of land use we studied were primary forest, degraded forest, plantation, pasture and cropland (Table 2.1; modified from Extended Data Table 1 in Newbold et al., 2015). We examine how land-use change affects day-time temperature at fine-scale spatial resolution, and we quantify the effects of: (1) forest conversion compared with forest degradation; (2) below-ground compared to above-ground; and (3) wet season conditions compared to the dry season. We focus on day-time temperatures because few studies collected night-time temperature, although we also separately test how the latter is impacted by land-use change for the subset of studies able to provide these data. Recent studies also highlight the importance of climatic extremes for species' survival (e.g. Christidis et al., 2013; Deutsch et al., 2008), hence we conduct additional analyses for those studies that provide these data.

Land-use type	Definition
Primary forest	Forest where any disturbances identified are very minor (e.g. a trail or path) or very limited in the scope of their effect (e.g. hunting of a particular species of limited ecological importance).
Degraded forest	Forest with one or more disturbances ranging from moderate intensity/breadth of impact (e.g. selective logging and bushmeat extraction), to severe intensity/breadth of impact (e.g. regrowth after clear-felling).
Plantation	Extensively managed or mixed timber, fruit/coffee, oil-palm or rubber plantations.
Cropland	Farming for herbaceous crops, without presence of livestock.
Pasture	Farming of livestock.

Table 2.1: Land use classification definitions (modified from Extended Data Table 1 in Newbold et al. (2015).

2.3 Methods

2.3.1 Literature search

We collated temperature data from peer-reviewed literature using ISI Web of Knowledge. The search terms were: "tropic* AND (temperature OR local climate) AND (land use OR landuse OR land cover OR landcover OR urban* OR city OR cities OR agri* OR arable OR built* OR metropol* OR deforest* OR forest*) AND (change OR expansion OR growth OR encroach* OR modif* OR conversion OR convert*)". We refined the search output by including only the following research areas: "environmental sciences ecology", "remote sensing", "agriculture", "biodiversity conservation", "forestry", "urban studies"; this returned 1,372 published studies. Excluding book chapters (21) and articles that were deemed irrelevant based on the title (298) or abstract (484) reduced the total to 525 articles. We reviewed each of these articles manually. Additional unpublished data (two studies) were also provided by co-authors (P.G., L.K.G.).

2.3.2 Selection criteria

All data originated from studies with at least two different sites in at least two different land-use types. Sites were located between 23.44° North and South, and the natural vegetation type was defined by authors as forest. Sites were fully contained within the land-use type of interest and positioned beneath the canopy (where applicable). Within a single study, sampling methodology was consistent across all sites and land-use types. Differences between studies, such as soil depth or the use of radiation shields for

dataloggers, were accounted for by the analytical approach (see 'Statistical analyses'). All sites within a single study differed in elevation by no more than 150 m.

Data collected through remote sensing or from meteorological stations were excluded, because they are inherently unrepresentative of local climatic conditions in forested areas. Meteorological stations are established to strategically avoid the very same local conditions in which we are primarily interested (Frenne and Verheyen, 2016). Acceptable methods of temperature measurement were those taken *in situ*, using a thermometer, temperature probe or temperature dataloggers. We included temperature data reported as an average across multiple spatial replicates for each land-use type within a study, provided that (1) the area over which data were averaged and (2) the number of spatial replicates within this area was consistent across different land-use types within the study. We set the maximum area over which data could be averaged as 1 ha, to ensure our study focused on temperature changes at a fine spatial scale. Aggregated spatial replicates of measurements within 1 ha were considered as a single site. Where raw data were provided, a single site comprised the individual point at which measurements were taken.

We included data reported as an average across multiple temporal replicates within a study site, provided that (1) the period of time over which data were averaged and (2) the number of temporal replicates within this period was within either day or night and was consistent across different sites within the study. We set the maximum time period over which data could be averaged as 183 days (half a year), provided this time period was entirely within either the dry season or the wet season, as defined by the authors. Aggregated temporal replicates within a study site were recorded as a single observation. Where raw data provided more than one measurement per day, we calculated a daily mean for each study site (between sunrise and sunset only), each of which represented a distinct observation. If night-time data were available, we applied the same approach for observations measured between sunset and sunrise. For those studies providing more than one temperature observation per day or night, we also calculated temperature minima and maxima for the time period(s) available (day or night).

2.3.3 Data collation

Where possible, temperature data were extracted from text, tables or graphs in the publication. Data in graphs were extracted using DigitizeIt (www.digitizeit.de; Scheffers et al., 2014b). We also extracted: site coordinates and elevation; site descriptions of sufficient detail to enable categorisation into land-use types; season (dry or wet); time of measurements (day or night); and whether temperature was recorded above- or below-ground. In many cases, temperature data or methodological information were

reported inadequately or not at all, in which case authors were contacted directly for information.

In some cases we were unable to retrieve all the required methodological information, and made estimates. We estimated coordinates from Google Earth, based on detailed descriptions in the text, and we estimated elevation from coordinates using a global digital elevation map at 3-arc second resolution (Jarvis et al., 2008). Unless authors had explicitly stated that data were collected during day or night, we determined this by comparing the time of data collection to the time of sunrise and sunset, estimated from the date of collection and the site coordinates using solar calculations developed by the National Oceanic and Atmospheric Administration (NOAA, nd), and implemented in R using custom functions (https://github.com/rasenior/SolarCalc). Our main analyses use day-time temperature only because very few studies considered night-time temperature, though we retained night-time temperature data where they were available for an additional, simplified analysis.

We assigned categories of land use based on Extended Data Table 1 in Newbold et al. (2015), which comprise 'primary forest, 'degraded forest' (renamed from 'secondary'), 'plantation', 'pasture' and 'cropland' (Table 2.1). 'Urban' could not be included due to insufficient data.

2.3.4 Statistical analyses

Each data point in our main analysis comprised an observation of day-time temperature in a particular land-use type. We modelled each temperature observation against land-use type using a linear mixed effects model, implemented in the `lme4` package (Bates et al., 2015) in R (R Core Team, 2017). Studies differed substantially in methodology and location, hence the identity of the study from which data were taken was included as a random intercept term. Exploratory plots suggested that the slope of the relationship between land-use type and temperature, as well as the intercept, varied by study. The decision to include a random slope of land-use type, with respect to study identity, was determined using AIC with the full fixed effects structure (Zuur, 2009). Fixed effects were then selected using backward stepwise model simplification (Zuur, 2009), with the following categorical variables: land-use type (five levels); position relative to ground level (above- or below-ground); and season (dry or wet season), as well as pairwise interactions between land-use type and the latter two variables. We tested interactions using likelihood ratio tests, and then removed interactions to test main effects independently. For a subset of studies with suitable data, we used an analogous approach with only land-use type included as a fixed effect, to model nocturnal temperature and also temperature minima and maxima (for day-time and night-time separately).

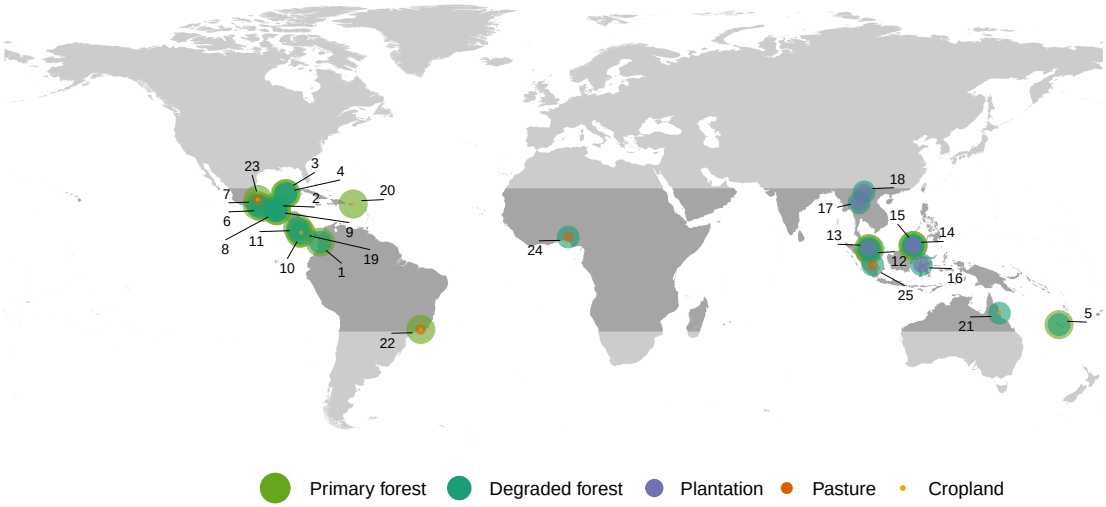

Figure 2.1: Locations of the 25 studies contributing data to the analyses. Point labels correspond to the study number in Table 2.1. The shading and size of concentric points corresponds to different land-use types, to indicate the data provided by each study.

Model estimates of local temperature are presented relative to the model estimate for primary forest (above-ground and in the dry season). Both the position relative to ground level and seasonality interacted with land-use change to influence local temperature, but for clarity we discuss each explanatory variable separately. As such, temperature differences between primary forest and altered land-use types are averages across all combinations of position and season. The influence of position on these thermal differences is presented as an average across seasons, and the influence of seasonality is an average across positions.

2.4 Results

In total, 25 studies met the criteria for inclusion (Table 2.2). Studies spanned 12 countries, across every continent within the tropics (Figure 2.1), and provided 113,894 observations of day-time temperature (Figure 2.2 and Figure A.4). Most observations represented either a single temperature observation within, or mean temperature across, a single day at the point location where measurements were taken. Six studies reported temperature at a coarser temporal resolution (mean = 107 days; minimum = 14 days; maximum = 183 days), and six studies reported temperature at a coarser spatial resolution (mean = 527 m^2; minimum = 64 m^2; maximum = 1,000 m^2). The maximum elevational difference between sites within a single study ranged from 0 to 141 m (mean = 33 m), and site elevation was random with respect to land-use type (LMM, χ^2 = 19.33, df = 14, P > 0.05; Figure A.5). We were also able to obtain 113,459 night-time temperature observations (including temperature extremes) from 10 studies, plus 113,230 observations of day-time temperature extremes from 11 studies; but

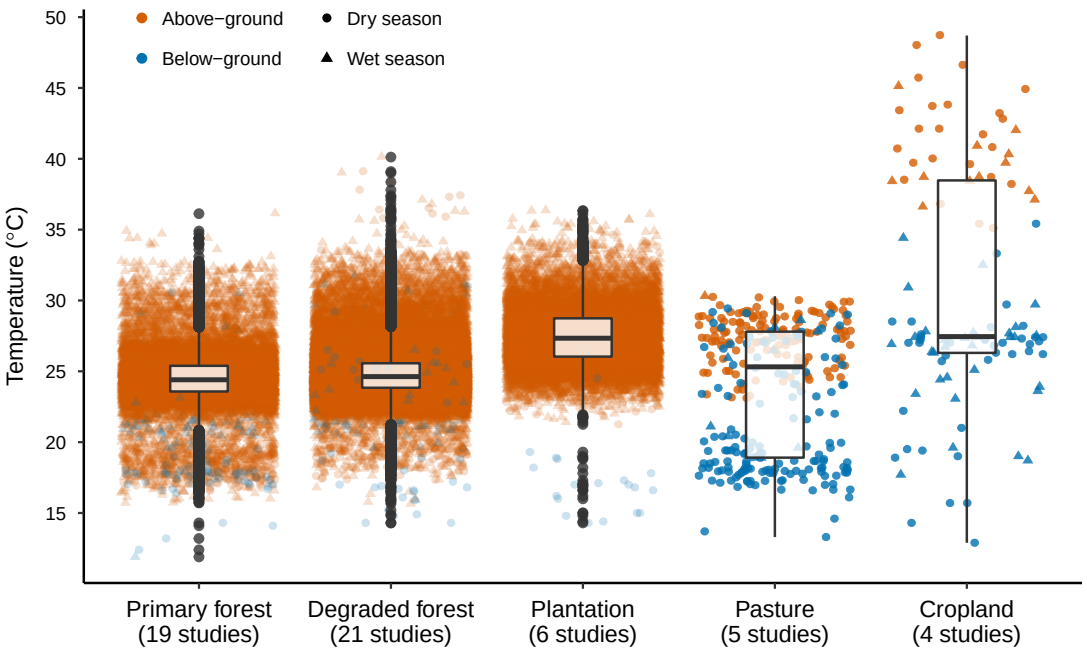

Figure 2.2: Raw day-time temperature against land-use type, across all studies contributing data to the analyses (plotted by study in Figure A.4). Point shading indicates temperatures measured above-ground (orange) or below-ground (blue), and different symbols indicate temperatures measured during the dry season (circles) or wet season (triangles).

none of these data were collected in cropland or pasture.

In all cases, the final model included a random slope for land-use type ('LUT') and random intercept with respect to the identity of the study ('studyID') from which data originated. The final model of day-time temperature ('temp_day') included land-use type, position relative to ground level ('position') and season, as well as pairwise interactions between land-use type and the latter two fixed effects:

```
lmer(temp_day ~ LUT*position + LUT*season + (LUT|studyID))
```

The final models of (1) night-time temperature, and temperature extremes (minimum and maximum) (2) during the day and (3) during the night, all had the same model structure, with land-use type as the only fixed effect:

```
lmer(temp ~ LUT + (LUT|studyID))
```

2.4.1 Effect of land-use change

Altered land-use types were substantially hotter than primary forest (LMM, χ^2 = 29.49, df = 4, P < 0.001; Table 2.3; Figure 2.3), and the magnitude of the warming broadly matched the intensity of vegetation change associated with each land-use type. Thus, degraded forests

Study	Country	Land-use type					Position		Season	
		Primary forest	Degraded forest	Plantation	Pasture	Cropland	Above-ground	Below-ground	Dry season	Wet season
1. González del Pliego (nd)	Colombia	X	X				X		X	
2. González-Di Pierro et al. (2011)	Mexico	X	X				X			X
3. Goode (nd)	Mexico	X	X				X		X	X
4. Goode and Allen (2009)	Mexico	X	X				X		X	X
5. Ibanez et al. (2013)	New Caledonia	X	X				X		X	X
6. Lebrija-Trejos et al. (2011)	Mexico	X	X				X	X	X	X
7. Negrete-Yankelevich et al. (2007)	Mexico	X	X					X		X
8. Santos (2011)	Mexico	X	X				X	X		X
9. Santos and Benítez-Malvido (2012)	Mexico	X	X				X	X		X
10. Sonnleitner et al. (2009)	Costa Rica	X	X				X		X	
11. Wood and Lawrence (2008)	Costa Rica	X	X					X		X
12. Yashiro et al. (2008)	Malaysia	X	X					X	X	X
13. Adachi et al. (2006)	Malaysia	X	X	X				X	X	
14. Hardwick and Orme (2016)	Malaysia	X	X	X			X		X	X
15. Hardwick et al. (2015)	Malaysia	X	X	X			X		X	X
16. Klein et al. (2002)	Indonesia		X	X			X			X
17. Wangluk et al. (2013)	Thailand		X	X				X	X	X
18. Werner et al. (2006)	China		X	X				X	X	
19. Holl (1999)	Costa Rica	X			X		X	X	X	
20. Liu and Zou (2002)	Puerto Rico	X			X			X	X	X
21. King et al. (1998)	Australia		X		X		X	X		X
22. Badejo et al. (2004)	Brazil	X			X	X		X		X
23. Campos (2006)	Mexico	X			X	X		X	X	X
24. Badejo (1990)	Nigeria		X			X		X	X	X
25. Furukawa et al. (2005)	Indonesia		X			X	X	X	X	X

Table 2.2: Summary of the 25 studies contributing data to analyses. Study number corresponds to point labels in Figure 2.1. Crosses indicate the land-use types, position(s) relative to ground level and season(s) considered by each study.

in our sample were the most similar to primary forest with an average difference of only +1.1°C, which was not statistically significant based on 95% confidence intervals (Figure 2.3). By contrast, converted habitats in our dataset - plantation, pasture and cropland - were, on average, hotter than primary forest by 2.7°C, 6.2°C and 7.6°C, respectively. Results were robust to resampling from studies that provided disproportionate numbers of observations (Appendix A.1; Figure A.1).

Night-time temperature, and day-time and night-time temperature extremes, showed varying results relative to primary forest in the two altered land-use types for which data were available: degraded forest and plantation. In all cases, sample sizes were very limited and confidence intervals were large, hence results should be interpreted with caution. Night-time temperature in degraded forest and plantation did not differ from that of primary forest (LMM, χ^2 = 2.09, df = 2, P > 0.05; Figure A.2), and neither did night-time minimum temperature (LMM, χ^2 = 2.31, df = 2, P > 0.05; Figure A.3d). Maximum night-time temperature was slightly higher overall in degraded forest and plantation compared to primary forest (LMM, χ^2 = 6.35, df = 2, P < 0.05; Figure A.3c), although pairwise differences were not statistically significant according to 95% confidence intervals. There was no difference between primary forest and degraded forest and plantation in terms of day-time maximum temperature (LMM, χ^2 = 4.87, df = 2, P > 0.05; Figure A.3a), or day-time minimum temperature (LMM, χ^2 = 4.60, df = 2, P > 0.05; Figure A.3b).

2.4.2 Above- versus below-ground

The warming effect of land-use change was much stronger above-ground than below-ground (LMM, χ^2 = 1115, df = 4, P < 0.001; Table 2.3; Figure 2.3a). The average difference between the local temperature of altered land-use types and primary forest was greater if measured above-ground rather than below-ground, by 1.9°C in plantation, 4.3°C in pasture, and 11.4°C in cropland. In degraded forest, the temperature relative to primary forest was very similar above- (+1°C) and below-ground (+1.1°C). Notably, the buffering effect below ground was so great that any difference between primary forest and impacted land uses was effectively negated in all land-use types but pasture (based on 95% confidence intervals; Figure 2.3a).

2.4.3 Dry versus wet season

Seasonality had some influence on the relationship between land-use change and temperature (LMM, χ^2 = 14.91, df = 4, P < 0.01; Table 2.3; Figure 2.3b), but the direction of the interaction varied by land-use type, and in all cases the effect size was very small. In degraded forest and plantation, seasonality had no appreciable effect on temperature

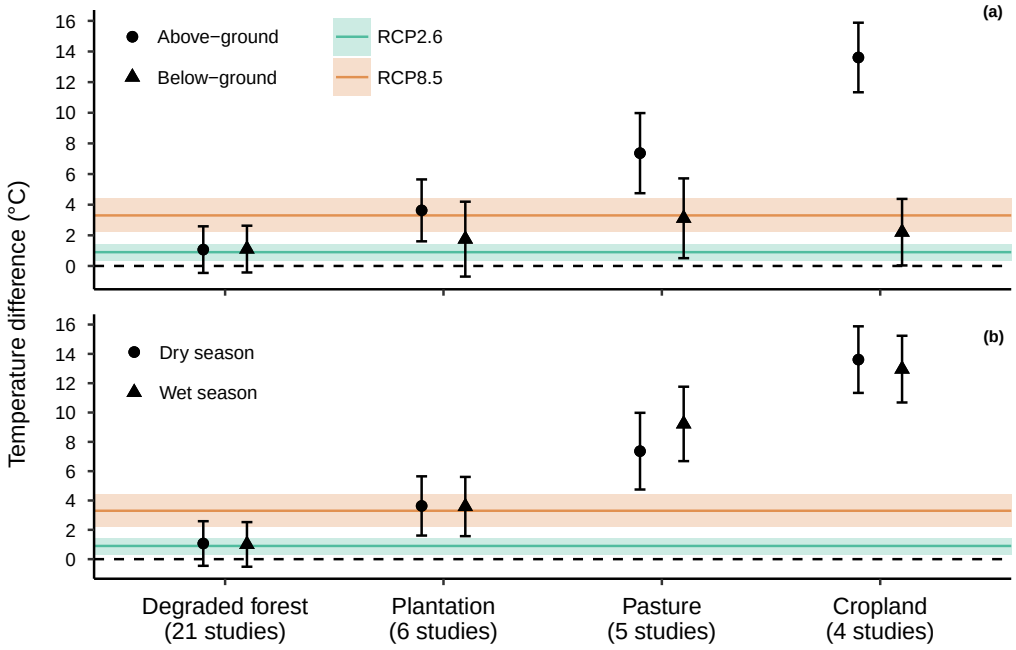

Figure 2.3: Model estimates of local day-time temperature in altered land-use types relative to primary forest (depicted by the black dashed line). In panel (a), different symbols denote position relative to the ground (above-or below-ground), and the season is held at the reference level (dry season). In panel (b), different symbols denote the season (dry or wet), and the position relative to the ground is held at the reference level (above-ground). Error bars are 95% confidence intervals. Solid lines indicate projected warming in the tropics for the period 2081-2100 compared to the period 1986-2005, as a result of global climate change (IPCC, 2013). Shaded bands indicate 5%-95% ranges from the distribution of the climate model ensemble. Colours represent the lowest and highest warming scenarios (RCP2.6 and RCP8.5, respectively).

relative to primary forest (dry vs. wet season: +0.1°C in both degraded forest and plantation). In contrast, the temperature difference between pasture and primary forest was 1.9°C greater in the wet versus dry season, while in cropland the differential was 0.6°C greater in the dry versus wet season.

2.5 Discussion

Our results show that land-use change increases local temperature in the tropics (Figure 2.3). In all conditions where this relationship was evident, the temperature rise due to land-use change exceeded that predicted for the tropics by the end of the 21st Century under the minimum climate warming scenario (+0.9°C in RCP2.6; IPCC, 2013), and frequently also exceeded the maximum warming scenario (+3.3°C in RCP8.5; IPCC, 2013). Previous studies show that land-use change tends to increase local temperature (e.g. Davin and de Noblet-Ducoudré, 2010; Findell et al., 2007; Loarie et al., 2009; Luskin and Potts, 2011; Ramdani et al., 2014; Tuff et al., 2016) but this is the first study, to our knowledge, that demonstrates this effect across many locations in the tropics at a site-level resolution (< 1 ha), considering multiple modes of land-use change concurrently, and comparing the relationship above- and below-ground and between wet and dry seasons.

2.5.1 Thermal differences between land-use types

Human-impacted land-use types are likely hotter than intact primary forest because of changes in evapotranspiration and the amount of solar radiation reaching the Earth's surface (Davin and de Noblet-Ducoudré, 2010; Findell et al., 2007; Oke, 1987). Degradation and deforestation cause a lowering and thinning of the canopy, and reduction in rooting depth, leaf area index and surface roughness, all of which reduce evapotranspiration (Davin and de Noblet-Ducoudré, 2010; Findell et al., 2007; Hardwick et al., 2015; Kumar and Shahabuddin, 2005; Okuda et al., 2003; Snyder et al., 2004), and thereby increase temperature (Foley et al., 2005; Oke, 1987). Changes to canopy architecture and a reduction in the number of sub-canopy vegetation strata also cause warming by increasing the amount of solar radiation reaching the ground (Murcia, 1995; Oke, 1987). Our land use categories encompass a spectrum of vegetation change, from relatively little change in degraded forests (where some trees and a closed canopy are maintained) to maximal change in pasture and cropland (where trees are replaced with herbaceous plants). Accordingly, degradation had the smallest average effect (+1.1°C), followed by plantation (+2.7°C), and then pasture (+6.2°C) and cropland (+7.6°C).

Land-use type	Position	Season	Temp. vs. PF	Lower CI	Upper CI	LUT mean	Position	Position mean	Position effect (AG-BG)	Season	Season mean	Season effect (dry-wet)
Degraded forest	AG	Dry	1.1	-0.5	2.6	1.1	AG	1	0.1	Dry	1.1	0.1
		Wet	1	-0.5	2.5					Wet	1	
	BG	Dry	1.1	-0.4	2.6		BG	1.1				
		Wet	1	-0.5	2.6							
Plantation	AG	Dry	3.6	1.6	5.6	2.7	AG	3.6	1.9	Dry	2.7	0.1
		Wet	3.6	1.6	5.6					Wet	2.6	
	BG	Dry	1.8	-0.7	4.2		BG	1.7				
		Wet	1.7	-0.7	4.2							
Pasture	AG	Dry	7.4	4.7	10	6.2	AG	8.3	4.3	Dry	5.2	-1.9
		Wet	9.2	6.7	11.8					Wet	7.1	
	BG	Dry	3.1	0.5	5.7		BG	4				
		Wet	5	2.4	7.5							
Cropland	AG	Dry	13.6	11.3	15.9	7.6	AG	13.3	11.4	Dry	7.9	0.6
		Wet	13	10.7	15.2					Wet	7.3	
	BG	Dry	2.2	0	4.4		BG	1.9				
		Wet	1.6	-0.6	3.7							

Table 2.3: Model estimates (with 95% confidence intervals) of local day-time temperature in altered land-use types relative to primary forest (PF), with respect to position relative to ground level and season. 'Position effect' refers to the difference between temperature measured above-ground (AG) versus below-ground (BG), averaged across seasons. 'Season effect' refers to the difference between temperature measured in the dry season versus the wet season, averaged across positions. All figures are quoted in °C.

We expected that the same mechanisms underlying the warming effect of land-use change would also result in increased day-time temperature extremes and decreased night-time temperatures in altered land-use types, relative to primary forest (Chen et al., 1995; Oke, 1987). Unfortunately, the data available were very limited, including only three of the five land-use types (primary forest, degraded forest and plantation), and resulting in extremely large confidence intervals (Figure A.2 and Figure A.3). We urge caution when interpreting our results, which suggested either no effect or an extremely weak effect of land-use change on temperature extremes and night-time temperature; clearly more data are needed to reliably test these relationships.

2.5.2 Interaction with position relative to ground level and seasonality

We found that local warming effects of tropical land-use change are negated below-ground, despite the strength of the relationship above-ground (Table 2.3; Figure 2.3a). This can largely be attributed to the higher specific heat capacity of soil compared to air (Oke, 1987). Greater availability of water may also play a role, permitting thermal energy to be dissipated through the evaporation of water rather than increasing temperature (Christidis et al., 2013; Davin and de Noblet-Ducoudré, 2010; Oke, 1987). We expected the latter effect to result in increased buffering during the wet season (cf. Davin and de Noblet-Ducoudré, 2010; Findell et al., 2007), but instead we found that seasonality had a very limited influence on temperature relative to primary forest (Table 2.3; Figure 2.3b). The strongest influence was in pasture, where the effect of land-use change was greater in the wet season. Potentially longer grass in pasture in the wet season could decrease albedo compared to pale exposed soil in the dry season, while the same pattern could be avoided in cropland through dry season irrigation. That said, pasture and cropland had the least data of all land-use types, and we advise that these results be interpreted with caution.

2.5.3 Implications for biodiversity

For tropical biodiversity, there are several key implications of our findings. Firstly, forest species persisting through forest conversion have already experienced thermal change similar, if not greater, in magnitude to that predicted by global climate change (IPCC, 2013). Historically the tropics have experienced relatively stable climatic conditions (Mora et al., 2013) and tropical species possess narrow thermal niches, with many already occupying the upper bounds of that niche (Deutsch et al., 2008; Freeman and Class Freeman, 2014; Sunday et al., 2014; Tewksbury et al., 2008). Dispersal towards more favourable climatic conditions is limited by low dispersal ability (Van Houtan et al., 2007), a scarcity of suitable destinations

(Colwell et al., 2008), and the necessity to pass through an increasingly hostile land-use matrix to reach target habitat (Brook et al., 2008; Scriven et al., 2015; Thomas et al., 2004). There is already some evidence that higher temperatures in the tropics are associated with lower species abundance (e.g. for arthropods: Foster et al., 2011), and there are also fitness costs associated with long-term persistence in suboptimal climatic conditions (du Plessis et al., 2012; Gunderson and Leal, 2016). Without any further temperature change some species persisting in converted environments may already be committed to extinction, particularly species that are unable to utilise microhabitats with favourable microclimates (González del Pliego et al., 2016; Scheffers et al., 2014a). Under predicted climate change, increasing average temperature and the increasing frequency and intensity of droughts (Chou and Lan, 2012; IPCC, 2013) will likely push many species beyond their upper thermal limits, especially in heavily degraded or converted habitats.

That said, we find several circumstances where warming through land-use change is mitigated. Degraded forests were not significantly hotter than primary forests (according to 95% confidence intervals; Figure 2.3). This is encouraging because degraded forests are likely to become the most widespread land-use type in future (Hurtt et al., 2011), and many studies have demonstrated their capacity to retain species of conservation concern (Edwards et al., 2011, 2014c; Gibson et al., 2011; Putz et al., 2012). For all altered land-use types, the warming effect was limited below-ground, highlighting a crucial thermal refuge for species that are able to occupy the soil, and suggesting that above-ground microhabitats, such as deadwood and epiphytes, might fulfil a similar role (González del Pliego et al., 2016; Scheffers et al., 2014a). Thermal refugia may not be a permanent solution for avoiding climate change, and sensitive species may find that even relatively cold microhabitats are still too hot (e.g. below-ground in pasture was 4°C warmer than primary forest; Table 2.3; Figure 2.3), but refugia could at least provide species with more time to respond to suboptimal climatic conditions (Hannah et al., 2014).

2.5.4 Caveats and knowledge gaps

By collating site-level data reported from the literature, we were able to achieve high geographical coverage and fine spatial resolution that is lacking in previous studies, but this technique is biased by the availability of data towards particular regions and land-use types (Figure 2.1), and relies heavily on substituting space for time, which can misrepresent anthropogenic impacts (França et al., 2016). In particular, there was only one study located in Africa, and Southeast Asian studies provided all of the plantation data and no cropland data. Future research should seek to explicitly consider how tropical land-use change affects: vegetation structure (e.g. using Leaf Area Index cf. Hardwick et al., 2015), relative humidity (Ewers and Banks-Leite, 2013; Luskin and Potts, 2011), nocturnal climatic

conditions (Chen et al., 1995; Dubreuil et al., 2011), extremes of temperature (Christidis et al., 2013), and rates of temperature change (Scheffers et al., 2014a); preferably at a range of spatiotemporal scales (Wiens and Bachelet, 2010) and with a standardised methodology to simplify comparisons across studies.

2.5.5 Conclusions

Our study confirms that tropical land-use change leads to warming at a local scale (< 1 ha) across the tropics, of a magnitude comparable to that predicted from global climate change. We find pantropical evidence that the effects of land-use change on temperature are ameliorated below-ground, and absent in degraded forests. Many studies collect site-level climate data, and through sharing of these data and collaboration between scientific disciplines, there is much that can be done to integrate theoretical and empirical understanding of the processes that govern climate at different scales. This will greatly advance our knowledge of potential synergies between two of the greatest drivers of biodiversity loss – land-use change and climate change – and highlight mitigating factors, such as thermal microrefugia, which could be a pragmatic focus for conservation management.

2.6 Code availability

R functions used to estimate time of sunset and sunrise can be downloaded from GitHub (https://github.com/rasenior/SolarCalc).

2.7 Data availability

The collated dataset can be found on Dryad (https://doi.org/10.5061/dryad.g4000). Note that in many cases these data were aggregated for analyses. For finer resolution data please refer to the original data sources.

2.8 Acknowledgements

We thank the following people for providing temperature data: Julieta Benítez Malvido, Stephen Hardwick, Karen Holl, Thomas Ibanez, and Bráulio Santos. A considerable amount

of data was provided by the Stability of Altered Forest Ecosystem (SAFE) Project, for which we acknowledge their primary sponsor: the Sime Darby Foundation. We thank Tim Newbold for statistical advice. R.A.S. was funded by a NERC studentship through the ACCE (Adapting to the Challenges of a Changing Environment) Doctoral Training Partnership (Grant No. NE/L002450/1); P.G. was supported by CONACyT, Scholarship 359063. We also thank two anonymous referees for their comments, which greatly improved the manuscript.

Chapter 3

A framework for quantifying fine-scale thermal heterogeneity using thermography

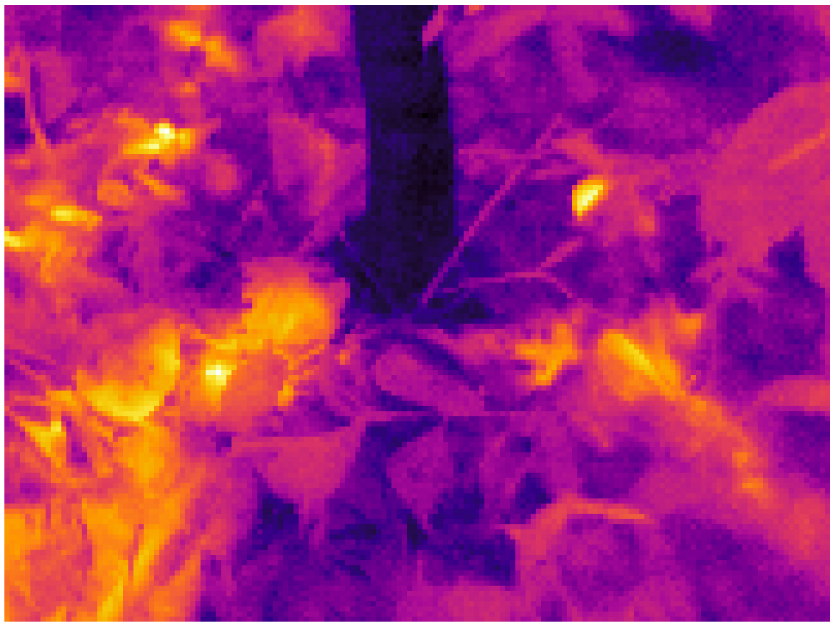

Thermal image of rainforest floor.

This chapter is currently in preparation for submission to *Ecography* as:

Senior RA, Hill JK, Edwards DP. A framework for quantifying fine-scale thermal heterogeneity using thermography.

3.1 Abstract

Variation in temperature at a fine spatial scale creates critically important microclimates for many organisms. Quantifying thermal heterogeneity at this scale is challenging and, until recently, has been largely restricted to the use of dataloggers to record air temperature. Thermography is becoming an increasingly viable alternative. A single thermal photo contains thousands of spatially explicit surface temperature measurements, making them ideal for rapidly assessing temperature variation at fine scale. To date, the technology and data have been underexploited in terrestrial ecology, partly because there is limited technical support. Here, we present a framework and R package for processing thermal images and other gridded temperature data, demonstrated using thermal images from selectively logged and unlogged forests of Borneo. We quantified heterogeneity in the understorey using metrics that capture both the frequency distribution and spatial distribution of temperature. Thermal heterogeneity was similar in logged and unlogged forests, but showed clear patterns over the day. When average temperature reached its maximum – around noon – we observed peaks in thermal diversity, the deviation of temperature extremes from the average, and in the area of statistically-defined 'hot spots'. At the same time, 'cold spots' were more irregularly shaped and less spatially clustered, which could make them easier for organisms to locate when they are most necessary (i.e. when average temperatures are highest). To illustrate how our approach can be applied to other temperature data we used mean monthly temperature for Borneo from WorldClim2 (~1 km^2 resolution). Thermal diversity and spatial clustering of cold spots were highest in September and October, which could be related to the transition from dry to rainy season. Put together, our framework simplifies the processing of thermal data, and our metrics capture key spatiotemporal temperature trends that could underpin species' responses to environmental change.

3.2 Introduction

A key way in which organisms will respond to future climate change is adaptation *in situ* (Hannah et al., 2014). On a daily basis, mobile organisms respond to extremes of heat by exploiting fine-scale (mm to m) thermal heterogeneity (González del Pliego et al., 2016; Scheffers et al., 2014a). Over longer time periods, climate at this scale ('microclimates') can also maximise fitness and thus influence the fine-scale distribution of less mobile species (Maclean et al., 2017). The same mechanisms could temper species' exposure to global climate change (Scheffers et al., 2014b; Suggitt et al., 2018), particularly in structurally complex habitats like tropical rainforests (Scheffers et al., 2017a). To accurately predict

species' responses to climate warming in these places we must therefore be able to efficiently and effectively capture thermal heterogeneity at fine scale.

The use of temperature dataloggers has been instrumental in advancing our knowledge of temperature at biologically relevant spatial scales (Bramer et al., 2018). However, dataloggers can only record the air temperature in their immediate vicinity, and so must be highly replicated in space and in a variety of microhabitats to capture spatial temperature variation. Additionally, the vast majority of terrestrial organisms are very small, flat, or thigmothermic (i.e. thermoregulate via direct contact with a surface), hence surface temperature is often more biologically relevant than is air temperature (e.g. Kaspari et al., 2015).

Technological advances in recent years have made thermal cameras an increasingly affordable and practical complement to dataloggers (Faye et al., 2016; Scheffers et al., 2017a). A single thermal image provides thousands of spatially explicit surface temperature measurements at the mm-cm scale. With such a wealth of data and limited guidance on how to process and analyse it, both the technology itself and the data provided have not been utilised to their full potential within terrestrial ecology. Faye et al. (2016) provide an excellent starting point from which to formulate a framework. Using visual images (red, green and blue spectral bands) in combination with thermal images, collected using an unmanned aerial vehicle (UAV), Faye et al. demonstrate how thermography can be used to compare thermal heterogeneity between different surfaces (in this case, bare soil versus crop surface), and suggest various metrics to capture different facets of thermal heterogeneity. However, while the use of UAVs in complex habitats is indeed becoming more feasible (Sanchez-Azofeifa et al., 2017), for the foreseeable future it is likely that thermography in these places will most commonly consist of thermal photos collected manually in the field, and there is no comparable toolbox for these data.

Both Faye et al. (2016) and Scheffers et al. (2017a) provide introductory R scripts to facilitate the processing of thermal photos. However, batch processing of data from thermal images is rarely straightforward, while parameters such as emissivity strongly influence the accuracy of measurements but may not be well understood by the novice user (Bramer et al., 2018).The development of the `Thermimage` package (Tattersall, 2017) in R has considerably eased extraction and conversion of raw data from FLIR thermal cameras specifically, but this package does not directly facilitate processing in batch nor does it calculate (or suggest) what metrics are most appropriate to quantify thermal heterogeneity using thermal images.

The most appropriate metrics to capture thermal heterogeneity will depend on the taxonomic group and research questions of interest. Temperature varies across time and space in a multitude of ways that can easily be captured by thermal images; it is important

to exploit the information provided without becoming overwhelmed. Both Shi et al. (2016) and Faye et al. (2016) provide a useful summary of some important metrics, and Faye et al. notably introduce a spatial component by borrowing metrics from landscape ecology, such as Shape Index and Cohesion Index (McGarigal et al., 2012). Extending this approach reveals other techniques that could be useful in this context, such as hot spot analysis (Getis and Ord, 1996).

In this study, we introduce an R package – `ThermStats` – which combines ideas, techniques and metrics from previous work into one simple framework for quantifying heterogeneity in thermal images. Using images collected in primary and selectively logged forests on Borneo, we illustrate the utility of our package for comparing thermal heterogeneity over time and between forest types. In addition, while the package was designed with fine-scale data in mind, we use temperature data for Borneo at 1 km^2 resolution from the WorldClim2 database (Fick and Hijmans, 2017) to demonstrate how our metrics of thermal heterogeneity can also be calculated for other kinds of gridded temperature data.

3.3 Methods

3.3.1 Step 1: Data collection

High resolution surface temperature measurements can easily be collected in the field using a handheld thermal camera. We used a FLIR Systems, model E40 camera, which costs ~US$4,000, weighs 825 g, and takes 19,200 measurements (160 x 120 pixels) in a single photo (FLIR, 2016; Scheffers et al., 2017a). Various other models are available, including the smaller and more affordable FLIR ONE smartphone attachment at ~US$300, 34.5 g and a resolution of 80 x 60 pixels. As with any field study, the sampling design should aim to achieve sufficient coverage over the study area and over time, such that the images are representative samples of the treatments of interest. For example, a single image of the ground from 1 m away encompasses an area of 0.9 x 1.1 m using a FLIR E40 camera (FLIR, 2016), and so it may be necessary to take multiple photos in different cardinal directions and at different times of day to effectively represent the temperature of a study plot (Chapter 4; Scheffers et al., 2017a).

Before any data are collected, we recommend users familiarise themselves with the technology. There are various sources of the infrared radiation detected by a thermal camera, but we want to focus only on the radiation emitted by the object of interest, which is a function of its temperature. The amount of radiation emitted by a particular object, for a given temperature, depends on its emissivity. A perfect blackbody has an emissivity

of 1, while surfaces that an ecologist is likely to photograph typically have an emissivity ranging from 0.92 (for dry, bare soil; FLIR, 2016) to 0.99 (for green broadleaf forest; Snyder et al., 1998). Additionally, the temperature and relative humidity of the atmosphere and the distance between the object and the camera will all affect (1) the amount of emitted radiation that is absorbed by the atmosphere and (2) the amount of radiation that originates from the atmosphere itself, with some of this also being reflected by the object (reflected apparent temperature).

To accurately quantify surface temperature, environmental parameters (emissivity, reflected apparent temperature, atmospheric temperature, atmospheric relative humidity and object distance) can be set in the camera or defined during data processing (see 'Step 3: Conversion of raw data'). The benefit of the latter approach is that the user can measure atmospheric temperature and relative humidity concurrently with thermal image collection, and these parameters can then be set for each image individually. Object distance should be minimised, and it is usually advisable to keep this value constant. Emissivity can either be estimated from the literature (cf. Scheffers et al., 2017a) or sampled in the field (FLIR, 2016). Reflected apparent temperature can also be sampled (FLIR, 2016), although for high emissivities and short object distances, relatively little radiation is reflected and thus apparent temperature can be assumed to equal the atmospheric temperature (Tattersall, 2017). It is recommended that thermal cameras are regularly calibrated (FLIR Systems suggest doing so once per year).

3.3.2 Step 2: Data extraction

A single thermal photo from a model E40 camera comprises 160 x 120 pixels, each of which is a unique measurement of received infrared radiation encoded as a raw 16-bit value. Data can be extracted into a .csv file using the freely available FLIR Tools software (https://www.flir.com/products/flir-tools; cf. Scheffers et al., 2017a), but we do not recommend this because it cannot be done in batch, there is less transparency regarding the conversion of raw values to temperature, and FLIR Tools uses interpolation to elevate the number of pixels (up to 320 x 240 for a model E40 camera). A quicker and more flexible approach is to use the R package `Thermimage` (Tattersall, 2017). The function `readflirJPG` is able to extract all raw data from a FLIR thermal image, and can be implemented in batch using the function `batch_extract` in our package, `ThermStats`.

3.3.3 Step 3: Conversion of raw data

The raw values embedded in a FLIR thermal image can be converted to temperature in °C using equations from infrared thermography (Tattersall, 2017; FLIR, 2016). This

is made simple by the function `raw2temp` in the `Thermimage` package, which can be implemented in batch in our package using the function `batch_convert`. Several default values are defined in `raw2temp`, but the most accurate temperature conversion will be achieved when the environmental parameters, described in 'Step 1', are defined by the user. Notably, default emissivity is 1, but should realistically take a value between 0.95 and 0.97 (Tattersall, 2017), while the default relative humidity of 50% is excessively low for moist habitats like tropical rainforest. Conversion of raw data also requires various calibration constants that are specific to each camera. These can be retrieved from a thermal image using the `Thermimage` function `flirsettings`, which is done automatically within our `batch_extract` function.

3.3.4 Step 4: Calculate metrics of thermal hetereogeneity

The most relevant metrics to quantify thermal heterogeneity depend on the particular research questions. The function `get_stats` takes a single thermal dataset, in the form of a matrix or raster, and calculates user-defined summary statistics across all pixels. Standard summary statistics could include measures such as mean and standard deviation, but may also include metrics like thermal richness (the number of unique temperature values) and thermal diversity indices (cf. Faye et al., 2016). Several helper functions are available to implement less standard summary statistics. Based on discussions in Faye et al. (2016) and Shi et al. (2016), we recommend some suitable statistics in Table 3.1.

The function `get_stats` identifies hot and cold spots in thermal images using a standalone function `get_patches`. Hot and cold spots are based on the Getis-Ord local statistic (Getis and Ord, 1996), calculated using the `spdep` package (Bivand and Piras, 2015). The statistic is calculated for individual pixels by comparing its value to that of neighbouring pixels. The size of the neighbourhood and style of spatial weighting are specified by the user (these arguments are passed directly to the relevant functions in the `spdep` package). High positive values exceeding the Z-value threshold (defined according to the sample size; Getis and Ord, 1996) are classified as hot spots, and low negative values as cold spots. Several spatial statistics are then calculated to characterise the hot and cold spots (Table 3.2; cf. Faye et al., 2016). There is an option to return patch outlines as a `SpatialPolygonsDataFrame`, which can be plotted on the temperature data using `plot_patches` alongside an (optional) histogram of the temperature distribution (Figure 3.1).

We assume that for most users the spatial unit of replication will comprise multiple thermal images. In this case, the user can specify a grouping variable in `stats_by_group`. Matrices from each group will be bound together and `get_stats` applied over the combined matrix. We assume the images are not adjacent in space, and therefore pad matrices with NA values

Summary statistic	Description
Average temperature	Provides context for all other statistics, and could be used as a measure of the macroclimate for small, surface-dwelling organisms. The median is more robust than the mean to spurious extreme values that can sometimes arise in thermal images.
Temperature extremes	While more rarely encountered, extreme values can be more significant to organisms, for example by exceeding upper thermal limits or by providing cool refugia from average conditions. The difference between extremes provides a measure of thermal diversity/stability (Shi et al., 2016), while the difference between extremes and average temperature provides a measure of the potential for thermal buffering. Again, we suggest the 5^{th} and 95^{th} percentiles are more robust to spurious extreme values than the minimum and maximum (respectively).
Temperature variability	Over space and time, the standard deviation or coefficient of variation of temperature represents another measure of thermal stability (Shi et al., 2016), which may be particularly significant for organisms requiring constant temperatures, e.g. juveniles with a lower capacity for thermoregulatory behaviours. In contrast, for other mobile organisms – particularly ectotherms – high thermal diversity is likely to maximise opportunities for thermoregulation.
Thermal diversity indices	Captures both the richness and evenness of different temperatures. Similar to temperature variability, the biological relevance of this measure is through its influence on the necessity and potential for thermoregulation. As discussed by Faye et al. (2016), Shannon's thermal diversity index quantifies how reliably one can predict the temperature of a pixel sampled at random from the temperature data. Simpson's thermal diversity index is similar, but instead captures the likelihood of two pixels being the same temperature (or temperature class) when taken at random from the thermal landscape.

Table 3.1: Suggested summary statistics that can be applied by `get_stats`.

before binding. Table D.2 gives an example of the output from `stats_by_group`.

3.3.4.1 Case studies

We demonstrate our framework and R package using fine-scale data collected in the field with a FLIR thermal camera. To investigate how thermal heterogeneity varies over time and with selective logging, we sampled surface temperature in a large area of contiguous forest in Malaysian Borneo in the years 2014 and 2015, using a FLIR Systems model E40 thermal

Patch statistic	Description	Biological relevance
Area (absolute)	Total number of pixels	Larger or more numerous microclimates increase opportunities for thermoregulation.
Area (proportion)	Proportion of all pixels which are inside hot/cold spots	Where a greater proportion of pixels fall inside microclimates there is likely to be higher thermal diversity.
Abundance	Number of distinct hot/cold spots	More numerous microclimates increase opportunities for thermoregulation.
Density	Number of hot/cold spots per unit area	Larger microclimates increase opportunities for thermoregulation.
Shape Index	Irregularity in shape of hot/cold spots, with 1 being perfectly regular i.e. a square (McGarigal et al., 2012)	More irregular microclimates may be less thermally stable but easier to locate, because of the greater proportion of edge.
Aggregation Index	Degree of clustering in space of hot/cold spots, with zero representing no clustering (He et al., 2000)	Dispersed, non-clustered microclimates are easier for animals to locate (Sears et al., 2016).
Patch Cohesion Index	Physical connectedness of hot/cold spots (Schumaker, 1996)	More connected microclimates may facilitate more efficient travel.

Table 3.2: Patch statistics calculated for hot and cold spots by the function `get_stats`.

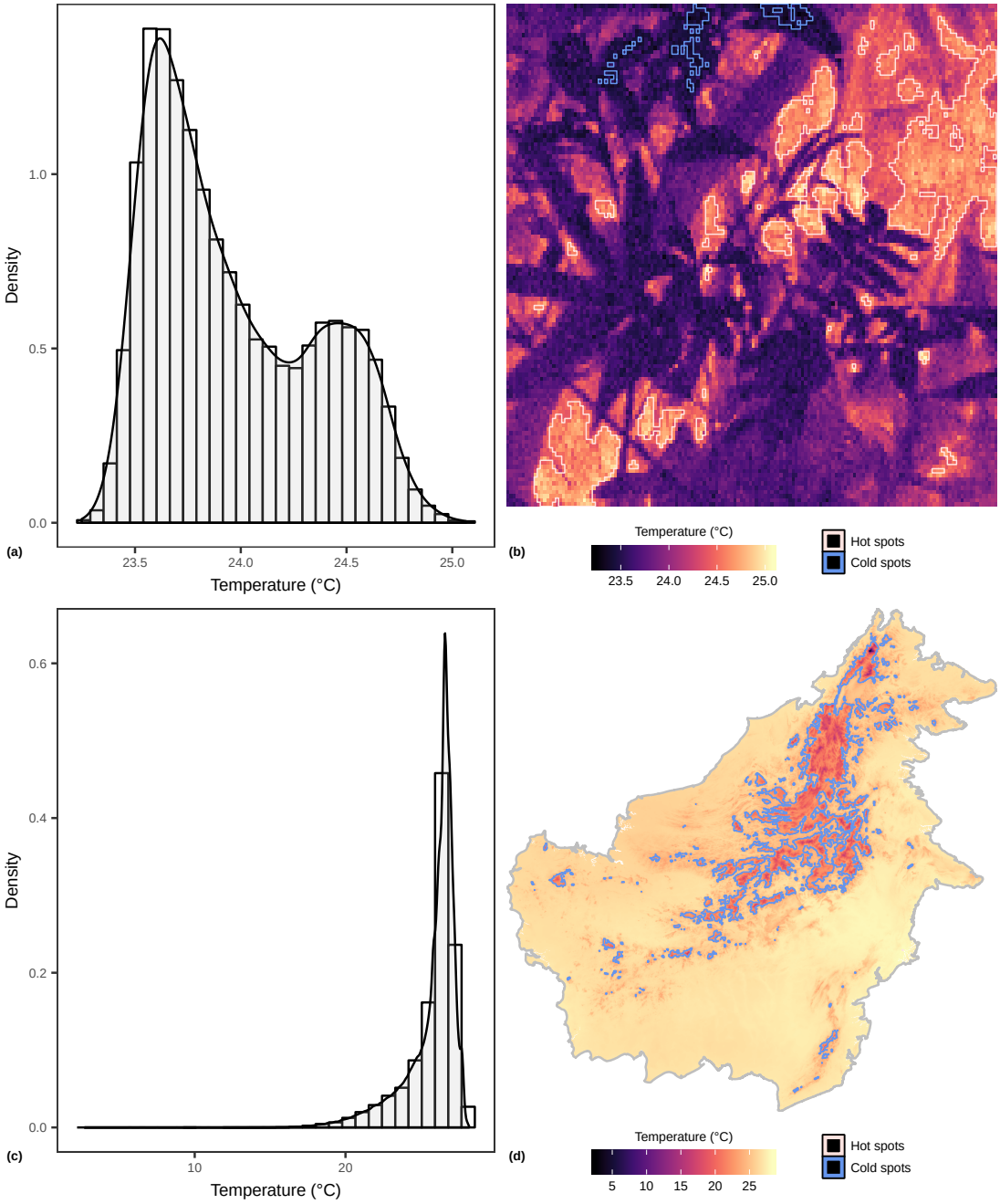

Figure 3.1: Examples of temperature distribution (left column) and thermal images (right column) for temperature data collected at fine and coarse spatial scales (top and bottom rows, respectively). Pixels are shaded from cold (purple) to hot (yellow). Hot spots (outlined in pink) and cold spots (outlined in blue) were identified using the Getis-Ord local statistic of each pixel.

camera. In both years, photos were taken at the centre of plots spaced along existing transects, with six transects in undisturbed primary forest (Danum Valley Conservation Area; 4°57045.2“N, 117°48010.4”E), and six transects in adjacent forest that had been commercially selectively logged twice between 1987 and 2007 (Ulu Segama-Malua Forest Reserve, 4°57042.8“N, 117°56051.7”E). Plots were sampled repeatedly from the coolest to the hottest part of the day (05:00-14:30 h). In each sampling event, thermal images were taken at the centre of the plot in four orthogonal directions, with the camera held at breast height and pointing 45° downwards (relative to the ground). A single pixel represents roughly 0.57 cm^2. In total we collected 2,972 photos across 144 plots. For full details see Scheffers et al. (2017a) and Chapter 4.

For all analyses, each metric of thermal heterogeneity was calculated across all four photos taken each time a plot was sampled. We focused on the following summary statistics from Table 3.1: median temperature; Shannon Diversity Index; upper temperature range (95^{th} percentile - median); and lower temperature range (median - 5^{th} percentile). We identified hot and cold spots using a neighbourhood size of eight pixels (k = 8 in `spdep::localG`), with row standardised neighbour weights (style = “W” in `spdep::nb2listw`). For hot and cold spots separately, we calculated the following spatial statistics (Table 3.2): average area per patch (total area divided by number of patches, to correct for plots with missing photos); average number of patches per unit area (density); Shape Index; and Aggregation Index. Overall we expected forests to be more thermally homogenous early in the day and to increase in heterogeneity towards the hottest part of the day, around noon, as microclimates increasingly deviate from the average temperature. Loss of vegetation, such as through logging, tends to decrease absorption and reflection of incident radiation and reduce heat loss through evapotranspiration (Oke, 1987; Sears et al., 2011), so we might expect logged forests to be more thermally homogenous than unlogged forests. However, there is also evidence that after selective logging there is rapid horizontal growth in the canopy (Asner et al., 2004), corresponding to rapid thermal recovery (Chapter 4).

We used Generalized Additive Mixed Effects Models (GAMMs) to model the various thermal heterogeneity metrics against forest type (categorical: primary or logged) and time of day, smoothed with a cubic regression spline. All models were fit using the `gamm4` package (Wood and Scheipl, 2017) in `R` (version 3.5.0; R Core Team, 2018). We included a random intercept term for ‘year’, and for ‘plot’ nested in ‘transect’ to account for spatial pseudoreplication. All metrics were modelled with a Gaussian error distribution, except for Aggregation Index which is proportion data (number of edges shared by pixels of the same class divided by the maximum number that could be shared; He et al., 2000), and was therefore modelled using a binomial error distribution. Statistical significance was inspected using likelihood ratio tests, dropping each fixed effect in turn and comparing it to the full model (Zuur, 2009).

Although our framework was designed with fine spatial scales in mind, thermal heterogeneity metrics can be calculated for any gridded temperature data. We therefore include an additional assessment of thermal heterogeneity across Borneo, using average monthly temperature (hereafter: temperature) for 1970-2000 from WorldClim2 (Fick and Hijmans, 2017) at 30 arc-second resolution (approximately 1 km^2 at the equator). We calculated the same heterogeneity metrics as in the field study, but focused only on cold spots (because there were very few hot spots). Seasonality is limited on Borneo so we expected that thermal heterogeneity would not change markedly over the year, but may be higher in the dry season – roughly July to October (McAlpine et al., 2018) – when average temperatures are higher and there is less buffering by high water availability. We modelled these metrics against month using Generalized Additive Models (GAMs), smoothed with a cubic regression spline, using the `mgcv` package in R (Wood, 2017). As with the field study, a Gaussian error distribution was used for all but the Aggregation Index, which used a binomial error distribution. Model inference was based on a likelihood ratio test of the full model compared to a model without the fixed effect of month.

3.4 Results

3.4.1 Field study

All measures of thermal heterogeneity were comparable between primary and unlogged forest ($P > 0.05$; Figure 3.2), but showed clear patterns over the day. Median temperature was lowest around dawn (~06:00 hr) and increased steeply thereafter until reaching a plateau around noon ($\chi^2 = 999$, $P < 0.001$; Figure 3.2a). The thermal Shannon Diversity Index showed a similar pattern, reaching maximum diversity at noon ($\chi^2 = 175$, $P < 0.001$; Figure 3.2b). Although less pronounced, noon peaks were also observed for the upper temperature range (95^{th} percentile minus median; $\chi^2 = 59.2$, $P < 0.001$; Figure 3.2c) and lower temperature range (median minus 5^{th} percentile; $\chi^2 = 20.6$, $P < 0.001$; Figure 3.2d). Together these measures suggest that overall variation in temperature and the deviation of extreme values from the average all increase from dawn to noon.

The spatial distribution of hot and cold spots is less intuitive, but did also vary temporally. For hot spots, the average area peaked around noon ($\chi^2 = 38.8$, $P < 0.001$; Figure 3.2e) when their density ($\chi^2 = 64.2$, $P < 0.001$; Figure 3.2g), and Shape Index ($\chi^2 = 69.6$, $P < 0.001$; Figure 3.2i) were near their minimum values. The Aggregation Index of hot spots reached its lowest value after dawn and increased thereafter ($\chi^2 = 14600$, $P < 0.001$; Figure 3.2k). Thus, throughout the morning hot spots became larger but fewer in number, with a more irregular shape and increased spatial clustering.

Cold spot distribution showed slightly different patterns in the timing of peaks and troughs, compared to hot spots. The average area of cold spots was highest early in the morning and decreased thereafter (χ^2 = 5.79, P < 0.05; Figure 3.2f), although their density remained constant (χ^2 = 1.77, P = 0.183; Figure 3.2h). The Shape Index of cold spots decreased after dawn to its minimum value, and subsequently increased (χ^2 = 27.7, P < 0.001; Figure 3.2j). Aggregation Index, in contrast, increased to its maximum value after dawn, and subsequently decreased (χ^2 = 60000, P < 0.001; Figure 3.2l). Overall, cold spots were larger, more regularly shaped and more clustered in the morning compared to noon.

3.4.2 Remote study

Thermal heterogeneity on Borneo varied over the year for most metrics considered. While average temperature peaked most notably around April-May (F = 7.26, P < 0.05; Figure 3.3a), the thermal Shannon Diversity Index was greatest around September and January (F = 11.8, P < 0.01; Figure 3.3b) and the upper temperature range (95^{th} percentile minus median) had an inverse pattern to median temperature, being lowest in May and highest in December (F = 14.6, P < 0.01; Figure 3.3c). There was no clear seasonality in the lower temperature range (median minus 5^{th} percentile; F = 2.68, P = 0.119; Figure 3.3d), nor the area (F = 1.72, P = 0.248; Figure 3.3e) and density (F = 1.93, P = 0.21; Figure 3.3f) of cold spots. The Shape Index of cold spots was highest in June and lowest in September (F = 4.58, P < 0.05; Figure 3.3g), in contrast to the Aggregation Index of cold spots which peaked in September (Deviance = 42.6, P < 0.001; Figure 3.3h). Taken together, these results suggest that there is some annual variation in thermal heterogeneity, with more clustered and regularly shaped cold spots and greatest thermal diversity around September.

3.5 Discussion

Our R package presents users with a simple protocol for processing and analysing thermal images. Although tailored towards images collected in the field using a FLIR camera, we demonstrate its applicability for other forms of gridded temperature data. In particular, we facilitate the calculation of various metrics of thermal heterogeneity collated from the literature (Faye et al., 2016; Shi et al., 2016), which are considered biologically important in the context of thermoregulation and are not readily captured by existing methods.

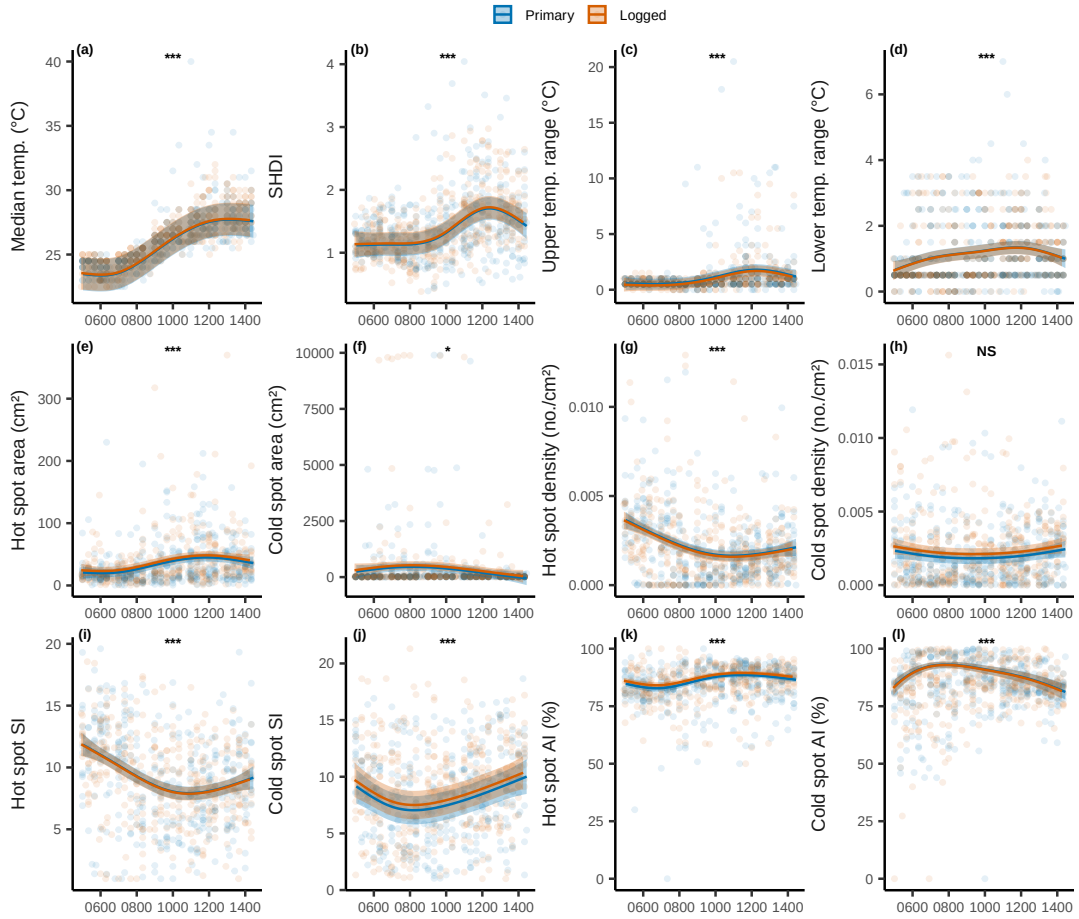

Figure 3.2: Trends in various measures of thermal heterogeneity over the day (06:00-14:30 hrs) for fine-scale temperature data collected using a thermal camera in primary (blue) and logged forests (orange). From left to right and top to bottom, the metrics are: median temperature (a); thermal Shannon Diversity Index (b); 95th percentile minus median temperature (c); 5th percentile minus median temperature (d); the average area (cm^2) per hot spot (e); the average area (cm^2) per cold spot (f); the number of hot spots per unit area (g); the number of cold spots per unit area (h); the Shape Index of hot spots (i); the Shape Index of cold spots (j); the Aggregation Index of hot spots (%) (k); and the Aggregation Index of cold spots (%) (l). Solid lines are model-predicted values with 95% confidence intervals. Semi-transparent background points represent the raw data. Statistically significant differences are indicated by asterisks: 0.01 < P < 0.05 (*); 0.001 < P < 0.01 (**) and P < 0.0001 (***).

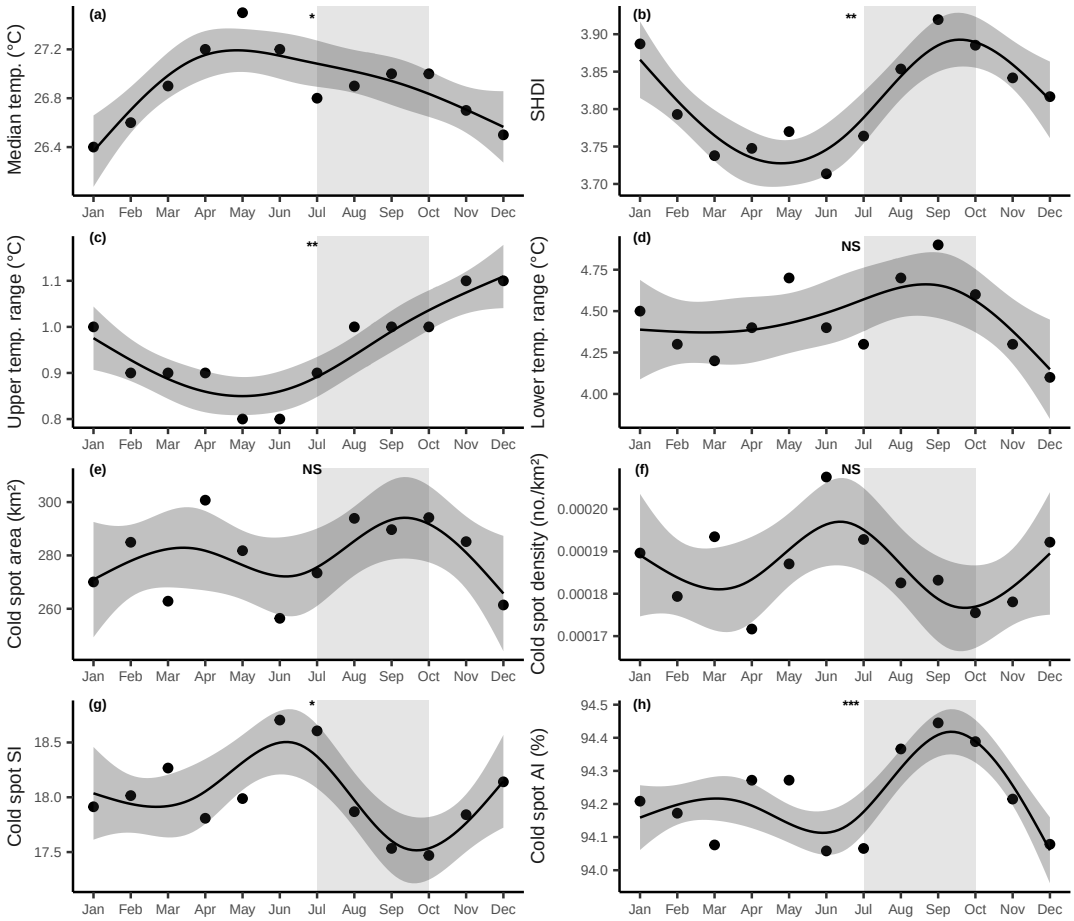

Figure 3.3: Trends in various measures of thermal heterogeneity over the year for temperature data from WorldClim2. From left to right and top to bottom, the metrics are: median temperature (a); thermal Shannon Diversity Index (b); 95th percentile minus median temperature (c); 5th percentile minus median temperature (d); the average area (km^2) per cold spot (e); the number of cold spots per unit area (f); the Shape Index of cold spots (g); and the Aggregation Index of cold spots (%) (h). Solid lines are model-predicted values with 95% confidence intervals. Points represent the raw data. Statistically significant differences are indicated by asterisks: 0.01 < P < 0.05 (*); 0.001 < P < 0.01 (**) and P < 0.0001 (***). The dry season is indicated by a light grey vertical band from July to October.

3.5.1 Case studies

We found a strong effect of time on nearly all metrics of fine-scale thermal heterogeneity, in both intensively logged and unlogged forests on Borneo. Average temperature was lowest around dawn (~06:00 hrs) and peaked around noon (~12:00 hrs). Organisms are most likely to be seeking above-average temperatures for basking after sunrise, at which point hot spots were smaller in area but more numerous, more irregular in shape and less clustered, thus potentially easier to locate (Sears et al., 2016). Conversely, cold spots are necessary to buffer organisms against extremes of heat, which are most likely encountered at noon. At this time there was the greatest difference between minimum and average temperature, and cold spots were likely to be easier to locate because of a more irregular shape and lack of spatial clustering. Temperature variation in both time and space was comparable between forest types (Figure 3.2), confirming the findings of Chapter 4 that within a few years of recovery, intensively logged forest can have an equal capacity for thermal buffering as nearby unlogged forest.

Despite the coarseness of the data from WorldClim2 and general lack of seasonality on Borneo (e.g. Walsh and Newbery, 1999), some temporal patterns were apparent. Namely, thermal diversity and clustering of cold spots were highest in September and October when the regularity of cold spot shape was lowest (Figure 3.3). This marks the end of the dry season (McAlpine et al., 2018), at which point lower water availability may decrease heat loss through evaporation (Oke, 1987), causing some locations to deviate more from the regional average temperature and thereby increasing overall thermal diversity.

3.5.2 Caveats and considerations

It is important to consider the strengths and weaknesses of thermography when deciding on the most appropriate methodology to answer the research questions of interest. Thermal cameras cannot directly measure sub-surface temperatures and are not as well suited for capturing temporal variation as dataloggers. Although affordable smartphone attachments are now available, thermal cameras may still be more expensive than dataloggers (depending on the quantity of dataloggers required), and can be sensitive to extreme weather conditions common to regions such as the tropics and Arctic (FLIR, 2016). Bramer et al. (2018) is an excellent resource for ecologists seeking best practice for using dataloggers; we hope that our study and the references herein offer something analogous for ecologists using thermography.

3.5.3 Summary

Fine-scale temperature variation across space and time has a huge influence on species' ecology, which will become increasingly pertinent as average temperatures rise under global climate warming. We showcase how our R package and framework can be used to quantify thermal heterogeneity in tropical forests using data at a fine spatial scale, collected using a FLIR thermal camera. We also show how our metrics can be calculated for other kinds of gridded temperature data, such as remotely sensed data. By simplifying and streamlining the processing of increasingly available thermal imagery, our approach enables researchers to more readily address key issues in ecology and conservation.

3.6 Code availability

The R package `ThermStats` can be downloaded from GitHub: https://github.com/rasenior/ThermStats. Bug reports and suggested enhancements can be submitted to: https://github.com/rasenior/ThermStats/issues.

3.7 Acknowledgements

Thanks to Manoela S. Machado Mollinari for helpful discussions. R.A.S. was funded by a NERC studentship through the ACCE (Adapting to the Challenges of a Changing Environment) Doctoral Training Partnership (Grant No. NE/L002450/1).

Chapter 4

Tropical forests are thermally buffered despite intensive selective logging

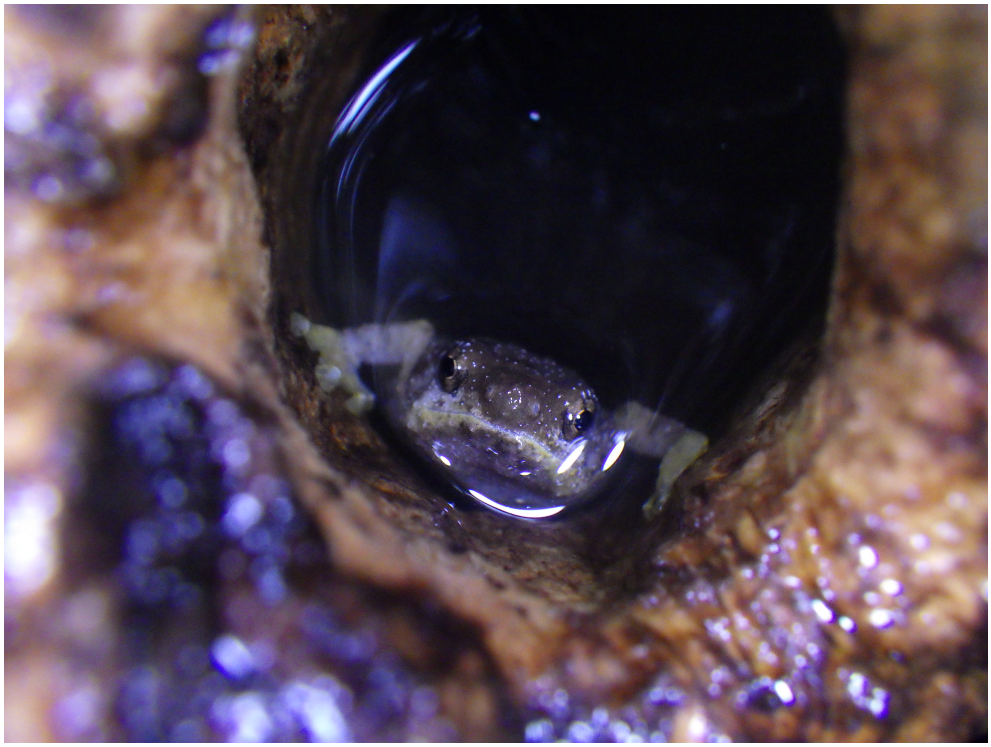

Bornean tree hole frog (*Metaphrynella sundana*).

This chapter has been published as:

Senior RA, Hill JK, Benedick S, Edwards DP. Tropical forests are thermally buffered despite intensive selective logging. Global Change Biology. 2018;24:1267–1278.

4.1 Abstract

Tropical rainforests are subject to extensive degradation by commercial selective logging. Despite pervasive changes to forest structure, selectively logged forests represent vital refugia for global biodiversity. The ability of these forests to buffer temperature-sensitive species from climate warming will be an important determinant of their future conservation value, although this topic remains largely unexplored. Thermal buffering potential is broadly determined by: (1) the difference between the 'macroclimate' (climate at a local scale, m to ha) and the 'microclimate' (climate at a fine-scale, mm to m, that is distinct from the macroclimate); (2) thermal stability of microclimates (e.g. variation in daily temperatures); and (3) the availability of microclimates to organisms. We compared these metrics in undisturbed primary forest and intensively logged forest on Borneo, using thermal images to capture cool microclimates on the surface of the forest floor, and information from dataloggers placed inside deadwood, tree holes and leaf litter. Although major differences in forest structure remained 9-12 years after repeated selective logging, we found that logging activity had very little effect on thermal buffering, in terms of macroclimate and microclimate temperatures, and the overall availability of microclimates. For 1°C warming in the macroclimate, temperature inside deadwood, tree holes and leaf litter warmed slightly more in primary forest than in logged forest, but the effect amounted to less than 0.1°C difference between forest types. We therefore conclude that selectively logged forests are similar to primary forests in their potential for thermal buffering, and subsequent ability to retain temperature-sensitive species under climate change. Selectively logged forests can play a crucial role in the long-term maintenance of global biodiversity.

4.2 Introduction

Land-use change is a profound threat to Earth's terrestrial biodiversity (Maxwell et al., 2016; Sala et al., 2000). Most of this biodiversity is found in tropical regions (Jenkins et al., 2013), where rates of deforestation and forest degradation are among the highest globally (Hansen et al., 2013). The detrimental impacts of deforestation on tropical biodiversity are well known (Barlow et al., 2016; Gibson et al., 2011); however, tropical forest degradation via commercial selective logging is 20 times more widespread than on-going conversion (Asner et al., 2009; Hansen et al., 2008), making it important to understand the value of these disturbed forests for biodiversity. Selectively logged forests constitute a large and effective refuge for species of conservation concern that cannot survive in deforested land (Edwards et al., 2011; Edwards and Laurance, 2013; Gibson et al., 2011). Protecting selectively logged forests may be a cost effective way to retain tropical biodiversity (Edwards et al., 2014c), but

this is heavily contingent on the assumption that these forests will maintain their current conservation value into the future.

Several factors may influence the value of selectively logged forests for biodiversity in the long-term, and a key consideration is the interaction of multiple drivers of biodiversity loss (Brook et al., 2008; Mantyka-pringle et al., 2012; Sirami et al., 2017). The impacts of climate change are particularly important, and increasingly so as this century progresses (Chou et al., 2013; IPCC, 2013; Sala et al., 2000). Novel (non-analogous) climatic conditions are predicted to appear first in the tropics (Mora et al., 2013), where many species have narrow thermal limits (Deutsch et al., 2008; Khaliq et al., 2014; Tewksbury et al., 2008) and where there is limited dispersal potential owing to poor dispersal ability of many species (Van Houtan et al., 2007). This vulnerability of tropical species is compounded by an absence of target habitats containing analogous climates (Colwell et al., 2008), and widespread deforestation creating a hostile matrix through which dispersal must occur (Brook et al., 2008; Scriven et al., 2015). The ability of tropical species to withstand climate change, and so avoid extinction, is likely to be highly dependent on their ability to adapt *in situ* within existing forest areas. The extent to which species persistence can be facilitated within selectively logged forests will, therefore, greatly influence the conservation value of these habitats.

In primary forests and secondary forests re-growing on abandoned farmland, previous studies found that organisms – particularly ectotherms – avoid suboptimal temperatures in the wider 'macroclimate' (climate at a spatial scale of m to ha) by moving locally into 'microclimates': climate at a fine-scale, mm to m, that is distinct from the macroclimate (González del Pliego et al., 2016; Scheffers et al., 2014a,b). Climate at this fine-scale is more relevant for the majority of terrestrial biodiversity, which primarily consists of small-bodied ectotherms (Potter et al., 2013; Nadeau et al., 2017; Suggitt et al., 2011). Indeed, the vast proportion of terrestrial species are small in size, flat in shape, or thermoregulate via contact with vegetation, and so it is important to consider microclimates close to, and including, the surfaces on which these species live (Kaspari et al., 2015; Scheffers et al., 2017a).

The most informative fine-scale temperature data are derived from point measurements that are highly replicated in both space and time, and demonstrate that loss of vegetation cover causes local daytime warming (Ewers and Banks-Leite, 2013; González del Pliego et al., 2016; Hardwick et al., 2015; Senior et al., 2017). Selective logging affects vegetation by lowering and thinning the canopy, reducing leaf area index (Ewers et al., 2015; Hardwick et al., 2015) and the number of vegetation strata, and creating large forest gaps (Kumar and Shahabuddin, 2005; Okuda et al., 2003). As such, the understorey of logged forests likely receives a greater amount of solar radiation, partitioned increasingly as direct rather than diffuse radiation (Oke, 1987), although these impacts diminish rapidly as selectively logged forests recover (Asner et al., 2004). The most tangible impact on the local climate

could be an overall increase in the day-time temperature of logged forests, increasing the necessity for thermal buffering. Simultaneously, the potential for thermal buffering may be compromised if forest structural changes also influence the temperature and distribution of cool microclimates, particularly if their temperature becomes more similar to that of the wider macroclimate (e.g. Caillon et al., 2014), or there are simply fewer cool microclimates available overall. Conversely, enhanced air-mixing in more open logged forests might create cooler and less variable microclimates. Previous evidence suggests that the availability of cool 'microhabitats' (localised environments within which cool microclimates are contained; González del Pliego et al., 2016; Scheffers et al., 2014a; Shi et al., 2016) can be reduced (e.g. leaf litter; Saner et al., 2009) or increased (e.g. deadwood; Carlson et al., 2017) by selective logging, implying that forest quality alters thermal environments.

A key novel question that we address in this paper is whether vegetation changes following commercial selective logging reduce the potential for thermal buffering. We focused on cool microclimates in the understorey only (climate at mm to m scale that is cooler than the macroclimate and located within ~2 m of the forest floor). Microclimates on the surface of the forest floor were captured by a thermal camera, while dataloggers were used to capture microclimates within cool understorey microhabitats: leaf litter, tree holes and deadwood (González del Pliego et al., 2016; Scheffers et al., 2014a,b). We determined thermal buffering potential according to: (1) the microclimate temperature relative to that of the macroclimate; (2) the daily variation in microclimate temperature; and (3) the availability of microclimates in space. The first two are roughly measures of microclimate 'quality' – they examine how effectively an organism will be buffered from macroclimate warming, assuming it moves into the microclimate. The third captures the likelihood that organisms can locate and move into suitable microclimates, according to the occurrence, distribution and thermal diversity of microclimates within the habitat (Caillon et al., 2014; Sears et al., 2011). We predicted that logged forests would be structurally distinct from primary forest, and we tested the hypothesis that this would lead to reduced thermal buffering potential and, subsequently, impaired ability of temperature-sensitive species to respond *in situ* to excessively high temperatures in the wider macroclimate.

4.3 Methods

4.3.1 Study area

Sampling took place in in an extensive area of contiguous forest in Sabah (Malaysian Borneo; Figure 4.1a). This area represents over 10,000 km^2 of lowland dipterocarp forest, comprising production forest and areas of undisturbed protected forest (Reynolds et al., 2011). In this

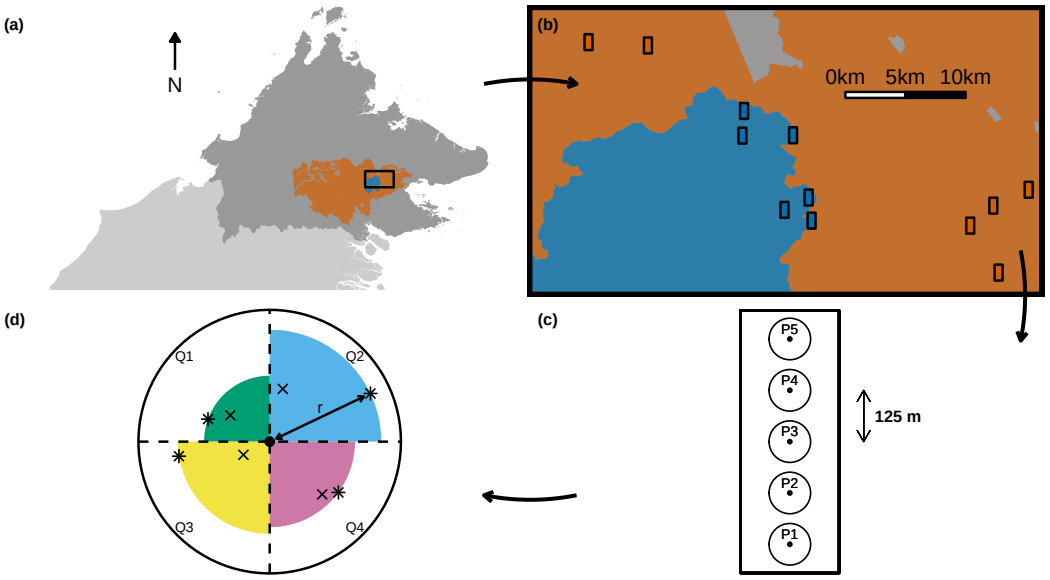

Figure 4.1: Study location in Malaysian Borneo (a), and distribution of sites (b): six sites in primary forest (blue) and six sites in logged forest (orange). Each site comprised five plots along an existing transect, with plot centres separated by 125 m (c). Tree and sapling stand basal area was calculated from the distance to and circumference of the nearest two trees and saplings in each of four quadrants centred on the plot centre (d; see Appendix B.1 for more details). Curved arrows indicate the direction of magnification, from panels a-d.

study, we sampled sites in forest that had been commercially selectively logged twice (Ulu Segama-Malua Forest Reserve, 4°57'42.8"N, 117°56'51.7"E). The area was first logged from 1987-1991, using tractors and high-lead extraction techniques to harvest commercial trees (those in the family Dipterocarpaceae) with stems > 0.6 m diameter at breast height (D.B.H.), and yielding ~113 m^3 of timber per hectare (Edwards et al., 2014b; Fisher et al., 2011). Between 2001 and 2007, the area was re-logged and the minimum harvested tree diameter reduced to > 0.4 m D.B.H., yielding an additional 31 m^3/ha of timber (Fisher et al., 2011). Thus, we sampled sites that had been heavily disturbed about 10 years prior to the study, at which point 67% of the forest had an average density of < 10 trees per hectare with a D.B.H. greater than 40 cm (Reynolds et al., 2011). The area has been recovering naturally since logging operations ceased. Control sites were located in undisturbed, protected primary forest (Danum Valley Conservation Area; 4°57'45.2"N, 117°48'10.4"E).

4.3.2 Sampling design

We sampled twelve sites, six in twice-logged forest and six in primary forest, along existing transects (Figure 4.1b; Edwards et al., 2011, 2014b). Sites were more than 2 km apart, and at least 100 m from forest edges. Within each site, we established five plots 50 m in diameter, with plot centres spaced at 125 m intervals along the transect (Figure 4.1c; 60 plots in

total). Fieldwork was conducted from April to July 2015, during the severe El Niño-Southern Oscillation (ENSO) event of 2015-2016 (NOAA Climate Prediction Center, 2015) when mean daily temperature was 2.26°C higher and mean daily rainfall was 2.09 mm lower than the 5-year average (across April to July for the years 2007 to 2011; data from weather station at Danum Valley Field Centre).

Forest structure

To quantify the level of disturbance to the forest from selective logging, we used an established methodology for assessing forest structure in each plot (Hamer et al., 2003; Lucey and Hill, 2012). The variables we measured were: the stand basal area (m^2/ha) of mature trees (circumference > 0.6 m) and saplings (circumference 0.1-0.6 m), based on the distance to and circumference at breast height of the two nearest trees and saplings in each of four quadrants centred on the plot centre (Figure 4.1d); the coefficient of variation for the basal area of trees and of saplings; the proportion of mature trees that were dipterocarps (indicative of mature, complex forest); percentage canopy cover; and visual estimates of percentage vegetation cover at ground (1.5 m above ground), understorey (15 m above ground) and canopy (the main stratum of leaf cover > 15 m above ground) height. For full methodological details see Appendix B.1.

Quantifying surface microclimates

Fine-scale surface temperature of the forest floor is particularly relevant for small-bodied, surface-dwelling organisms, such as many insect and reptile species. We measured surface temperature within each plot using an infrared camera (FLIR Systems, model E40). Macroclimate temperature was defined as the air temperature at 1.5 m above-ground, measured using a whirling hygrometer. Each site was visited on two days, and each plot within the site was sampled five times each day between 05:00 hrs to 14:30 hrs. During each sample of any given plot, the observer stood at the centre of the plot, took a single hygrometer reading and then, holding the camera at breast height and pointing 45° downwards (relative to the ground), took a photo in four orthogonal directions (Scheffers et al., 2017a). Each thermal image comprised 19,200 distinct observations of surface temperature (one per pixel), and covered a surface area of approximately 1 m^2. In total, we recorded 2,400 thermal images (4 images per plot x 5 repeats x 2 site visits x 60 plots).

For all subsequent analyses, a unique data point comprised thermal information from the four photographs taken each time a plot was sampled: 76,800 observations of surface temperature measurements for each plot (i.e. combining 19,200 observations from the four

photos taken in each orthogonal direction). For details of thermal image data extraction and processing see Appendix B.2. The temperature of cool surface microclimates was defined as the 5th percentile (i.e. coolest) across all 76,800 pixels. For some organisms, the efficacy of thermal buffering also depends on the thermal stability of microclimates (Shi et al., 2016). We calculated daily variation in surface microclimate temperature as the difference between the minimum and maximum microclimate temperature, for each day and for each plot.

To identify spatially-explicit patches of warm and cool pixels (Figure 4.2) we calculated the Getis-Ord local statistic for each pixel within the neighbourhood of the nearest eight pixels, using the function `localG` in the `spdep` package in R (Bivand and Piras, 2015; R Core Team, 2017). Pixels with a Z-value of ≥ 3.886 were defined as being within warm patches, and those with a Z-value of ≤ -3.886 within cool patches (Getis and Ord, 1996). Thermal diversity was defined as the difference between the median temperature of the warmest warm patch minus the median temperature of the coolest cool patch (hereafter: 'patch temperature range'). The average surface area of cool patches was calculated as the total number of pixels within cool patches, multiplied by the surface area of one pixel (0.516 cm^2), and divided by the total number of cool patches across the four photos. Finally, spatial configuration of cool patches was quantified using the Aggregation Index: the number of edges that cool patches share, divided by the maximum number of edges that they could possibly share (Caillon et al., 2014; He et al., 2000). Higher values of the Aggregation Index indicate increased clustering of microclimates in space, which makes them more difficult for organisms to track (Sears et al., 2016).

Quantifying microclimates in leaf litter, tree holes and deadwood

Many ectotherms, such as amphibians, spend some or all of their time exploiting cool microclimates inside microhabitats, which thermal images are unable to capture. We selected three types of microhabitat known to provide cool microclimates (González del Pliego et al., 2016; Scheffers et al., 2014a,b), and placed one temperature datalogger (HOBO pendant datalogger, Onset, model UA-001-64K or model UA-002-64K) per plot in each microhabitat type: deadwood (> 10 cm stem diameter), tree holes (> 2 cm at widest point of entrance hole, < 2 m above the ground) and leaf litter (1.5 m left of the plot centre). The hygrometer measurements of macroclimate temperature were not always synchronised with the dataloggers inside microhabitats, hence we additionally measured macroclimate temperature using a datalogger suspended 1.5 m above the ground at the centre of each plot, shielded against direct radiation and precipitation by an inverted plastic funnel (Scheffers et al., 2014a; Shoo et al., 2010).

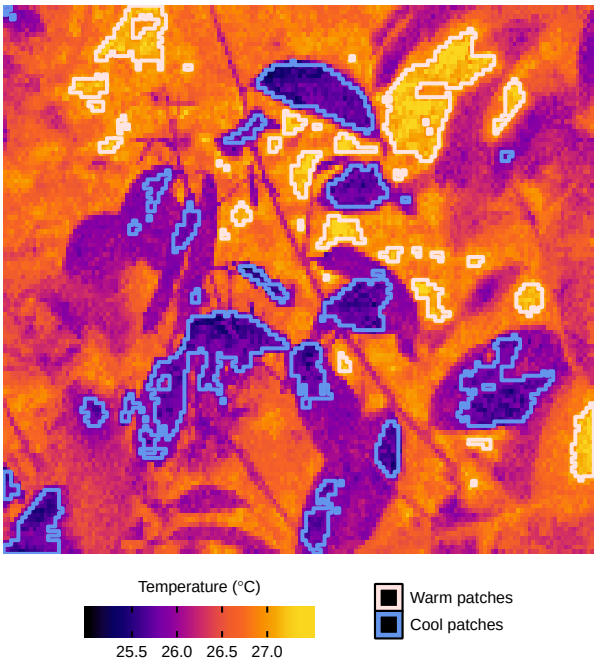

Figure 4.2: Example thermal image. Pixels are shaded from cold (purple) to hot (yellow). Warm patches (outlined in pink) and cool patches (outlined in blue) were identified using the Getis-Ord local statistic of each pixel.

All dataloggers recorded temperature every 20 minutes for six consecutive days, occurring within one week of thermal image collection. For qualitative comparison with thermal images and to lessen the degree of temporal autocorrelation, microclimate temperatures for each of the three microhabitats in each plot were calculated as the median of six daily measures, computed for each two-hour interval during the same time period as when thermal images were collected (i.e. 04:40 to 14:40 hrs). Our analyses focused on day-time thermal buffering, but we also ran analogous models for the full 24 hours to explore night-time thermal buffering (see Appendix B.5). In the main text, we only present data for day-time measurements because this is most relevant to organisms seeking to avoid extremes of heat, and because findings were qualitatively similar. Variation in temperature for microclimates inside microhabitats was defined as the daily range (95^{th} percentile minus 5^{th} percentile) of raw temperatures for each day, in each plot.

To estimate the occurrence of microclimates inside microhabitats, we measured the volume of leaf litter, tree holes and deadwood within a 50 x 5 m subplot centred on each plot centre (60 sub-plots in total), with the long edge running parallel to the transect. For full methodological details see Appendix B.3. We divided microhabitat volume by the total area surveyed to generate microhabitat volume per m^2 forest, for each plot.

4.3.3 Variables analysed

Forest structure

We examined the impact of selective logging on forest structure using linear mixed effects models to compare nine structural response variables between logged and primary forests: stand basal area of trees and of saplings; the coefficient of variation across individual basal areas of trees and of saplings; proportion of trees that were dipterocarps (binomial data: dipterocarp versus non-dipterocarp); percentage canopy cover (proportion data); and percentage vegetation cover at ground, understorey and canopy strata (proportion data). We found that tree stand basal area (m^2/ha) was a good measure of changes in forest structure from logging activity (LR = 8.102, P < 0.01; Figure C.4a; see 'Results' for full details), hence we use this variable as a continuous measure of disturbance (henceforth: forest quality) in all our analyses exploring the thermal buffering potential of logged and unlogged forests.

Macroclimate and microclimate temperature

Macroclimate temperature is the temperature at a relatively coarse spatial scale, and was captured in this study using both a hygrometer and suspended datalogger (measuring the same variable but at different times). The macroclimate does not affect thermal buffering potential *per se*, but it does dictate the overall necessity for thermal buffering. We modelled hygrometer and datalogger temperature separately, including forest type (logged or primary forest) and forest quality as explanatory variables (see Appendix B.4).

To assess the impact of selective logging on the ability of microclimates to buffer organisms from macroclimate warming, we modelled microclimate temperature against forest quality, forest type and macroclimate temperature, including an interaction term between the latter two variables. The slope of the relationship between microclimate and macroclimate temperature is a measure of the rate of change. Surface microclimate temperature refers to the 5^{th} percentile of surface temperature observations (i.e. coolest) for each plot, and this was compared against macroclimate temperature as measured by the hygrometer. Microclimate temperature inside leaf litter, tree holes and deadwood refers to the two-hourly median temperature recorded by dataloggers inside microhabitats, and this was compared against macroclimate temperature as measured by a suspended datalogger.

To capture the impact of logging on the thermal stability of microclimates, we modelled microclimate temperature range against forest type and forest quality. For surface microclimates, the range was the daily range of surface temperature observations (the 5^{th}

percentiles, i.e. coolest surface temperatures). For microclimates inside microhabitats, the range was the daily range (95^{th} percentile minus 5^{th} percentile) of the raw temperature observations. All models were run separately for surface, leaf litter, tree hole and deadwood microclimates.

Microclimate availability

Microclimate occurrence was modelled separately for surface microclimates (i.e. the average surface area of cool patches), and those inside leaf litter, tree holes and deadwood (each quantified by their average volume per m^2 forest). The thermal diversity of surface microclimates was captured by the temperature range between the warmest warm patch and the coolest cool patch. The spatial configuration of surface microclimates refers to the Aggregation Index of cool patches (binomial data: edges shared by cool patches versus edges not shared by cool patches). For all models, the fixed effects were forest type (logged or primary forest) and forest quality (i.e. tree stand basal area).

4.3.4 Statistical analyses

All data were analysed using mixed effects models in R (version 3.3.0; R Core Team, 2017). To account for spatial pseudoreplication, forest structure models included 'site' as a random intercept term, and all other models included 'plot' nested within 'site'. Temperature data were recorded at multiple time points, hence the full models were visually assessed for evidence of temporal autocorrelation of residuals (function `acf` in the `nlme` package; Pinheiro et al., 2017), and a correlation structure for both date and time was incorporated where necessary (the specific structure was chosen using AIC; Zuur, 2009). For binomial data (proportion of dipterocarps and surface microclimate Aggregation Index) we used generalized linear mixed effects models (GLMMs) with a binomial error distribution, fitted using the package `lme4` (Bates et al., 2015) and tested for overdispersion. Diagnostic plots were assessed for all models to confirm model fit and, where necessary, we modified the variance structure of the residuals (Zuur, 2009) and transformed variables to normality. For true proportion data (percentage canopy cover and percentage vegetation cover), the transformation used was a modification of the empirical logit (Warton and Hui, 2011).

For all models, statistical significance was inspected using likelihood ratio tests, dropping each fixed effect in turn and comparing it to the full model (Zuur, 2009). The significance of main effects involved in an interaction was assessed in the same way, except reduced models were compared to a full model without the interaction term. The basic structure for most response variables (RV) was:

```
RV ~ forest_type + forest_quality + (1|transect/plot) + cor(~
date_time|transect/plot)
```

4.4 Results

4.4.1 Changes in forest structure after logging

Following two rounds of commercial selective logging, tree stand basal area – our measure of forest quality – was 23.4 m^2/ha in logged forest, compared to 39.5 m^2/ha in primary forest (LR = 8.102, P < 0.01; Figure C.4a). Logged forests thus contained far fewer large trees than did primary forests. There were also more large saplings in logged forest (9.55 m^2/ha) than in primary forests (6.77 m^2/ha; LR = 4.239, P < 0.05; Figure C.4b), and trees were less variable in size (LR = 13.038, P < 0.001; Figure C.4c). There was no difference between forest types in terms of the variability of size among saplings (LR = 0.114, P = 0.736; Figure C.4d).

Changes to forest structure from selective logging were also evident in the overall amount of vegetation cover. Although there was no observed difference between logged forest and primary forest in percentage vegetation at ground level (LR = 2.758, P = 0.097; Figure C.4g), the proportion of trees that were dipterocarps (χ^2 = 2.42, P = 0.12; Figure C.4e) or the percentage canopy cover (LR = 0.874, P = 0.35; Figure C.4f), we did find that percentage vegetation cover was higher in primary forest than in logged forest in both the understorey (primary = 68.2%; logged = 54.4%; LR = 5.288, P < 0.05; Figure C.4h), and in the canopy (primary = 23.1%; logged = 8.6%; LR = 9.174, P < 0.01; Figure C.4i). Thus, 9-12 years after logging there were significant differences in forest structure between logged and primary forests. This was especially true for the components of forest structure that typically indicate the presence of large, mature trees and high structural complexity, and which might be expected to influence microclimates and the availability of microhabitats.

4.4.2 Macroclimate and microclimate temperature in logged and primary forest

Despite differences in forest structure, we found no difference in macroclimate temperature of logged and primary forests, whether measured by the hygrometer (LR = 0.081, P = 0.776; Figure C.2a) or suspended datalogger (LR = 0, P = 0.983; Figure C.2b). Macroclimate temperature was also consistent across varying levels of forest quality, for temperature measured via the hygrometer (LR = 0.022, P = 0.883; Figure C.2a) and suspended datalogger

(LR = 0.527, P = 0.468; Figure C.2b). Thus, the necessity for thermal buffering was comparable between the two forest types.

Absolute microclimate temperature was comparable between forest types for all of the microclimates considered: surface (LR = 0.447, P = 0.504; Figure 4.3e), deadwood (LR = 0.206, P = 0.65; Figure 4.3f), tree holes (LR = 2.759, P = 0.097; Figure 4.3g) and leaf litter (LR = 1.616, P = 0.204; Figure 4.3h). We found that the relationship between microclimate temperature and macroclimate temperature was slightly steeper in primary forest compared to logged forest for deadwood (LR = 7.268, P < 0.01; Figure 4.3b), tree holes (LR = 13.657, P < 0.001; Figure 4.3c) and leaf litter (LR = 28.914, P < 0.001; Figure 4.3d). However, for 1°C macroclimate warming (from the median value) the maximum difference in microclimate warming between forest types was < 0.1°C, and no such interaction was apparent for surface microclimates (LR = 1.197, P = 0.274; Figure 4.3a). Similarly, for a 1 m^2/ha increase in forest quality (i.e. tree stand basal area), tree hole temperature was slightly warmer (LR = 4.661, P < 0.05; Figure 4.3g), but the size of this effect was negligible (+0.00194°C), and not evident for other microclimates (P > 0.05; Figure 4.3e-h). Thus we conclude that effects of logging on microclimate temperature were generally not evident, or minimal.

The final facet of microclimate temperature that we considered was daily temperature variation. This too was comparable between logged and primary forests for microclimates at the surface (LR = 0.437, P = 0.508; Figure 4.4a), as well as those inside deadwood (LR = 0.02, P = 0.889; Figure 4.4b), tree holes (LR = 3.242, P = 0.072; Figure 4.4c) and leaf litter (LR = 2.449, P = 0.118; Figure 4.4d). Microclimate temperature variation was also consistent across different levels of forest quality (P > 0.05; Figure 4.4).

In summary, selective logging had little observed impact on absolute microclimate temperature or its daily variation. There was some evidence that thermal buffering potential was slightly enhanced for deadwood, tree holes and leaf litter inside logged forest, but the effects were extremely small and not evident for microclimates at the surface.

4.4.3 Microclimate availability in logged and primary forest

The thermal buffering potential within a habitat depends not only on the temperature of microclimates relative to the macroclimate, but also on the overall availability and thermal diversity of those microclimates. The occurrence of surface microclimates was not impacted by forest type (LR = 0.872, P = 0.35; Figure 4.5b), and the average volume of microhabitats (per m^2 forest) was similar in logged and primary forest for deadwood (LR = 0.263, P = 0.608; Figure 4.5d), tree holes (LR = 3.053, P = 0.081; Figure 4.5e) and leaf litter (LR = 0.162, P = 0.687; Figure 4.5f). There was no observed impact of forest quality on the occurrence of

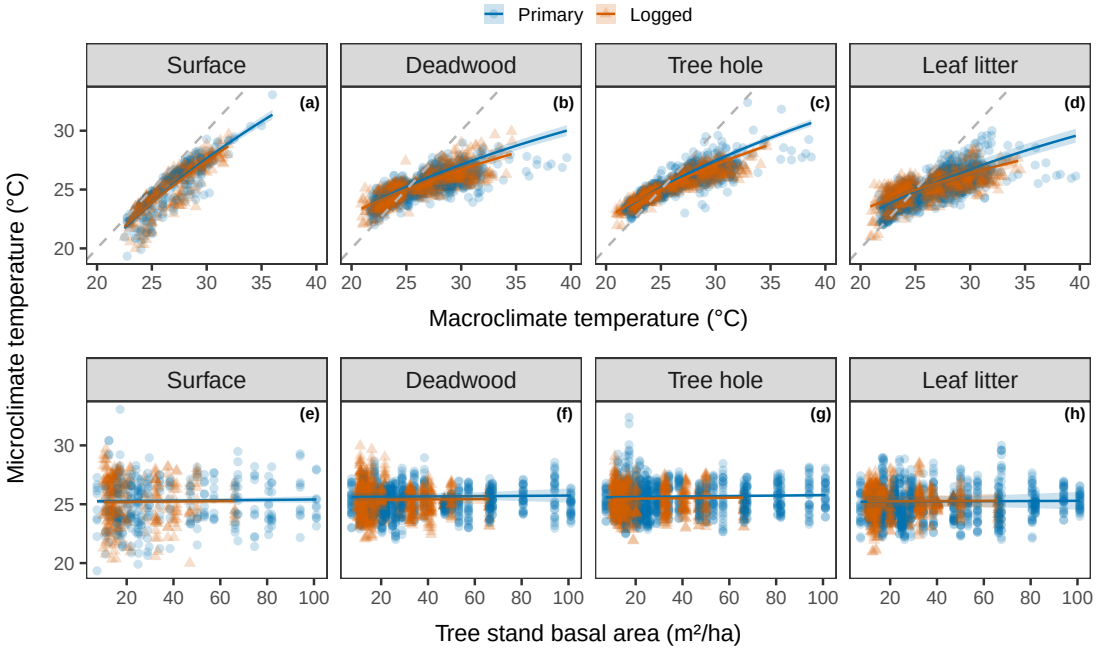

Figure 4.3: Comparison between primary forest (blue) and logged forest (orange) in terms of: (a-d) the relationship between microclimate temperature and macroclimate temperature; and (e-h) absolute microclimate temperature across varying levels of forest quality (measured as tree stand basal area). Microclimates were measured at the surface (a, e), and inside deadwood (b, f), tree holes (c, g) and leaf litter (d, h). The grey dashed lines in panels a-d indicate zero temperature buffering, where the microclimate temperature is equal to the macroclimate temperature. In all panels, shaded bands are 95% confidence intervals.

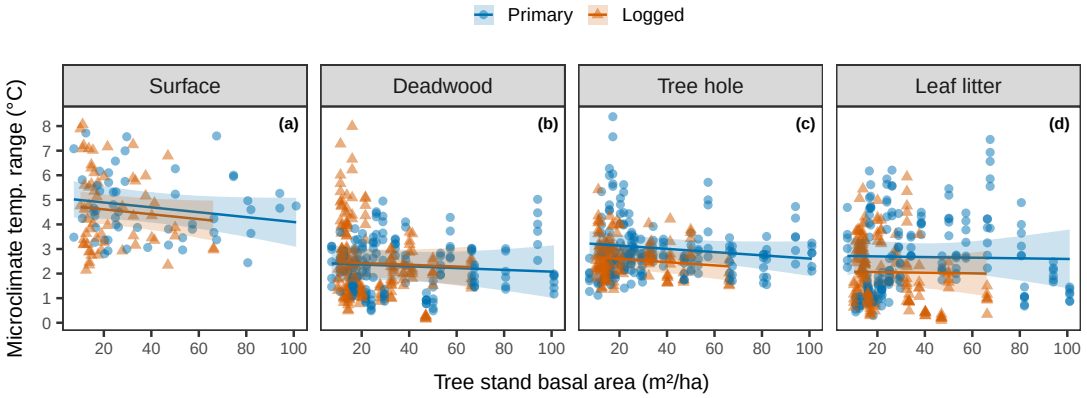

Figure 4.4: The influence of forest type (primary or logged) and forest quality (measured as tree stand basal area) on microclimate temperature range. Daily range for surface microclimates (a) was calculated as the difference between the maximum and the minimum microclimate temperature (itself calculated as the 5th percentile temperature across four photos taken at each visit to each plot). For microclimates inside deadwood (b), tree holes (c) and leaf litter (d), the daily range was the difference between the 95th percentile and 5th percentile of raw temperature measurements. Primary forest data points are depicted as blue circles and logged forest as orange triangles. Shaded bands represent 95% confidence intervals.

surface microclimates (LR = 1.324, P = 0.25; Figure 4.5b) or the volume of deadwood (LR = 3.78, P = 0.052; Figure 4.5d) and tree holes (LR = 2.172, P = 0.141; Figure 4.5e). In contrast, we found that leaf litter volume increased by 12.3 cm^3/m^2 for a 1 m^2/ha increase in forest quality (i.e. tree stand basal area; LR = 7.056, P < 0.01; Figure 4.5f).

Using thermal images we were able to quantify the thermal diversity and spatial configuration of surface microclimates. Thermal diversity has a bearing on the diversity of organisms that are able to find microclimates meeting their thermal requirements (which vary according to species, age, time of day, seasonality, etc.). Spatial configuration influences the ease with which organisms can utilise microclimates. We found that the temperature range spanned by surface microclimates (both warm and cool patches) was comparable between logged and primary forests (LR = 0.276, P = 0.599; Figure 4.5a) and with varying forest quality (LR = 3.552, P = 0.059; Figure 4.5a). The same was true for the Aggregation Index of cool surface patches, both between logged and primary forest (χ^2 = 0.312, P = 0.576; Figure 4.5c) and with different levels of forest quality (χ^2 = 0.183, P = 0.669; Figure 4.5c).

Overall, the availability of microclimates was minimally affected by selective logging, regardless of whether microclimates were located at the surface or inside microhabitats. This was true for various different components of microclimate availability, including their occurrence, thermal diversity and spatial configuration.

4.5 Discussion

Forest degradation by commercial selective logging affects huge expanses of the tropics (Asner et al., 2009; Lewis et al., 2015). Southeast Asia has experienced the most intensive selective logging of all tropical rainforests (Lewis et al., 2015), and in our study area ~145 m^3 of timber was removed per hectare. Despite these forests having only a maximum of 12 years post-logging recovery (Fisher et al., 2011), and the coincidental occurrence during data collection of abnormally hot and dry conditions associated with the strongest El Niño-Southern Oscillation (ENSO) event since 1998 (NOAA Climate Prediction Center, 2015), we found very few thermal differences associated with selective logging. This is an important finding for tropical conservation because it suggests that the potential for thermal buffering will not limit the ability of selectively logged forests to maintain high biodiversity under climate change.

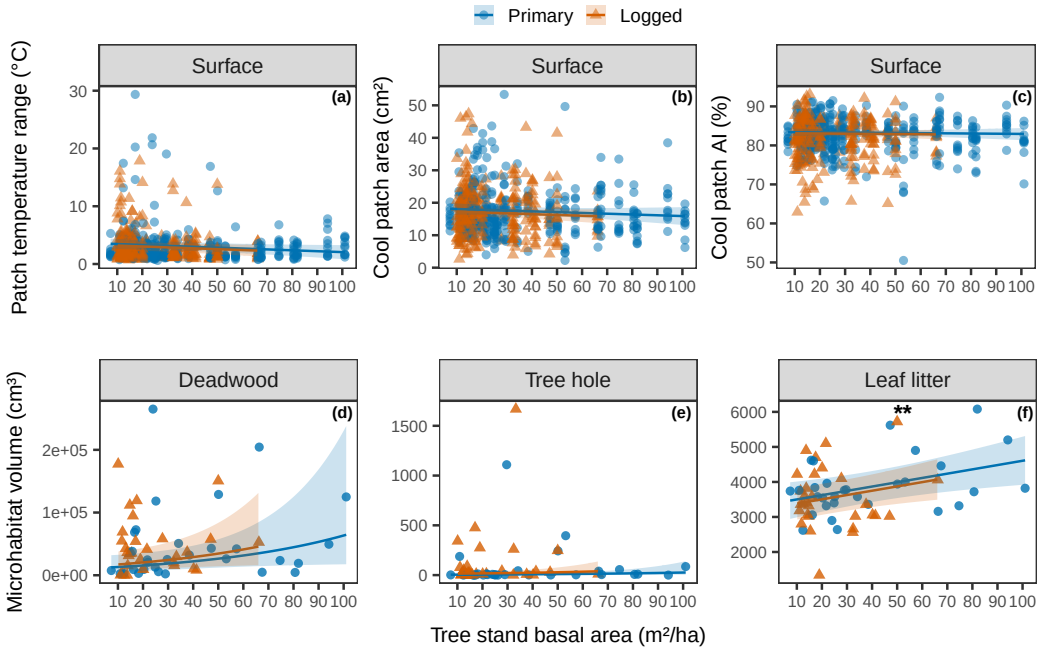

Figure 4.5: The influence of forest type (primary or logged forest) and forest quality (measured as tree stand basal area) on microclimate availability. Results for surface microclimates (top row) include: the temperature range from the warmest warm patch to the coolest cool patch (a); the average surface area of cool patches (b); and the Aggregation Index of cool patches (c). The volume (per m^2 forest) of microhabitats typically associated with microclimates (bottom row) is shown for deadwood (d), tree holes (e) and leaf litter (f). Primary forest data points are depicted as blue circles and logged forest as orange triangles. Shaded bands represent 95% confidence intervals. Asterisks in panel f denote a statistically significant difference at $0.001 < P < 0.01$ (**).

4.5.1 Forest structure

At a local scale (m to ha), climate is highly dependent upon vegetation (Oke, 1987; Sears et al., 2011). Selective logging operations generally target larger and older trees, leading to many associated changes in vegetation structure (Edwards et al., 2014c; Kumar and Shahabuddin, 2005; Okuda et al., 2003). A clear signal of historical logging in our study area was a reduction in stand basal area of mature trees by 40.8% (Figure C.4a; Berry et al., 2008), accompanied by reduced variation in tree basal area (Figure C.4c), and reduced vegetation cover at ≥ 15 m height (Figure C.4h,i). The increase in stand basal area of saplings by 41.1% (Figure C.4b) is evidence that there has been substantial natural regeneration in the intervening years.

4.5.2 Macroclimate and microclimate temperature

Although primary forest contained more large trees (Figure C.4a), the absence of any long-term effect of selective logging on percentage canopy cover (Figure C.4f) suggests that forest vegetation as a whole – regardless of how it was distributed vertically – intercepted comparable amounts of incoming solar radiation in both logged and primary forests. This finding is in keeping with previous studies observing rapid horizontal canopy growth following selective logging (e.g. Asner et al., 2004). Alternatively, vegetation in logged forest may have intercepted less incoming radiation than in primary forest (i.e. if there was less vegetation overall), but reflected a greater proportion of what was intercepted, owing to the higher albedo of habitats with an abundance of non-tree species (Davin and de Noblet-Ducoudré, 2010; Edwards et al., 2014c; Oke, 1987). In either case (or in combination), given comparable levels of solar radiation reaching the forest floor of logged and primary forests, it follows that the temperature at coarse and fine scales (macroclimate and microclimate temperatures) should also be comparable (Figure 4.3 and Figure C.2).

The temperature of cool microclimates relative to average conditions is what largely determines their ability to buffer macroclimate warming (González del Pliego et al., 2016; Scheffers et al., 2014a; Shi et al., 2016). Given that selective logging did not affect absolute temperature of the macroclimate (Figure C.2) or microclimates (Figure 4.3), we can infer that there was no overall effect of selective logging on the difference between micro- and macroclimate temperature. There was also no evidence that selective logging impacted overall daily variation in microclimate temperature (Figure 4.4). There were some impacts of logging on the relationship between microclimate and macroclimate temperature for microclimates inside deadwood, tree holes and leaf litter (Figure 4.3), but the effect sizes for these interactions were extremely small. The maximum difference in microclimate warming between logged and primary forests was < 0.1°C for 1°C of macroclimate warming. As such,

we conclude that even when selective logging had a statistically significant influence on thermal buffering potential, the effect was small and of limited biological relevance.

4.5.3 Microclimate availability

Even if microclimates are present and effective at buffering temperature change, overall rarity or isolation could render them functionally redundant to some species (Sears et al., 2011, 2016). We demonstrate that lower forest quality was associated with less leaf litter (Figure 4.5; cf. Saner et al., 2009), but forest quality and forest type had little effect on the occurrence of microclimates at the surface or inside deadwood and tree holes. This is contrary to expectations from previous studies (Ball et al., 1999; Blakely and Didham, 2008). However, high volumes of deadwood could be maintained in logged forest by lower decomposition rates (Ewers et al., 2015; Yeong et al., 2016; but see Hérault et al., 2010), and large remnant pieces from harvest operations. In undisturbed forests, tree holes tend to be associated with larger, older trees (Blakely and Didham, 2008; Lindenmayer et al., 2000). A comparable quantity of tree holes might be found in logged forests because of damage from logging operations (Edwards et al., 2014c), increased wind in gaps (Chen et al., 1995) and remnant large trees that were specifically avoided by logging companies because of hollow boles. Additionally, we assessed tree holes in the understorey only, and differences may well manifest at higher forest strata.

The availability of microclimates to organisms is also influenced by their thermal diversity and distribution in space. We found that patches of warm and cool microclimates on the surface of the forest floor spanned a temperature range of about 3°C, regardless of logging activity (Figure 4.5a). Cool patches were generally highly clustered in space (Aggregation Index of 83.3%), but this was not affected by logging (Figure 4.5c). Thermal diversity and spatial configuration of microclimates are relatively novel facets of thermal buffering potential (but see: Caillon et al., 2014; Faye et al., 2016; Sears et al., 2016); they are likely determined by the composition of the forest floor and the relative radiative properties of these different components (e.g. bare soil versus leaves versus water; Oke, 1987; Snyder et al., 2004). We therefore suggest that these characteristics of the forest floor were comparable between forests despite the large differences in forest structure that were evident after logging.

4.5.4 Caveats and future research directions

The potential for thermal buffering and its general necessity are influenced by moisture levels, as well as temperature (McLaughlin et al., 2017). Many ectotherms, including amphibians (Duellman and Trueb, 1986) and isopods (Hassall et al., 2010), can survive in

hot temperatures for longer if relative humidity is sufficiently high to prevent desiccation. Although we did not measure fine-scale vapour pressure deficit (a variable combining both temperature and relative humidity), we did find that coarse-scale vapour pressure deficit measurements from the hygrometer and from hygrochron iButtons (Appendix B.4) showed little variation within or between forests (Figure C.2).

Relative climates in primary and logged forests could be very different above the understorey, which we were unable to capture in our study. Some ectotherms move down from the upper strata to exploit more favourable temperatures lower down (Scheffers et al., 2013). Hence, if temperatures in higher strata are in fact hotter in logged forest compared to primary forest, it is possible that species could move to utilise the favourable temperatures of the understorey of logged forest that we demonstrate here, potentially resulting in a 'flattening' of species' vertical distributions.

While thermal cameras are an important addition to the toolbox of microclimate research (Faye et al., 2016), it is also important to remember that they are just one element. Thermal cameras are well-suited to capturing temperature at a very fine-scale and with inherent spatial information, but differences in 3D topography of a surface could affect results (e.g. the real distance between neighbouring pixels can be more than is apparent in the 2D image). Additionally, although thermal cameras are ideal for measuring surface temperatures, they have a limited capacity to capture sub-surface temperatures, and hence we have used thermal imagery in combination with dataloggers.

The ability of selectively logged tropical forests to retain current levels of biodiversity will critically depend on their ability to protect species from the impacts of increasingly severe climate change. As average temperatures increase over this century, so too will the intensity and frequency of extreme climatic events. Thermal buffering will likely be crucial in allowing species to move locally to avoid suboptimal climates. We sampled in some of the most intensively logged forest in the tropics, during abnormally hot and dry conditions of a severe ENSO event; it is highly unlikely that our study would have failed to detect any appreciable thermal differences between primary and logged forests had they existed. Regardless of whether commercially selectively logged forests remain biologically or structurally distinctive from undisturbed forests, this study shows for the first time that they are functionally equivalent in the provisioning of cool microclimates, and underscores their vital role in conservation both now and under future climate warming.

4.6 Data availability

Data available from the University of Sheffield Online Research Data repository (https://doi.org/10.15131/shef.data.5414629).

4.7 Acknowledgements

Thanks to staff at Danum Valley Field Centre for logistical support; and Azlin Bin Sailim, Jessica Olid and Chloe Walker-Trivett for field assistance. R.A.S. was funded by a NERC studentship through the ACCE (Adapting to the Challenges of a Changing Environment) Doctoral Training Partnership (Grant No. NE/L002450/1).

Chapter 5

Global loss of climate connectivity in tropical forests

Mixed use tropical landscape in Bali.

This chapter is currently in preparation for submission to *Nature* as:

Senior RA, Hill JK, Edwards DP. Global loss of climate connectivity in tropical forests.

5.1 Abstract

Range shifts are a crucial mechanism enabling species to avoid extinction under climate change (Chen et al., 2011; Parmesan, 2006). The majority of terrestrial biodiversity is concentrated in the tropics (Jenkins et al., 2013), including species considered most vulnerable to climate warming (Tewksbury et al., 2008), but extensive and ongoing deforestation of tropical forests is likely to impede range shifts (McGuire et al., 2016; Taubert et al., 2018). We conduct the first global assessment of the potential for tropical species to reach analogous future climates – so-called 'climate connectivity' – and empirically test how this has changed in response to deforestation between 2000 and 2012. We find that over 62% of tropical forest (~7M km^2) is already incapable of facilitating range shifts to analogous future climates. In just 12 years over 27% of tropical forest experienced a loss of climate connectivity, with non-linear declines in connectivity as forest loss increased. On average, if species' ranges shift as far down climate gradients as permitted by existing forest connectivity, by 2070 organisms would still experience 0.69°C of warming under the least severe climate warming scenario, up to 2.5°C warming for the most severe scenario. Limiting further forest loss and focusing the global restoration agenda towards creating climate corridors are global priorities for improving resilience of tropical forests under climate change.

5.2 Main text

Globally, in paleoecological records and under modern climate change, species have moved polewards or upwards to avoid extinction under climate warming (Chen et al., 2011; Parmesan, 2006). Land-use change increasingly impedes range shifts by fragmenting natural habitat (Tucker et al., 2018). This is of particular concern in the tropics, where most remaining terrestrial biodiversity is harboured (Jenkins et al., 2013) and where most new agricultural land will be sourced (Lewis et al., 2015). Additionally, the tropics will experience the earliest appearance of novel climatic conditions (Mora et al., 2013), for which many tropical species will be unequipped because of their narrow thermal limits (Tewksbury et al., 2008) and limited dispersal relative to rates of climate change (Loarie et al., 2009; Opdam and Wascher, 2004).

The potential for species to shift their range in response to climate change depends both on the future availability of suitable habitat with an analogous climate, and the connectivity between that habitat and the species' current distribution (Littlefield et al., 2017). Many studies have addressed these factors individually, but few have integrated them to quantify the connectedness of natural areas to future climate analogues – hereafter: 'climate

connectivity' (Nuñez et al., 2013). Of those that do (Lawler et al., 2013; Littlefield et al., 2017; McGuire et al., 2016), none have applied the approach pantropically or considered how climate connectivity has changed over time.

Here we combine a high-resolution forest cover layer (Hansen et al., 2013) with current and projected future Mean Annual Temperature (Hijmans et al., 2005) (hereafter: temperature), to quantify across the tropics: (1) the potential for species to reach analogous future climate within existing forest cover, and (2) the change in this measure of climate connectivity from 2000 to 2012. Climate connectivity was calculated based on the method of McGuire et al. (2016), whereby natural land cover – here defined as cells with more than 50% forest cover (Hansen et al., 2013) – was partitioned into patches based on current temperature (~1950-2000; WorldClim v1.4), and each forest patch traced to the coolest patch that could be reached by traversing a gradient of hotter to cooler adjacent patches. All patches were then assigned mean future temperature for the year 2070 (average for 2061-2080), derived from the HadGEM2-AO general circulation model (IPCC, 2013) and Representative Concentration Pathway (RCP) 8.5, which is the most severe ('business-as-usual') IPCC scenario. To capture the extent to which forest cover enables species to reach a place that, under future climate warming, is the same as or cooler than their current location, climate connectivity was calculated as the current temperature of each patch minus the future temperature of its designated destination patch. Negative values indicate that the coolest reachable forest is still warmer under climate change than the current temperature, and inhabitant organisms would fail to reach an analogous climate under projected warming.

We found that, on average, if tropical species were only limited by climate connectivity and their range shifted as far along temperature gradients as permitted by current forest cover, they would still experience 2.5°C of warming under projected future climate change (median value across all realms; Figure 5.1a). By comparison, average warming without any movement would be 4°C. The average climate connectivity of discrete land masses varied by biogeographic realm ($F = 76.9$, $P < 0.001$; Figure 5.2a) with the Neotropics and Afrotropics the least well connected, resulting in unavoidable warming of -2.8°C and -2.7°C, respectively. Range-shifting species in Indomalaya, Australasia and Oceania would also fail to reach analogous temperatures, experiencing warming of -2.5, -2.3 and -2°C, respectively. This suggests that the average tropical forest, for any given realm, is not sufficiently connected along a temperature gradient to enable species to avoid climate change by shifting their distribution.

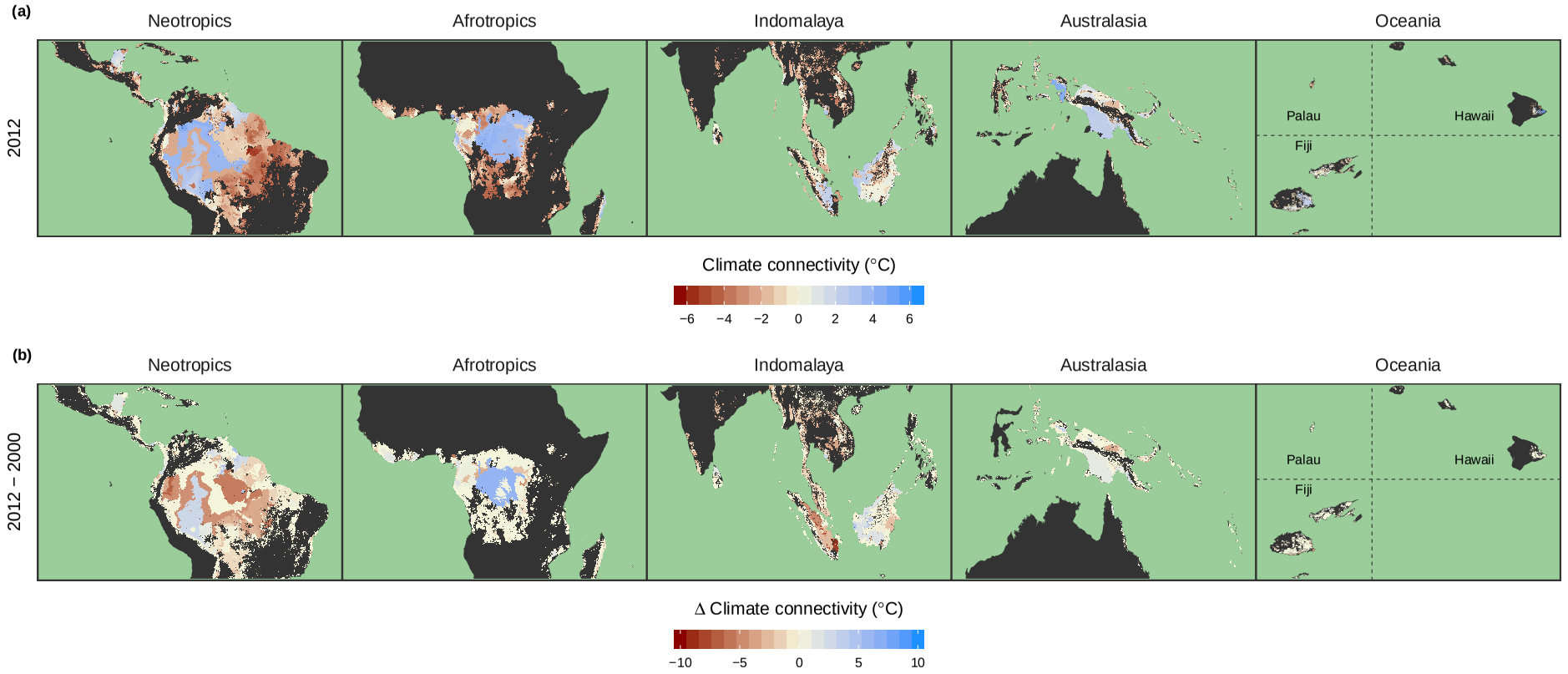

Figure 5.1: Climate connectivity in 2012 (a) and change in climate connectivity from 2000 to 2012 (b). Positive values (blue) indicate successful climate connectivity in panel (a), or a gain of connectivity in panel (b). Negative values (red) indicate unsuccessful climate connectivity in panel (a), or a loss of connectivity in panel (b). To aid visualisation we have shifted land masses in Oceania.

Overall, 62.2% of tropical forest area failed to achieve successful climate connectivity (≥ 0; median value across realms), whereby species' range shifts within existing forest cover could circumvent climate warming. This is comparable to the 59% observed in the continental United States by McGuire et al. (2016), and is all the more concerning because of the greater numbers of climate-vulnerable species with narrow thermal limits. Variation across biogeographic realms ($F = 120$, $P < 0.001$; Figure 5.2b) showed slightly different patterns than for average climate connectivity. Indomalaya was the least successful realm with 71.2% of its forested area failing to connect to climate analogues, followed by the Neotropics (66.9%), Oceania (62.2%), Afrotropics (62%), and Australasia (42.3%). As found in previous studies (Lawler et al., 2013; Littlefield et al., 2017), regions with large, contiguous forest patches connecting warmer lowland regions to cool uplands, such as the western Amazon, Congo Basin and parts of New Guinea (Figure 5.1a), can compensate somewhat for low average climate connectivity. That said, in these locations the total path distance from source to target patch was often substantial – up to 2,820 km for one source patch in the Neotropics – and this does not account for biogeographic barriers, such as major rivers. Climate connectivity was consistently low for regions with severe and extensive loss of lowland rainforests, such as Indochina, Brazilian Atlantic forest and West Africa (Haddad et al., 2015; Lewis et al., 2015).

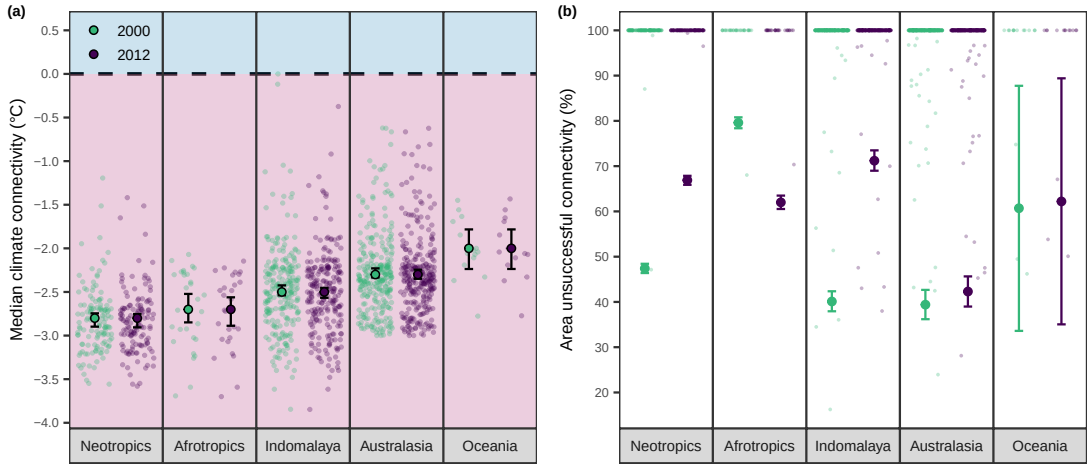

Figure 5.2: Climate connectivity of land masses in different biogeographic realms in the year 2000 (green) and 2012 (purple). Panel (a) shows results for median climate connectivity, with the dashed line indicating zero climate connectivity, at and above which successful climate connectivity is achieved. Panel (b) shows results for the proportion of total forested area that fails to achieve successful climate connectivity. Solid points are model-predicted values with 95% confidence intervals. Raw data are plotted in the background as semi-transparent points.

In only 12 years, change in climate connectivity was widespread – 26.6% of cells forested in 2000 or 2012 (~3M km^2) experienced loss of climate connectivity, compared to 10% of cells that experienced gains (Figure 5.1b). While average climate connectivity did not

differ between years ($F = 0.623$, $P = 0.43$; Figure 5.2a), the proportion of forested area that was unsuccessfully connected increased overall from 2000 to 2012 ($F = 193$, $P < 0.001$; Figure 5.2b), with variation between realms ($F = 256$, $P < 0.001$; Figure 5.2b). The biggest losses of climate connectivity were seen in Indomalaya (-31.1%), followed by the Neotropics (-19.5%), Australasia (-2.9%), and Oceania (-1.5%). Conversely, there was a considerable gain of connected forest area in the Afrotropical realm (+17.6%), likely driven by apparent tree cover gain in the central Congo basin (Hansen et al., 2013).

Loss of climate connectivity from 2000 to 2012 increased non-linearly with increasing area of forest loss ($F = 992$, $P < 0.001$; Figure 5.3). Notably, the proportion of tropical forest area losing climate connectivity appeared to increase rapidly beyond 1,000 km^2 of deforestation within a given land mass. The effect was clearest in Indomalaya and the Neotropics (Figure 5.3), probably because of the greater number of land masses experiencing such high levels of forest loss. A comparable effect is seen in the number and size of forest fragments created by forest loss (Taubert et al., 2018). We suggest that relatively low levels of forest loss reduce redundancy by removing links to future climate analogues, until a critical point is reached beyond which additional forest loss severs all links and climate connectivity falls below zero. Disproportionate benefits could come from reinstating these connections – particularly along elevational gradients (cf. Elsen et al., 2018) – through forest restoration initiatives such as the Bonn Challenge, which aims to restore 3.5 million km^2 by 2030. Habitat corridors are not appropriate for all taxa and locations (Early and Sax, 2011; Lees and Peres, 2008), but are likely to be of particular value in the locations where poor climate connectivity (Figure 5.1a) or high connectivity loss (Figure 5.1b) coincide with high species' vulnerability to climate change (Figure D.10; Pacifici et al., 2018) or high levels of endemism (Figure D.11).

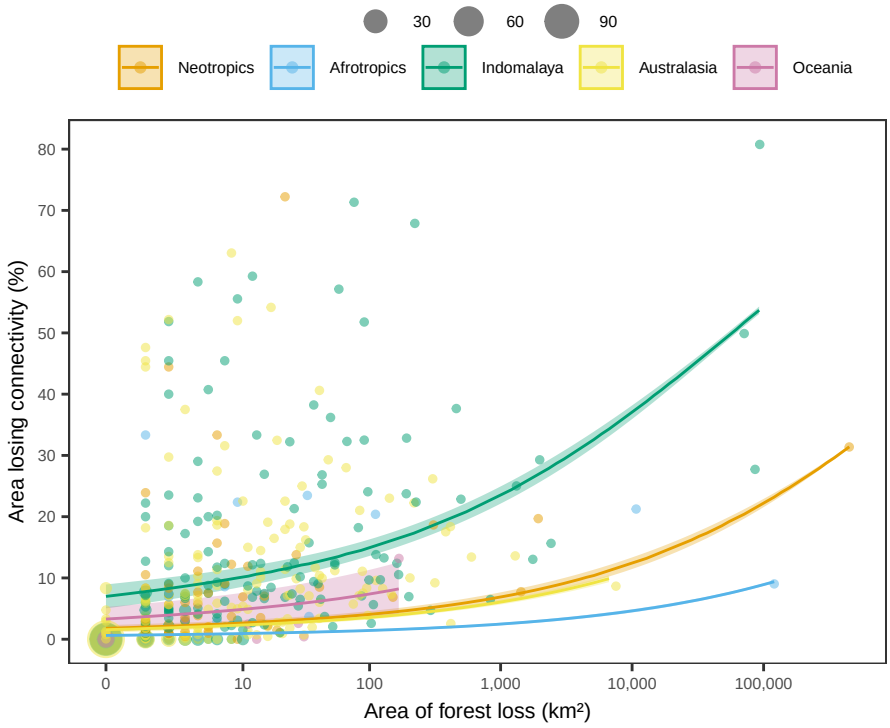

Figure 5.3: The proportion of total forested area in each land mass that lost climate connectivity between 2000 and 2012. Connectivity loss (% area) is plotted against increasing area of forest loss (log scale) and across different biogeographic realms (orange = Neotropics, blue = Afrotropics, green = Indomalaya, yellow = Australasia and pink = Oceania). Points correspond to raw data, with point size indicating the number of observations at that location. Fitted lines derive from model predictions with 95% confidence intervals.

The climate connectivity metric used here is a measure of the physical potential for thermally restricted groups of species to track climate through near-contiguous forest cover (cf. McGuire et al., 2016). We focus on broad trends and patterns across the Earth's most biodiverse terrestrial region, which requires assumptions and simplifications that inevitably render our results less applicable at finer spatial scales and for particular species (Brito-Morales et al., 2018). We do not incorporate any species-specific information, but note that other factors will affect both the need and capacity for species to shift their ranges, such as *in situ* adaptation (Hannah et al., 2014; Parmesan, 2006; Socolar et al., 2017) and dispersal limits (Schloss et al., 2012). We assumed that forest patches of 10 km^2 and above would be sufficiently large to facilitate species range shifts, but in reality minimum patch size will depend on the species of interest. Repeating our analyses with minimum patch sizes of 1, 5, 25 and 100 km^2 revealed qualitatively similar results (Appendix D.1).

Our estimates of climate connectivity are conservative because the forest cover layer does not distinguish between natural forest and tree plantations (Hansen et al., 2013). A precautionary reanalysis excluding tree plantations for the seven countries where plantation boundaries were available (Brazil, Cambodia, Colombia, Indonesia, Liberia, Malaysia, and

Peru) produced very similar results, except that from 2000 to 2012 the percentage of forest failing to connect to analogous climates decreased by 2.9% when including plantations, compared to an increase of 8.6% if they were excluded (see Appendix D.2). We do not use sub-canopy temperature nor account for forest quality, but note that thermal buffering by forest canopy varies little between pristine and degraded forests (Senior et al., 2018). Relative temperature change in the understorey, and thus our broad conclusions, should therefore be consistent across forests of different quality.

We focus on the most severe climate warming scenario (RCP8.5), which appears the most likely outcome (Sanford et al., 2014). Repeating our analysis for the least severe scenario (RCP2.6) resulted in similar overall trends, although we found that the proportion of successfully connected forest was enhanced and the loss of climate connectivity alleviated under this scenario (Appendix D.3). Other climate variables – particularly temperature extremes and precipitation – are important in determining the climatic niche of any given species. Unfortunately, projections of future precipitation under climate change remain highly uncertain (Corlett, 2012; IPCC, 2013) and are highly variable in space, both of which make it difficult to determine the gradient that species would have to follow to avoid deleterious changes in precipitation.

Our study is the first to quantify climate connectivity pantropically and over time. Loss of forest cover is extensive in the tropics (Hansen et al., 2013; Lewis et al., 2015) and causes widespread and accelerating fragmentation of remaining habitat (Taubert et al., 2018). Simultaneously, climate change poses an increasing risk to thermally-restricted forest specialists (Tewksbury et al., 2008); the ability of these species to track climate will be important in determining their risk of extinction under climate change. We found that, across most of the tropics, current forest cover is already insufficient to facilitate range shifts to future climate analogues. Furthermore, the relationship between loss of forest cover and loss of climate connectivity is such that the problem is likely to magnify as forest loss continues. Landscape planning for climate resilience should endeavour to limit the extent of forest loss to protect existing forest cover, via land-sparing approaches and carbon-based payments for ecosystem services. Where opportunities arise to protect or restore forest, such as through the global landscape restoration agenda, disproportionate gains may come from focusing on connecting forest along climate gradients (Elsen et al., 2018).

5.3 Methods

We focused our study pantropically, including all land masses located between ±23.4° latitude. For those land masses with a true extent beyond the tropics, boundaries were

buffered by 100 km to reduce artificial truncation of climate gradients (cf. McGuire et al., 2016). Maps were analysed at 1-km resolution projected into the World Cylindrical Equal Area projection. All spatial layers were processed with Python code implemented using the arcpy module in ArcMap version 10.4.1 (ESRI, 2011).

5.3.1 Climate-partitioned forest patches

Since we were interested in climate connectivity for species inhabiting tropical forests, we calculated climate connectivity based on movement along a temperature gradient within forested areas only. We defined cells as forest or non-forest using tree cover data from Hansen et al. (2013). For the year 2000, cells were defined as forested if they had > 50% tree cover (Hansen et al., 2013). Results are conservative because the Hansen et al. (2013) dataset does not differentiate between natural forest and tree plantations, but see Appendix D.2 for analyses excluding cells within tree plantations for those countries where plantation boundaries were available (Brazil, Cambodia, Colombia, Indonesia, Liberia, Malaysia, and Peru). For the year 2012, cells were classified based on forest loss and forest gain (Hansen et al., 2013) relative to forest cover in 2000. If a cell had experienced forest loss from 2000 to 2012, it had gone from a forested to non-forested state and the cell was classed as non-forest in 2012. Conversely, if a cell had experienced forest gain from 2000 to 2012, it had gone from a non-forested to a forested state; providing there had been no concomitant loss, the cell was classed as forest in 2012.

We partitioned forest patches using a present-day (~1950-2000), 30-arc-second global layer for Mean Annual Temperature (hereafter: temperature) from the WorldClim database (Version 1.4; Hijmans et al., 2005; McGuire et al., 2016), re-sampled to 1 km^2. The same approach was applied separately to forest cover in 2000 and 2012: temperature values were assigned to forested cells and reclassified to increments of 0.5°C (ranging from -18 to 32°C), based on evidence that tropical species are sensitive to this degree of temperature difference (e.g. Freeman and Class Freeman, 2014; Raxworthy et al., 2008). The resulting raster was converted to polygons, whereby neighbouring forest cells with the same reclassified temperature value were assigned to the same polygon (hereafter: forest patch). While our approach is not specific to any particular taxon, it may be helpful to consider the method in the context of range shifts by non-volant terrestrial animals (cf. Nuñez et al., 2013). We removed forest patches < 10 km^2, based on the assumption that they could not support a population for long enough to enable range shifts. See Appendix D.1 for the implications of varying minimum patch size. Patches within 2 km of each other were assigned to the same patch, conservatively assuming that populations could move across 2 km of non-forest to reach suitable habitat (cf. McGuire et al., 2016).

5.3.2 Climate connectivity

The logic behind the measure of climate connectivity in McGuire et al. (2016) is that it represents the maximum temperature differential between current and future conditions that can be achieved by traversing a gradient from hotter to cooler patches within existing natural habitat. We assigned mean current and future temperature to all forest patches, again using data from WorldClim. Future temperature was for the year 2070 (average for 2061-2080), derived from the HadGEM2-AO general circulation model (IPCC, 2013) and Representative Concentration Pathway (RCP) 8.5, which is the most severe ('business-as-usual') IPCC scenario. See Appendix D.3 for a re-analysis using RCP2.6, the least severe IPCC scenario.

To trace each forest patch to its final destination, we identified which patches were neighbours, and iterated over all unique temperatures from cooler to hotter, each time identifying the patch corresponding to that temperature and the identity of its coolest neighbour. For patches with no cooler neighbours, the final destination patch was assigned as itself. For all other patches, the destination was assigned as the final destination of its coolest immediate neighbour. This algorithm ensures that the coolest destinations are passed on with each iteration, enabling destination patches to extend beyond immediate neighbours. See Appendix D.4 for a full worked example (McGuire et al., 2016).

Once each origin patch has a designated final destination patch, climate connectivity is calculated as the temperature difference between them. The key question is whether forest cover is sufficient for organisms to reach a place that, under future climate warming, is the same as or cooler than their current location. Thus, climate connectivity is the current temperature of the origin patch minus the future temperature of the destination patch. Where this value is zero or positive, the patch has achieved successful climate connectivity: there is sufficient structural connectivity between forested areas for organisms to reach forest that is same as or cooler than the temperatures they currently experience. Negative values indicate that the coolest reachable forest is still warmer under climate change than the current temperature, and inhabitant organisms would fail to reach an analogous climate under projected warming.

5.3.3 Statistical analyses

All data were analysed in R (version 3.5.0; R Core Team, 2018). The specific variables included are detailed below. For all models, statistical significance was inspected by dropping each fixed effect in turn and comparing to the full model (Zuur, 2009). The significance of main effects involved in an interaction was assessed in the same way, except reduced models were

compared to a full model without the interaction term.

5.3.3.1 Current state of climate connectivity

Climate connectivity was necessarily calculated at a patch-level, but because patches themselves were not constant through time our spatial unit of replication was land mass. There were 697 land masses in total, comprising whole islands, such as Borneo and Madagascar, as well as sections of continents clipped to the extent of the tropics, such as for Africa and Australia. To assess current status we calculated median climate connectivity for each land mass, as well as the proportion of the total area of forested patches that failed to achieve successful climate connectivity (i.e. climate connectivity < 0).

Median climate connectivity (range = -3.8-0°C; n = 697) and percentage area of unsuccessful connectivity (range = 16-100%; n = 697) were modelled against year (categorical: 2000 or 2012) and biogeographic realm (categorical: Neotropics, Afrotropics, Indomalaya, Australasia, and Oceania), with an interaction between them, fit using the `lme4` package (Bates et al., 2015). Median climate connectivity was modelled using a linear model. Area of successful connectivity was modelled as a binary variable (sum patch area with climate connectivity < 0 versus sum patch area with climate connectivity ≥ 0), using a Generalized Linear Model (GLM) with a quasibinomial error distribution to account for overdispersion. For both response variables, model comparisons were performed using F tests.

5.3.3.2 Change in climate connectivity

Change of climate connectivity from 2000 to 2012 was first calculated at the level of the grid cell. For both years, we created a binary raster of climate connectivity, where cells were either successful (climate connectivity ≥ 0) or unsuccessful (climate connectivity < 0). Change was then calculated as climate connectivity in 2012 minus climate connectivity in 2000, and could take one of three values: no change (value of 0), loss of climate connectivity (value of -1), or gain of climate connectivity (value of 1). Where cells changed from a forested to a non-forested state, we assume a loss of climate connectivity for that cell. Where cells changed from a non-forested to a forested state (e.g. via secondary forest regrowth on abandoned farmland; Aide et al., 2013), we assume a gain of climate connectivity for that cell. For analyses, loss of climate connectivity was captured for each land mass (n = 695) by the proportion of the total area of forested cells (forested in either 2000, 2012 or both) that experienced a change from successful to unsuccessful climate connectivity. An analogous approach was applied to quantify gain of climate connectivity.

Area of connectivity loss was modelled as a binary variable (area losing connectivity versus

area not losing connectivity), against the explanatory variables: biogeographic realm and area of forest lost between 2000 and 2012. We used a Generalized Additive Model (GAM) implemented in the `mgcv` package (Wood, 2017), with a quasibinomial error distribution to account for overdispersion.

5.4 Code Availability

Custom Python code to calculate climate connectivity can be downloaded from GitHub (https://github.com/rasenior/ClimateConnectivity). These scripts have been directly adapted from the methods in McGuire et al. (2016), and the `R` code therein (https://github.com/JennyMcGuire/ClimateConnectivity).

5.5 Acknowledgements

We thank Jenny L. McGuire for making her code publicly available, and for providing us with additional help and guidance. We thank Michela Pacifici for providing maps of climate vulnerability, and BirdLife International for providing maps of Key Biodiversity Areas. Thanks also to Felix K. S. Lim, Philip J. Platts and Sarah A. Scriven for helpful discussions. R.A.S. was funded by a NERC studentship through the ACCE (Adapting to the Challenges of a Changing Environment) Doctoral Training Partnership (Grant No. NE/L002450/1).

Chapter 6

General Discussion

Frilled tree frog (*Kurixalus appendiculatus*).

6.1 Summary

The conservation of biodiversity globally depends in large part on the conservation of tropical biodiversity (Barlow et al., 2018). The biggest single driver of biodiversity loss is land-use change (Sala et al., 2000). In the tropics, this is largely driven by continuing deforestation to meet global food demands (Gibbs et al., 2010; Tilman et al., 2011), alongside extensive degradation by direct disturbances such as selective logging and fire, as well as indirect, secondary impacts such as edge effects from fragmentation and increased access for poachers from expanding road networks (Barlow et al., 2016; Haddad et al., 2015; Laurance et al., 2009). Simultaneously, the intensifying and inexorable threat of climate change will be felt keenly in the tropics (Corlett, 2011). Relative to the long periods of climatic stability that characterise this region, species' exposure to climate warming will be among the highest globally (Mora et al., 2013), compounded by high sensitivity of tropical species resulting from their restricted thermal tolerance (Deutsch et al., 2008; Khaliq et al., 2014; Tewksbury et al., 2008) and limited capacity for dispersal or adaptation (Hoffmann and Sgrò, 2011; Loarie et al., 2009; Moore et al., 2008; Opdam and Wascher, 2004). A key unknown, addressed in this thesis, is the extent to which the loss and degradation of tropical forests might exacerbate biodiversity loss by impeding species' ability to adaptively respond to climate change.

The main aims of this thesis were to determine how land-use change in the tropics impacts: (1) exposure to local warming, and the feasibility of both (2) microclimates and of (3) range shifts as mechanisms by which species can avoid extinction under global climate change. First, comparing local, site-level temperature in various different land-use types, I found that conversion of forest to farmland resulted in local warming of 1.6-13.6°C, but this was avoided below-ground and in degraded forests. To further investigate the thermal buffering potential of degraded forests I developed a framework and R package, which together facilitate assessment of thermal heterogeneity using thermal images. Combining this approach with temperature loggers and microhabitat assessments, I found that the potential for thermal buffering was similar in intensively logged forest and unlogged forests on Borneo, despite notable differences in forest structure. Even with thermal buffering the distribution of many species will shift as the climate warms, hence I used global forest cover and climate datasets to quantify, across the tropics, the extent to which range shifts to analogous future climates are facilitated by existing forest cover, and how this has changed with recent deforestation. I found that 62% of tropical forests already fail to connect to future climate analogues, and this will likely deteriorate further since 27% of these forests experienced loss of climate connectivity from 2000 to 2012, accelerating with increasing forest loss.

In the following chapter I synthesise all my results to illustrate how, overall, the loss and degradation of forests has impacted species' ability to respond to future climate change in the tropics. I conclude with recommendations for conservation practitioners and policy-makers, and some suggestions for priority research directions.

6.1.1 Climate at the fine scale

Until recently most studies of climate change impacts used very coarse resolution climate data – up to 10,000 times larger than the size of the study organism (Potter et al., 2013) – and did not integrate the combined effects of land-use change and climate change (Titeux et al., 2017). The findings of Chapter 2 highlight that coarse-scale data can mask important anthropogenic impacts at the level of the organism. Namely, that in many parts of the tropics where forest has been lost, extreme warming has already occurred as a result of conversion to agriculture. Degraded forests and below-ground habitat avoided local warming through land-use change, although Chapter 2 did not consider temperature at the micro-scale (mm to m; 'microclimates') that allows mobile organisms to behaviourally thermoregulate (González del Pliego et al., 2016; Scheffers et al., 2014a), and can even influence the fine-scale distribution of less mobile organisms (Maclean et al., 2017).

Capturing micro-scale, biologically-relevant temperature data has become increasingly feasible with the advent of small dataloggers and affordable thermal imaging technology (Scheffers et al., 2017a). The latter has, however, been underutilised at least in part because there is little guidance available for processing and analysing thermal images in ecology. I addressed this shortfall in Chapter 3, where I presented an `R` package – `ThermStats` – designed to streamline the processing of images from FLIR thermal cameras, and to calculate key metrics of thermal heterogeneity for any gridded temperature data.

In Chapter 4 I built on the findings of Chapter 2 by assessing microclimate availability and buffering capacity in intensively selected logged forests on Borneo, in comparison with nearby unlogged, primary forest. Using techniques developed in Chapter 3, combined with data from temperature loggers and microhabitat measurements, I found that not only are degraded forests and primary forests comparable in local temperature (cf. Chapter 2), but microclimates are similar in availability, thermal stability and ability to buffer organisms from warming at coarser spatial scales.

6.1.2 Climate at the coarse scale

Chapters 2 to 4 focused on the impact of land-use change on temperature at spatial scales of millimetres to hectares, which, in the context of climate change, is important for understanding the baseline temperature onto which global climate warming is projected, as well as the likely ability of organisms to utilise microclimates as a means to avoid suboptimal temperatures experienced at coarser spatial scales. However, even where microrefugia are available, and especially where they are not, global climate change could impact temperature at all spatial scales to the extent that organisms will need longer-term solutions to avoid extinction (Hannah et al., 2014). Range shifts are one such solution, and have been widely documented (Parmesan, 2006). In Chapter 5 I found that tropical forests are generally poorly connected along climate gradients, such that the average tropical forest will fail to facilitate species' range shifts to analogous future climates. Increasing loss of forest resulted in an accelerating loss of climate connectivity, suggesting that without intervention the current situation could decline rapidly.

6.2 Wider applicability of findings

6.2.1 Biological relevance

The results of Chapters 2 to 4 are most relevant for small-bodied ectotherms, which are strongly influenced by local and fine-scale temperature, and are widely known to utilise thermal variation at these spatial scales to avoid suboptimal climatic conditions at coarser scales (González del Pliego et al., 2016; Scheffers et al., 2014a). Small-bodied animals are more strongly influenced by surface temperatures and boundary layer climates (e.g. Kaspari et al., 2015) so our results are also relevant for small-bodied endotherms, although less is known about the extent to which they can and do utilise microclimates in tropical rainforests. While immobile species cannot directly utilise microclimates within generations, their fitness may still be affected by local temperature and by changes in fine-scale thermal heterogeneity, the latter potentially driving dispersal between generations and causing individuals to localise within particular microclimates (Maclean et al., 2015).

The findings of Chapter 5 are most immediately relevant for species that can disperse easily but require forest cover to do so, such as medium to large-sized, non-volant forest specialists (cf. Nuñez et al., 2013). The size of these organisms makes microclimates a less viable way to avoid climate warming in the long term, but also enhances their ability to disperse to more favourable climates. Poorer dispersers may be unable to keep pace with changing climate (Schloss et al., 2012), while range shifts of various species will be additionally shaped by

novel biotic interactions and reductions in habitat area at higher elevations (Elsen and Tingley, 2015; Mason et al., 2014).

A key consideration for future research is water balance. Moist habitats are more robust to temperature change because water has a higher specific heat capacity than air, requiring a greater input of thermal energy to achieve the same change in temperature. Increased water availability also increases evapotranspiration in forests, meaning that thermal energy is dissipated through the evaporation of water rather than a change in temperature (Oke, 1987). Additionally, water can determine species' sensitivity to temperature change. Amphibians, for example, have a semi-permeable skin and are prone to dessication in hot environments when water availability is low (Duellman and Trueb, 1986). A particularly useful metric is vapour pressure deficit – the difference between the amount of moisture in the air and how much moisture the air can hold when it is saturated – which can be measured at fine spatial scales using dataloggers that record both temperature and relative humidity. These dataloggers are prone to water damage (Bramer et al., 2018), but could provide valuable information for quantifying microclimates. The influence of water in shaping species' climate niche may also influence species' range shifts in a warming world. Precipitation data could provide a valuable extension to the approach of Chapter 5, although this is best applied at regional scale where future projections are more reliable and there is a clearer gradient that species would need to follow to avoid deleterious changes in precipitation.

Regardless of spatial scale, in this thesis I have only focused on species movement in two dimensions. In reality, tropical rainforests have a high degree of structural complexity in the third dimension, providing an additional climate gradient that species could exploit to cope with global climate warming (Scheffers et al., 2017b; Scheffers and Williams, 2018). With ever-improving technology, it is possible to apply the techniques of Chapter 3 and Chapter 4 vertically and in forests of varying human impact to create a fuller, more three-dimensional picture of how human activity affects thermal regimes in tropical forests. Thermal data could be collected more extensively using LiDAR (Jucker et al., 2018), by combining thermal imagery with unmanned aerial vehicles (Faye et al., 2016; Sanchez-Azofeifa et al., 2017), and by combining telemetry and dataloggers to record and recreate the thermal experiences of mobile species. Detailed ground-truthed data could be combined with above-canopy, remotely sensed data in correlative or mechanistic models (cf. Kearney and Porter, 2017; Maclean et al., 2017) to create sub-canopy climate layers, which could feed into Species Distribution Models or help us to understand other responses to climate change, such as local adaptation and acclimation.

6.2.2 Relevance across tropics and elsewhere

Chapters 2 and 5 had the broadest geographical relevance, since they were pantropical in scope. The representativeness of Chapter 2 was limited by the availability of temperature data in the literature, with Africa being particularly poorly represented. This is a problem noted in other large-scale ecological studies (e.g. Gibson et al., 2011; Spooner et al., 2018), and could compromise the generality of results because of the unique biogeography and land-use history of Africa (Hansen et al., 2008).

Chapter 4 focused on a region of the tropics where logging intensity was once among the highest globally (Lewis et al., 2015) but has since ceased entirely (Reynolds et al., 2011). Field studies such as this are inevitably site-specific, but combined with the framework of Chapter 3 and technological advances described above, the approach could be applied more extensively, for different modes of land-use change and of varying intensity and periods of recovery. Similarly, Chapter 5 considered only the effects of wholesale forest conversion because of limitations in the forest cover data available (Hansen et al., 2013). Techniques to remotely sense the age, quality and type of forest are still in development (Mitchell et al., 2017), but could in time allow a more nuanced assessment of climate connectivity across heterogenous forest landscapes.

This thesis focuses on tropical rainforests, but there are many priority regions for tropical conservation where natural vegetation is not closed canopy forest – for example, Brazil's cerrado and the Succulent Karoo of South Africa and Namibia (Myers et al., 2000). In these places, modification by humans is less likely to dramatically alter local and fine-scale temperature because there is naturally less thermal buffering by complex, three-dimensional vegetation. However, that is not to say that a small change in absolute temperature would not have ecological implications; this depends on the ecology of inhabitant species and their sensitivity to temperature change. The specific structures associated with microclimates will undoubtedly also vary by location, e.g. desert burrows and alpine boulder fields (Shoo et al., 2010). Climate connectivity is likely to be poor for many habitat types because of widespread habitat loss and resulting fragmentation. More intact regions tend to be those that are inhospitable to humans, such as taiga and deserts (Watson et al., 2016) and regions at very high elevation (Elsen et al., 2018). In these places, climate connectivity will be largely determined by the availability of analogous future climate, and this is more likely in areas of high topographic complexity (Elsen et al., 2018).

6.3 Recommendations for conservation

Land-use change is still the primary cause of species loss (Sala et al., 2000), and the lack of consideration of associated climatic effects suggests that its full impact may be underestimated and potentially confounded with climate change (Chapter 2; Oliver and Morecroft, 2014; Senior et al., 2017). As a growing driver of biodiversity loss, it is necessary to consider climate change and mitigate against it, but the priority for conservation research, practice and policy should – first and foremost – be to minimise land-use change and its negative consequences. A growing body of evidence suggests that a land sparing approach is often the best way to maximise biodiversity retention, whether the land use is agriculture (Phalan et al., 2011), selective logging (Edwards et al., 2015) or urban development (Collas et al., 2017).

On a local scale, enhancing thermal heterogeneity could increase the potential for thermal buffering, thus protecting species from climate change or, at the very least, providing more time for adaptation and dispersal (Hannah et al., 2014). Chapter 4 demonstrates that forest regeneration over a decade is sufficient for thermal recovery in the forest understorey after intensive selective logging. More research is needed to identify minimum recovery time, but it may be that active restoration or reduced impact logging could bolster thermal recovery further. One possible approach is *in situ* management of microrefugia, reviewed in Greenwood et al. (2016). It would be insightful to experiment with such interventions in different land-use types in the tropics, assessing impacts on fine-scale thermal heterogeneity using dataloggers or thermal imagery (cf. Chapters 3 and 4), as well as the impact on local biodiversity.

Given the potential value of logged tropical forests for buffering species against climate change (Chapter 4) and the well-established role of degraded forests in retaining species of conservation concern (Edwards et al., 2011; Gibson et al., 2011; Putz et al., 2012), it is critical that they too are incorporated into conservation planning. Without protection, logged forests are susceptible to over-harvesting as well as edge effects, fire, hunting and wildlife trade associated with the expanding networks of roads and skid trails (Edwards et al., 2014c; Laurance et al., 2014). With increasing forest degradation there is heightened risk of 'salvage' logging and, ultimately, conversion to agriculture (Edwards et al., 2014c). By managing forests designated for logging within larger, permanent timber estates, protocols can be implemented with sustainability and biodiversity retention in mind. For example: rotating cutting to allow for regeneration post-harvest; using reduced-impact logging techniques (Putz et al., 2008); and ensuring that mature forest is set-aside within the landscape to seed recovering sites and to provide habitat for disturbance-intolerant species (Edwards et al., 2014a,c). Sustainable timber harvesting can be promoted through schemes

like REDD+, through government regulations, and through market-based incentives ranging from positive publicity to certification schemes, such as the Forest Stewardship Council (Edwards et al., 2014a,c).

Chapter 5 outlined the importance of connecting tropical forest along climate gradients to facilitate species range shifts under future climate change. Reforestation is in line with the Bonn Challenge, which seeks to restore 350 million hectares by 2030. Expanding the protected area network would contribute to Aichi target 11, whereby at least 17% of terrestrial and inland water areas are protected by 2020 (CBD, 2010). A simple way to connect forest along climate gradients is to focus on elevational gradients, which are currently poorly connected (Elsen et al., 2018). This could have the additional benefit of conserving regions of topographic complexity and their associated microclimates, thus maximising species' options for responding to climate change (Suggitt et al., 2018). The results in Chapter 5 can be used to signpost to centres of poor climate connectivity, which would benefit from more targeted research at finer spatial resolutions, and tailored towards priority habitat types or taxa. Where it is not possible to connect current distributions to future climate analogues, well-planned translocation of poor dispersers can be a worthwhile and cost-effective solution to help imperilled species cope with climate warming (Willis et al., 2009).

6.4 Conclusions

The influence of ongoing forest degradation and conversion on the ability of tropical species to respond to climate change will have a major bearing on their long-term prospects. Tropical species represent a large, valuable and vulnerable pool of global biodiversity, the loss of which would invariably push us towards, and perhaps beyond, various planetary boundaries. Land-use change can directly and substantially alter local climate, but degraded forests and microhabitats are valuable assets to conservation through their ability to buffer species from climate warming. Forest protection and restoration can also help connect species to future climate analogues, which most tropical forests currently fail to do. To maximise climate resilience of tropical rainforests, practitioners and policy-makers should maximise the options available for species to respond to climate: minimising forest loss, permitting and facilitating the recovery of degraded forests, and planning forest loss, gain and restoration with climate gradients and connectivity in mind.

Appendix A

Supporting information for Chapter 2

A.1 Impact of unbalanced sampling

A.1.1 Methods

Some studies contributed substantially more temperature observations than others. To test whether these studies were unduly influencing our results, we established a threshold over which a given land-use type, in a given study, was deemed to have a disproportionate number of associated temperature observations. The threshold used — 2,071 observations — was the mean number of observations across all unique combinations of land-use type and study identity (55 in total). The same number of observations (2,071) was then randomly re-sampled from each of the land-use type and study combinations that exceeded the threshold. With this reduced and more balanced dataset we repeated the main analysis (see Chapter 2: 'Statistical analyses' for more details), modelling local day-time temperature ('temp_day') against land-use type ('LUT'), position relative to ground-level ('position') and season. The final model structure was unchanged, and included a random slope for land-use type and random intercept with respect to the identity of the study ('studyID') from which data originated:

```
lmer(temp_day  ~ LUT*position + LUT*season + (LUT|studyID))
```

A.1.2 Results

All results were qualitatively unchanged from those derived using the full dataset. Local day-time temperature was warmer in altered land-use types, compared to primary forest

(LMM, χ^2 = 32.19, df = 4, P < 0.001; Figure A.1). Averaged across above- and below-ground, and across seasons, the temperature differential was greatest in cropland (7.7°C), followed by pasture (6.4°C), plantation (3.2°C) and degraded forest (0.9°C).

The relationship between land-use type and temperature interacted with both position relative to ground level (LMM, χ^2 = 681, df = 4, P < 0.001; Figure A.1a) and season (LMM, χ^2 = 105.63, df = 4, P < 0.001; Figure A.1b). Specifically, the difference between altered land-use types and primary forest was greater above-ground than below-ground (Figure A.1a), and variable between seasons according to the land-use type (Figure A.1b).

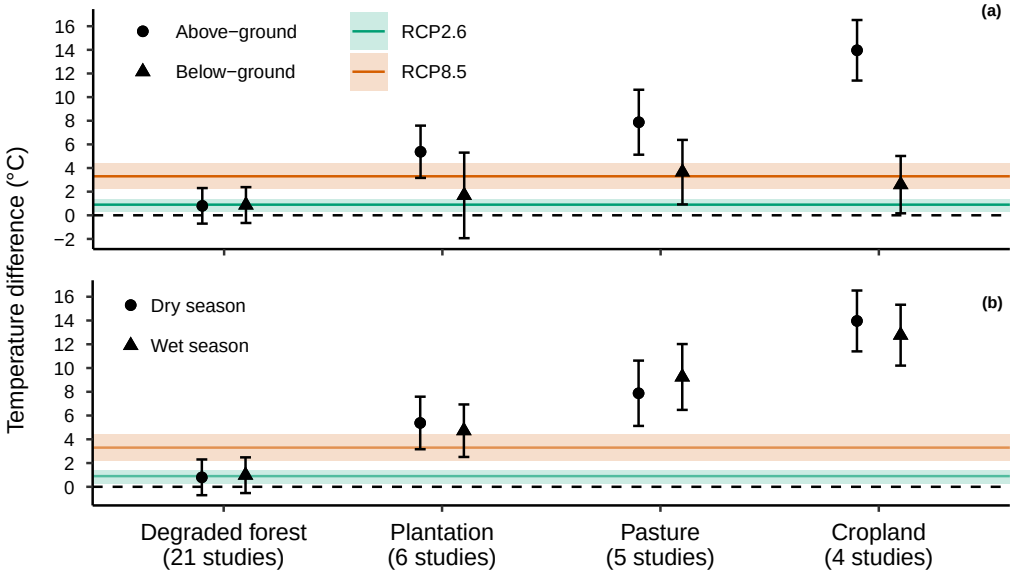

Figure A.1: Model estimates of the temperature difference between altered land-use types and primary forest, using a reduced dataset to balance sample sizes between the different studies that contributed data. Parameter estimates are standardised against the estimate for primary forest, which is represented by the dashed line. Error bars are 95% confidence intervals. Solid lines indicate projected warming in the tropics for the period 2081-2100 compared to the period 1986-2005, as a result of global climate change (IPCC, 2013). Shaded bands indicate 5%–95% ranges from the distribution of the climate model ensemble. Colours represent the lowest and highest warming scenarios (RCP2.6 and RCP8.5, respectively).

A.2 Supplementary figures

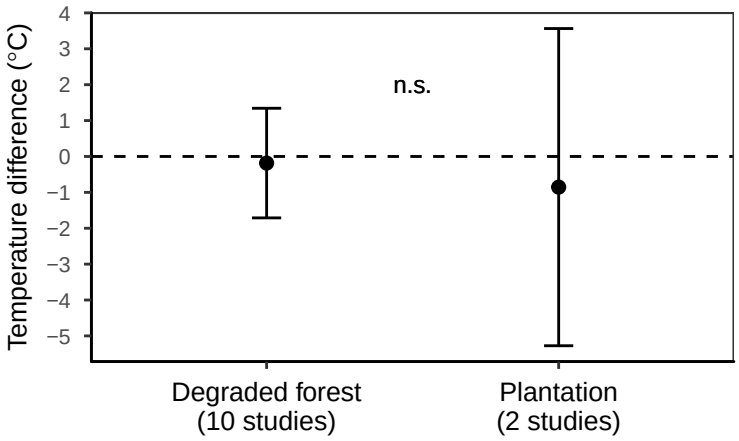

Figure A.2: Model estimates of the nocturnal temperature difference between altered land-use types and primary forest. Note that cropland and pasture are missing from this analysis because nocturnal temperature data for these land-use types were not available. Parameter estimates are standardised against the estimate for primary forest, which is represented by the dotted line. Error bars are 95% confidence intervals.

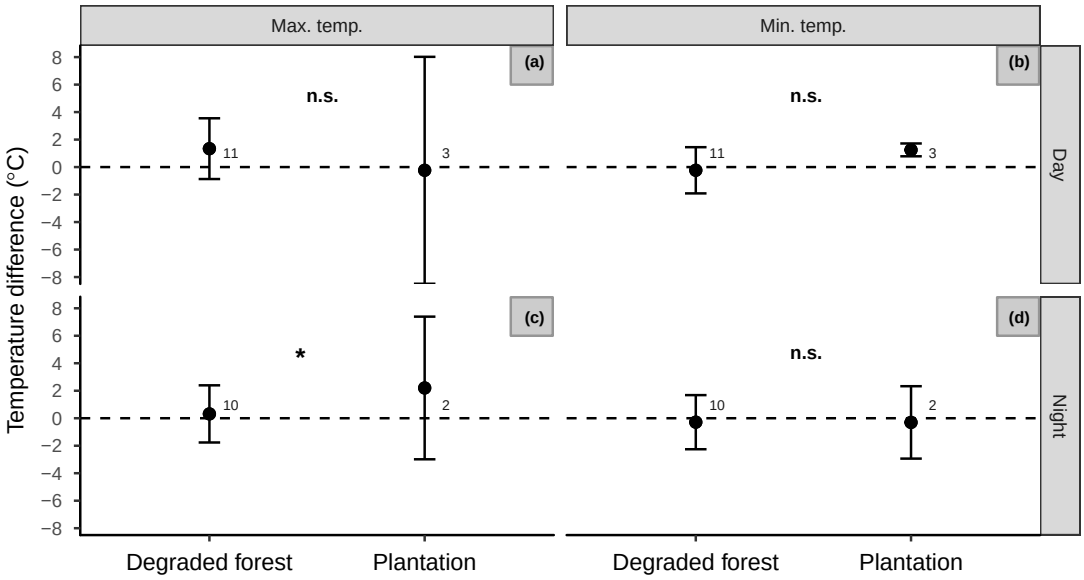

Figure A.3: Model estimates of the difference between altered land-use types and primary forest in terms of temperature extremes. Day-time results are depicted in panels (a) and (b), and night-time results in panels (c) and (d). Panels (a) and (c) indicate the effect of land-use change on maximum temperature, and panels (b) and (d) indicate the same for minimum temperature. Note that data for cropland and pasture are absent from this analysis because data for these land-use types were not available. Parameter estimates are standardised against the estimate for primary forest, which is represented by the dotted line. Error bars are 95% confidence intervals. The grey numbers next to points represent the number of studies providing the underlying data.

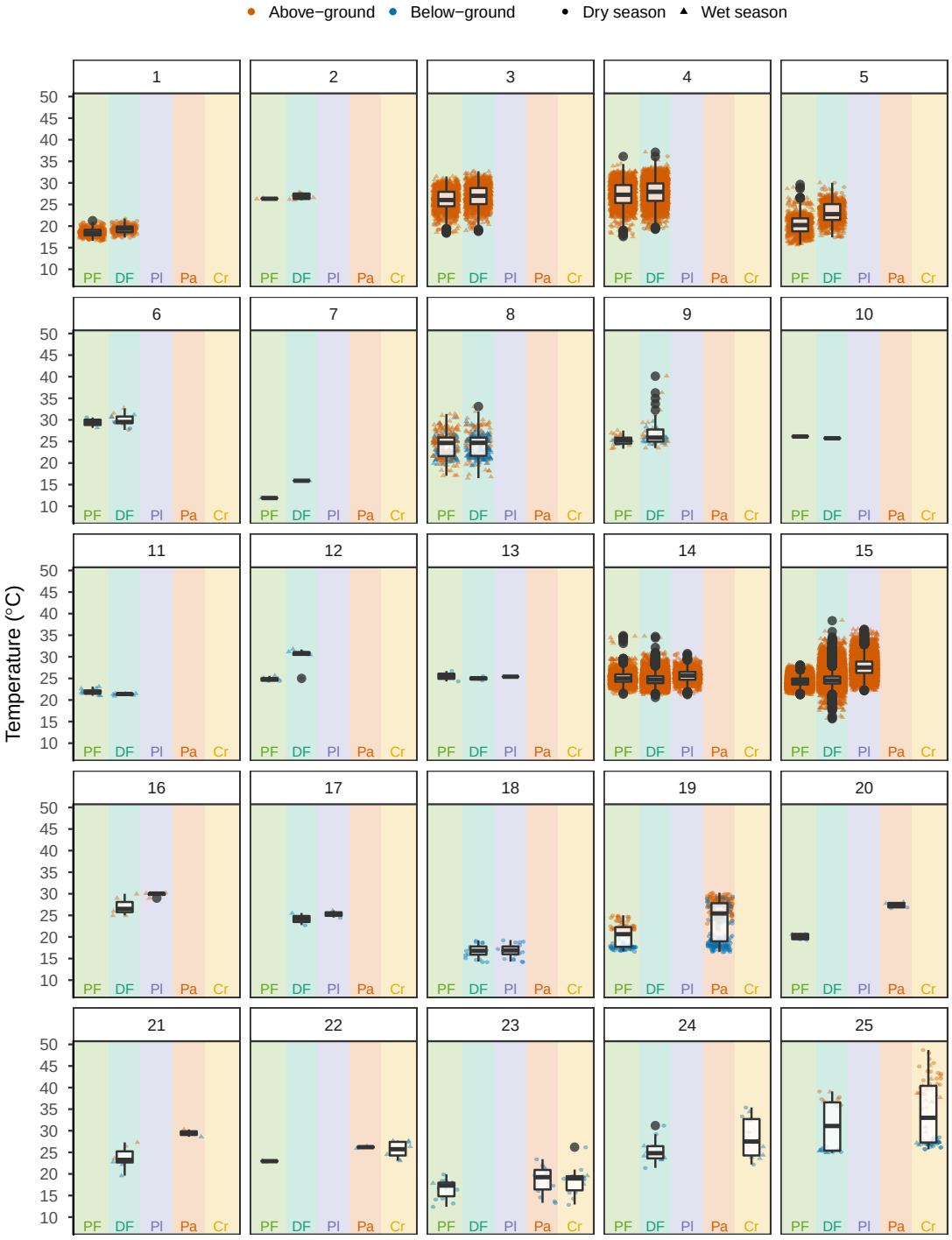

Figure A.4: Day-time temperature against land-use type for each study contributing data to the analyses. Panel numbers refer to the study number in the reference list of Table 2.2. Land-use types are: primary forest (PF), degraded forest (DF), plantation (Pl), pasture (Pa) and cropland (Cr). Panels are ordered by the combination of land-use types for which data was available: (1-12) PF + DF; (13-15) PF + DF + Pl; (16-18) DF + Pl; (19-20) PF + Pa; (21) DF + Pa; (22-23) PF + Pa + Cr; and (24-25) DF + Cr. Shading of points indicates temperatures measured above-ground (orange) or below-ground (blue), and point symbol indicates temperatures measured during the dry season (circles) or wet season (triangles).

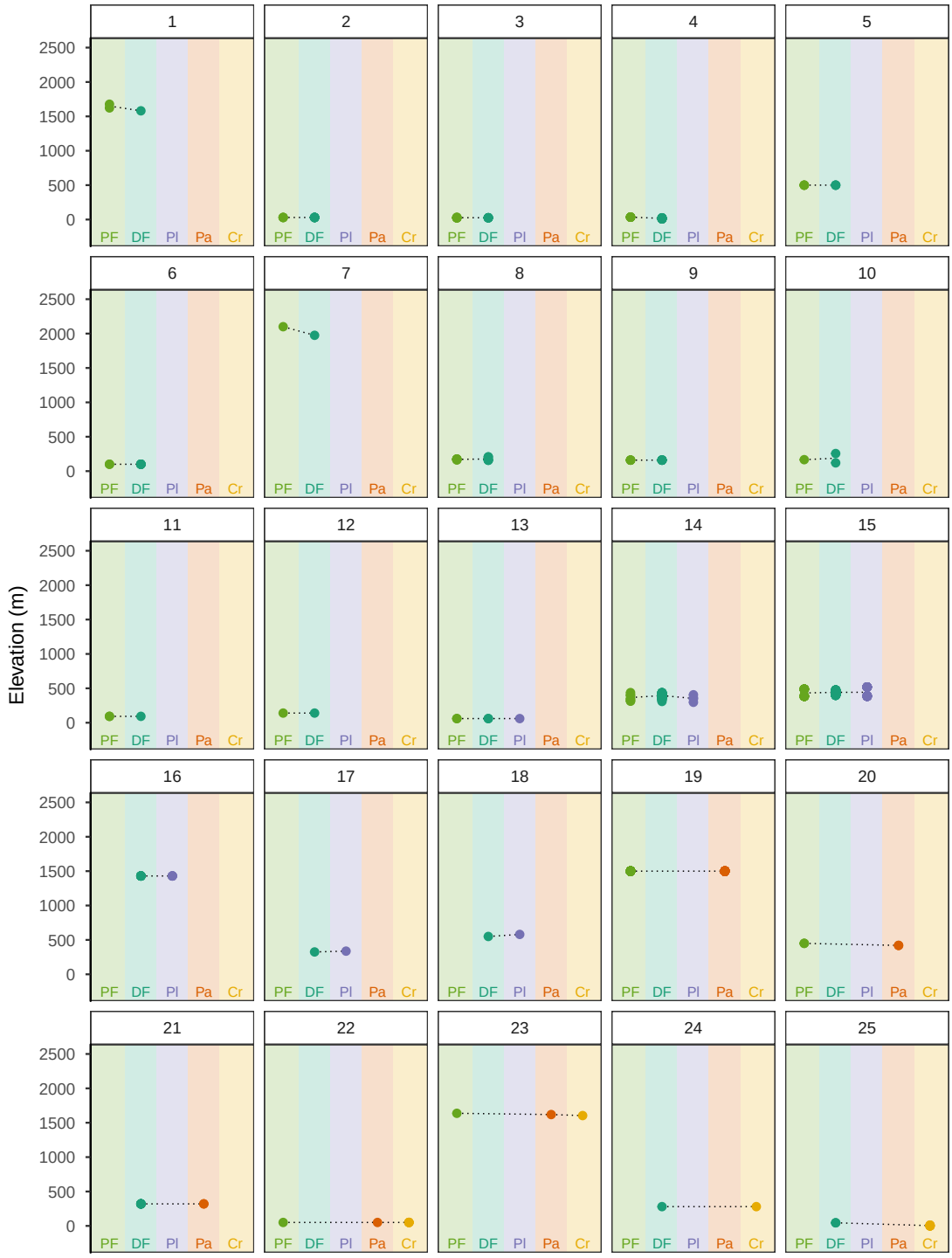

Figure A.5: Site elevation against land-use type for each study contributing data to the analyses. Panel numbers refer to the study number in the reference list of Table 2.2. Land-use types are: primary forest (PF), degraded forest (DF), plantation (Pl), pasture (Pa) and cropland (Cr). Panels are ordered by the combination of land-use types for which data was available: (1-12) PF + DF; (13-15) PF + DF + Pl; (16-18) DF + Pl; (19-20) PF + Pa; (21) DF + Pa; (22-23) PF + Pa + Cr; and (24-25) DF + Cr. Dotted black lines connect the mean elevation of all the sites within each land-use type.

Appendix B

Supporting information for Chapter 3

B.1 Package vignette

B.1.1 Summary

ThermStats is designed for biologists using thermography to quantify thermal heterogeneity. It uses the Thermimage package (Tattersall, 2017) to batch process data from FLIR thermal cameras, and takes inspiration from FRAGSTATS (McGarigal et al., 2012), SDMTools (VanDerWal et al., 2014), Faye et al. (2016) and Shi et al. (2016) to facilitate the calculation of various metrics of thermal heterogeneity for any gridded temperature data.

The package is available to download from GitHub using devtools:

```
devtools::install_github("rasenior/ThermStats")
library(ThermStats)
```

Once loaded, the code below can be followed step-by-step.

B.1.2 Extracting raw data

Data are extracted from FLIR images using batch_extract. This is a batch implementation of the readflirJPG function from Thermimage. It requires only the path to the directory of FLIR thermal images, and the freely available external software 'Exiftool' (https://www.sno.phy.queensu.ca/~phil/exiftool/). Besides raw data, this step also

retrieves camera-specific calibration parameters which are required later to convert raw data to temperature values.

```
# Batch extract images included in ThermStats installation
flir_raw <-
    batch_extract(in_dir = system.file("extdata",
                                       package = "ThermStats"),
                  write_results = FALSE)
```

B.1.3 Converting raw data to temperature

Raw data are encoded in each thermal image as a 16 bit analog-to-digital signal, which represents the radiance received by the infrared sensor. The function `batch_convert` converts these raw data to temperature values using equations from infrared thermography, via a batch implementation of the function `raw2temp` in `Thermimage`. It uses environmental parameters defined by the user, and the calibration constants extracted in `batch_extract`. See Chapter 3: 'Methods' for a full discussion of the different environmental parameters. In brief:

- Emissivity = the amount of radiation emitted by a particular object, for a given temperature.
- Object distance = the distance between the camera and the object of interest.
- Reflected apparent temperature = the temperature resulting from radiation that originates from the atmosphere and is reflected by the object.
- Atmospheric temperature = the temperature of the atmosphere.
- Relative humidity = the relative humidity of the atmosphere.

```
# Define raw data
raw_dat <- flir_raw$raw_dat
# Define camera calibration constants dataframe
camera_params <- flir_raw$camera_params
# Define metadata
metadata <- flir_metadata

# Create vector denoting the position of each photo in metadata
photo_index <- match(names(raw_dat),
                     metadata$photo_no)

# Batch convert
flir_converted <-
```

```
batch_convert(
    raw_dat = raw_dat,
    # Emissivity =
    # mean of the range in Scheffers et al. 2017
    E = mean(c(0.982,0.99)),
    # Object distance =
    # hypotenuse of a right triangle where the vertical side
    # is 1.3 m (breast height) & the angle down is 45 degrees
    OD = (sqrt(2))*1.3,
    # Apparent reflected temperature, atmospheric temperature
    # & infrared window temperature =
    # atmospheric temperature measured in field
    RTemp = metadata$atm_temp[photo_index],
    ATemp = metadata$atm_temp[photo_index],
    IRWTemp = metadata$atm_temp[photo_index],
    # Infrared Window transmission = default value of 1
    IRT = 1,
    # Relative humidity = relative humidity measured in field
    RH = metadata$rel_humidity[photo_index],
    # Calibration constants from 'batch_extract'
    PR1 = camera_params[,"PlanckR1"],
    PB = camera_params[,"PlanckB"],
    PF = camera_params[,"PlanckF"],
    PO = camera_params[,"PlanckO"],
    PR2 = camera_params[,"PlanckR2"],
    # Whether to write results or just return
    write_results = FALSE)
```

B.1.4 Calculating thermal statistics

Statistics can be calculated for individual temperature matrices, or across multiple matrices within a specified grouping. The latter is useful for sampling designs where multiple images are collected at each sampling event to capture temperature across a wider sampling unit, such as a plot. In either case, statistics include summary statistics specified by the user – for example, median, 5th and 95th percentiles and Shannon Diversity Index (SHDI) – as well as spatial statistics for hot and cold spots, identified using the Getis-Ord local statistic (Getis and Ord, 1996).

For an individual matrix, `get_stats` requires the user to specify the matrix and the desired statistics. Statistics can be calculated for geographic temperature data (in a matrix or raster format), in which case the user should also define the extent and projection of the data.

```
flir_stats <-
    get_stats(
        # The temperature matrix
        val_mat = flir_converted$`8565`,
        # The ID of the matrix
        matrix_id = "8565",
        # Whether or not to identify hot and cold spots
        get_patches = TRUE,
        # Size of the neighourhood (for calculating Getis-Ord stat)
        k = 8,
        # Neighbour weighting style (for calculating Getis-Ord stat)
        style = "W",
        # Matrix projection (only relevant for geographic data)
        mat_proj = NULL,
        # Matrix extent (only relevant for geographic data)
        mat_extent = NULL,
        # The data to return
        return_vals = c(
            # Temperature data as dataframe
            "df",
            # SpatialPolygonsDataFrame of patch outlines
            "patches",
            # Patch statistics dataframe
            "pstats"),
        # The names of the statistics functions
        # (used to name columns in the 'pstats' dataframe)
        pixel_fns = NULL,
        # The summary statistics of interest
        median, perc_5, perc_95, SHDI
    )
```

For grouped matrices, `stats_by_group` requires the user to supply a list of matrices along with metadata and the name of the variable in the metadata that defines the matrix grouping. Table B.1 shows the metadata used in the code snippet, where photo number ('photo_no') defines individual temperature matrices, and replicate identity ('rep_id') defines the grouping of photos. There are two replicates, 'T7P1' and 'T7P2', and each has

two associated photos.

photo_no	rep_id	atm_temp	rel_humidity
8565	T7P1	24.00	96
8583	T7P1	24.00	96
8589	T7P2	23.25	98
8613	T7P2	23.50	96

Table B.1: Example metadata denoting the grouping ('rep_id') of different temperature matrices. Statistics can be calculated over multiple matrices within a group, using the function `stats_by_group`.

By default, both `get_stats` and `stats_by_group` return a dataframe with patch statistics (Table B.2) for each matrix or matrix group, respectively.

median	perc_5	perc_95	SHDI	hot_shape_index	hot_aggregation
23.5	23	24.5	1.16	7.54	0.895
24.0	23	25.0	1.68	7.80	0.855

Table B.2: A snippet of hot spot patch statistics returned by `stats_by_group`, which implements `get_stats` within groups.

B.1.5 Plotting

In addition to patch statistics, `get_stats` can return (1) the temperature matrix in a dataframe format, and (2) a `SpatialPolygonsDataFrame` of its hot and cold spots. The function `plot_patches` can then recreate the original thermal image overlaid with outlines of hot and cold spots, and plot the temperature distribution (if `plot_distribution = TRUE`).

```
plot_patches(
    # The raw temperature data
    df = flir_stats$df,
    # The patch outlines
    patches = flir_stats$patches
)
```

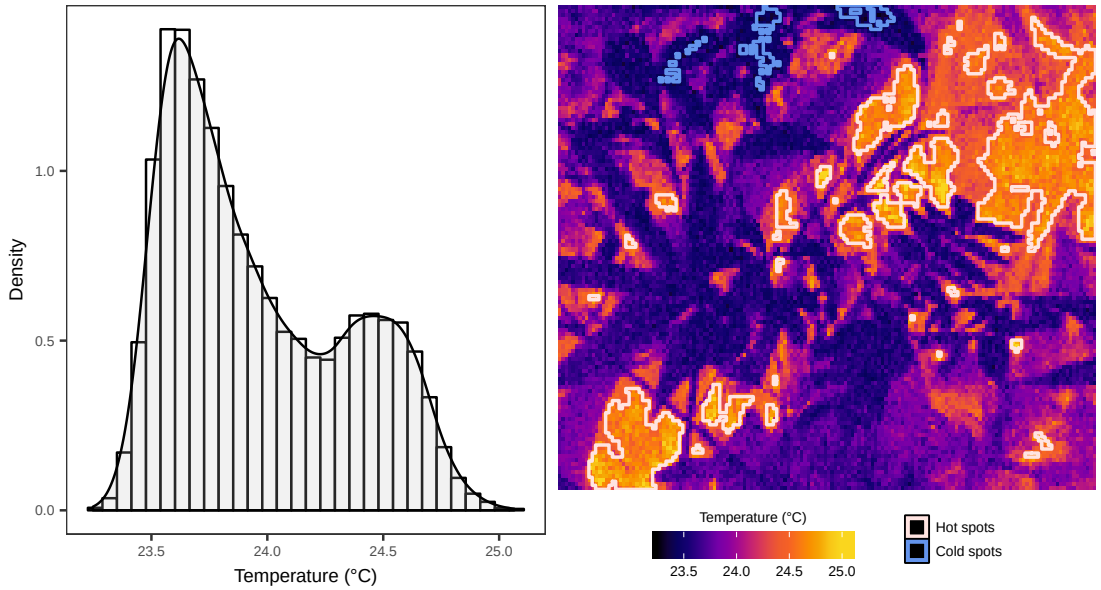

Figure B.1: The output of `plot_patches` includes a histogram and the original temperature data overlaid with outlines of hot and cold spots, identified using the Getis-Ord local statistic.

Appendix C

Supporting information for Chapter 4

C.1 Sampling methods for forest structure

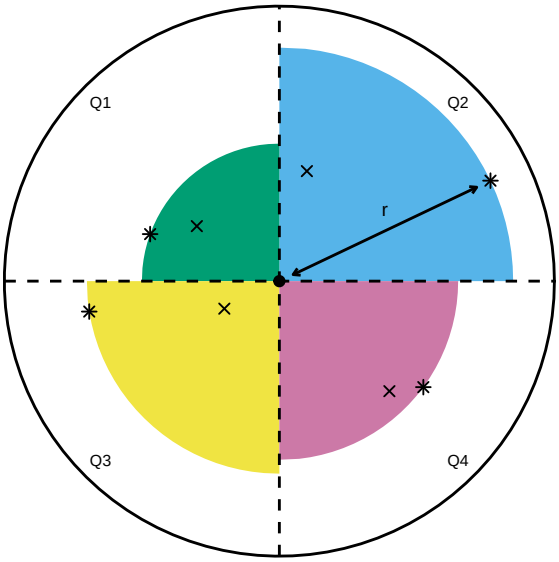

Figure C.1: Sampling design schematic.

Several different variables have been previously identified as efficiently capturing overall forest structure (Hamer et al., 2003; Lucey and Hill, 2012). Each plot (background circle in the schematic) was divided into quadrants (Q1-Q4). Within each quadrant we measured the distance to and circumference at breast height of the two nearest mature trees (circumference > 0.6 m) and saplings (circumference 0.1-0.6 m). Stand basal area (m^2/ha) was calculated separately for trees and for saplings. In the above schematic, tree/sapling individuals are depicted as points: there can be zero, one or two individuals in each quadrant; the nearest individual is represented by a cross, and the furthest individual as

a star. To estimate stand basal area, we calculated the basal area of each individual from its circumference at breast height, summed this across all observed individuals, divided by the true area of forest that was surveyed and multiplied by 10000 to convert units into the standard m^2/ha. The true area surveyed is depicted by coloured quadrants; this was calculated for each quadrant individually and then summed together. Each true quadrant area was calculated using the equation:

$$A = \frac{1}{4}\pi r^2$$

Where A is the area (m^2) and r is the distance to the furthest individual (tree or sapling; m).

To capture plot-level variation in basal area we calculated the coefficient of variation for trees and for saplings, and we also noted the proportion of observed tree individuals that were in the family Dipterocarpaceae, given the association of these species with mature, complex forest.

Finally, to capture the overall density of vegetation at the plot centre we measured percentage canopy cover using a spherical densiometer (Lemmon, 1956), and the same observer estimated percentage vegetation cover at three distinct forest strata: ground (1.5 m above ground), understorey (15 m above ground) and canopy (the main mat of leaf cover > 15 m above ground). Visual estimates of vegetation cover were made by imagining a horizontal gridded plane intersecting vegetation at the three different heights, and then estimating the percentage of grid cells occupied by vegetation.

C.2 Extracting and processing data from thermal images

Using infrared cameras to sample microclimates in the terrestrial realm is a relatively novel methodology (Scheffers et al., 2017a; but see: Caillon et al., 2014; Faye et al., 2016). There is, as yet, no standardised protocol, and there are numerous different choices of hardware. In this study, we used a FLIR Systems, model E40 camera. A single thermal image comprised 19,200 distinct measurements from the infrared sensor (one per pixel). These raw data can be extracted and converted to temperature in °C using the freely available software FLIR Tools (cf. Scheffers et al., 2017a). However, it is easier, faster and more thorough to use the R package `Thermimage` (Tattersall, 2017).

Raw data were first extracted from thermal images using the function `readflirJPG`, which produces a numeric matrix of the same dimensions as the original jpeg (160 x 120). The function `raw2temp` was then used to convert raw data into temperature using standard equations from infrared thermography (see `?Thermimage::raw2temp` for more details). At this point it is possible to specify various parameters that likely differ from the default settings. For emissivity we used a value of 0.986, which represents the mean of the range (0.982 to 0.990) for bare soil, leaf litter, live tree leaves and the bark of tree trunks in green broadleaf forests (Snyder et al., 1998). For atmospheric temperature and relative humidity, we used measurements taken using a whirling hygrometer immediately prior to each sampling event at each plot. We defined the distance between the camera and the surface as the hypotenuse of an isosceles right triangle with its vertical length equal to breast height: $1.3 \times \sqrt{2} = 1.84$ m. Finally, there are five different calibration constants (PlanckR1, PlanckB, PlanckF, PlanckO and PlanckR2) that are specific to each camera, and we retrieved these from thermal images using the function `flirsettings`. See Chapter 3 for a full description of these methods, combined into a framework and R package: `ThermStats`.

C.3 Sampling methods for microhabitat volume

We measured the volume of leaf litter in five 1 x 1 m quadrats, centred 2 m to the left of the transect edge, at 0, 10 and 20 m from the plot centre. Leaf litter was compressed inside a purpose-built compression cylinder with a plunger, and the volume read directly from a graduated scale on the cylinder (Parsons et al., 2009).

Within the subplot we measured the length and circumference at both ends of all intact deadwood (> 10 cm diameter). If only a portion of the deadwood was contained within the subplot, we measured that portion only. We calculated volume using Smalian's volume formula (Waddell, 2002):

$$V = \frac{l \cdot (\frac{\pi}{8}) \cdot (D_S^2 + D_L^2)}{10000}$$

Where V is volume (m^3), l is the length (m), D_S is the small-end diameter (cm), D_L the large-end diameter (cm). We also measured the maximum and minimum diameter of entrances to all tree holes (maximum entrance diameter > 2 cm and < 2 m high), and their internal volume. Approximating the entrance to an ellipse shape, we calculated entrance area using the standard equation for area of an ellipse:

$$A = \pi \times a \times b$$

Where A is entrance area (cm^2), a is the maximum diameter of the entrance (cm) and b is the minimum diameter (cm). Internal volume could not be adequately measured for one very large tree hole, hence the plot in which it was located was excluded from analyses.

C.4 Impact of logging on macroclimate

C.4.1 Methods

To interpret the impact of selective logging on thermal buffering by microclimates in a meaningful way it is also necessary to know whether macroclimate conditions are affected by selective logging. As discussed in the Materials and Methods, macroclimate temperature was measured prior to thermal image collection using a whirling hygrometer, and also by a temperature datalogger suspended at the centre of each plot (HOBO pendant datalogger, Onset, model UA-001-64K or model UA-002-64K).

The necessity for thermoregulation, however, is dependent not only on temperature, but also on water availability. Vapour pressure deficit (VPD) encompasses both temperature and relative humidity. We measured VPD in two ways. First, using dry-bulb (i.e. macroclimate temperature) and wet-bulb temperature from the whirling hygrometer. We also suspended one hygrochron iButton datalogger (Maxim, model DS1923) 1.5 m above the ground in the plot centre of a subset of plots, alongside the HOBO dataloggers measuring macroclimate temperature. We attempted to distribute our limited number of hygrochrons as evenly as possible; ultimately we collected data from 15 plots across all six sites in primary forest, and from 13 plots across five sites in logged forest. As there were five plots in each site (Figure 4.1), we placed dataloggers either in plots one, three and five, or plots one and five, depending on the number of hygrochrons available. Uneven sample sizes resulted because several hygrochrons were lost or broken. Hygrochrons measured relative humidity every 20 minutes for six days and, as in Chapter 4: 'Methods', a unique datapoint was the median value across each two-hourly increment from 04:40-14:40 hrs, on each day of recording for each of the 60 total plots.

Macroclimate VPD was calculated from saturated vapour pressure and relative humidity using the formula:

$$VPD = \frac{100-RH}{100} \times SVP$$

Where VPD is vapour pressure deficit (Pa), RH is relative humidity (%) and SVP is saturated vapour pressure (Pa). SVP was calculated from temperature:

$$SVP = 610.7 \times 10^{\frac{7.5 \times T_d}{237.3+T_d}}$$

Where T_d is macroclimate (dry-bulb) temperature (°C). Relative humidity can be estimated directly from a whirling hygrometer, but to reduce human error we calculated relative humidity using the equation:

$$RH = \frac{p}{SVP}$$

Where p is partial vapour pressure (Pa), estimated assuming ambient pressure of 1 atm:

$$p = SVR_w - 66.86 \cdot (1 + 0.00115 \cdot (T_w)) \cdot (T_d - T_w)$$

Where T_d is dry-bulb temperature (°C), T_w is wet-bulb temperature and SVP_w is saturated vapour pressure at the wet-bulb temperature, calculated in the same way as SVP, but substituting in T_w for T_d.

C.4.2 Statistical analysis

All supplementary analyses were carried out in an analogous way to the main analyses of microclimate temperature (see Chapter 4: 'Statistical analyses'). The response variables (macroclimate temperature or VPD, from either the hygrometer or dataloggers) were modelled against the fixed effects forest quality (measured as tree stand basal area; m^2/ha) and forest type (categorical: primary forest or logged forest), using linear mixed effects models implemented in the `nlme` package (Pinheiro et al., 2017) in R (R Core Team, 2017). Plot nested in site was included as a random intercept term, to account for spatial pseudoreplication. Temporal autocorrelation of residuals was evident (function `acf`), and we therefore included date and time in a correlation structure, with the best structure determined using AIC (Zuur, 2009). Statistical significance was inspected using likelihood ratio tests (see Chapter 4: 'Methods'; Zuur, 2009), and diagnostic plots were assessed to confirm model fit.

C.4.3 Results

Macroclimate temperature was comparable between primary and logged forest whether measured using a whirling hygrometer (LR = 0.081, P = 0.776; Figure C.2a) or suspended datalogger (LR = 0, P = 0.983; Figure C.2b), and was also unaffected by forest quality for both the hygrometer (LR = 0.022, P = 0.883; Figure C.2a) and datalogger measurements (LR = 0.527, P = 0.468; Figure C.2b). Similarly, macroclimate VPD did not differ according to forest type for either method of VPD measurement: hygrometer (LR = 1.344, P = 0.246; Figure C.2c) and suspended datalogger (LR = 3.489, P = 0.062; Figure C.2d). Neither did the two measures of macroclimate VPD vary with forest quality (P > 0.05; Figure C.2c-d). Thus, we found no evidence that selective logging impacted macroclimate temperature or macroclimate VPD.

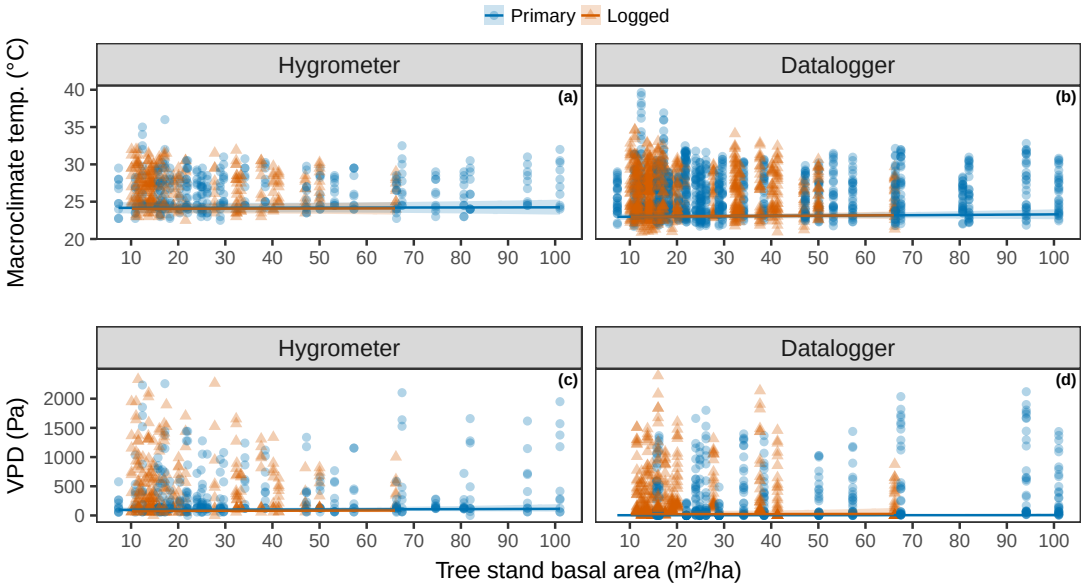

Figure C.2: The influence of forest type (primary or logged forest) and forest quality (measured as tree stand basal area; m^2/ha) on macroclimate temperature (top row) and macroclimate vapour pressure deficit (VPD; bottom row). Macroclimate measurements collected using a whirling hygrometer are shown in the left column, and from dataloggers in the right column. Datapoints from primary forest points are depicted as blue circles, and from logged forest as orange triangles. Shaded bands are 95% confidence intervals.

C.5 Impact of logging on microclimate over 24 hours

C.5.1 Introduction

We were primarily interested in the impact of selective logging on thermal buffering at times when buffering from extremes of heat is most necessary. In the main analyses, therefore, we limited our study to temperatures recorded between the coolest part of the day (around sunrise) and the hottest part of the day (around noon; cf. Scheffers et al., 2017a). However, the wealth of data recorded by dataloggers also enables us to investigate how thermal buffering varies over the full 24-hour period, and particularly during the day versus during the night. In the same way that we would expect logged forests to receive more incoming solar radiation during the day – because of reduced structural complexity and canopy cover (Kumar and Shahabuddin, 2005; Okuda et al., 2003) – we would also expect these forests to radiate heat more freely at night (Chen et al., 1995). Night-time conditions, although less thermally challenging, are still important biologically because nocturnal species can be inactive inside refugia during the heat of the day, but they must forage and seek mates at night if they are to survive and reproduce in the long-term.

C.5.2 Statistical anlaysis

We assessed the impact of selective logging on microclimate temperature in the same way as in Chapter 4: 'Methods', but using the full datalogger dataset. Each unique datapoint was the median of six repeated measures taken every 20 minutes for each two-hourly interval, for each of six sequential days and in each of the 60 total plots (5 plots x 12 sites). As these analyses were not compared alongside results from thermal images, the two-hourly intervals began from 00:00 hrs (rather than 04:40 hrs). For simplicity, data recorded between 06:00-18:00 hrs were defined as being during the day, and 18:00-06:00 as during the night. Analyses were carried out separately for day and night and for each microhabitat: deadwood, tree holes and leaf litter. Thus, for each analysis (out of six), there was a maximum of 4320 unique datapoints: 12 time intervals x 6 days x 5 plots x 12 sites.

As in Chapter 4, we used mixed effects models to analyse microclimate temperature as a function of forest quality (measured as tree stand basal area; m^2/ha), forest type (primary or logged forest) and macroclimate temperature, with an interaction between the latter two variables. Models were implemented in the `nlme` package (Pinheiro et al., 2017) in `R` (R Core Team, 2017). We included plot nested within site as a random intercept to account for spatial pseudoreplication, and both date and time in a correlation structure to account for temporal autocorrelation (the best structure was determined using AIC; Zuur,

2009). Statistical significance was inspected using likelihood ratio tests, first dropping the interaction and comparing to the full model, and then dropping main effects in turn and comparing to a model without the interaction term (Zuur, 2009).

C.5.3 Results

We found no effect of either forest quality or forest type on microclimates at the surface or inside deadwood and leaf litter ($P > 0.05$; Figure C.3). We found a very small effect of both variables on the absolute temperature of microclimates inside tree holes, during the day. At the median value of tree basal area, tree hole temperature in primary forest was 24.8°C compared to 24.9°C in logged forest (LR = 58.202, $P < 0.001$; Figure C.3b), and with an increase in forest quality (i.e. tree stand basal area) of 1 m^2/ha, tree hole temperature increased by 0.00504°C (LR = 57.814, $P < 0.001$). Evidently, these effects were extremely small, and therefore unlikely to be relevant to the majority of organisms.

Similarly, any effects of forest type on the relationship between microclimate and macroclimate temperature, while statistically significant, were small in real terms. During the day, 1°C of warming in the macroclimate (from its median temperature) corresponded to more warming in primary forest than in logged forest for tree holes (LR = 18.214, $P < 0.001$; Figure C.3b) and leaf litter (LR = 40.957, $P < 0.001$; Figure C.3c), but there was no difference for microclimates inside deadwood (LR = 0.254, $P = 0.614$; Figure C.3a). At night, 1°C of cooling in the macroclimate corresponded to more cooling in primary forest than in logged forest for microclimates inside deadwood (LR = 8.589, $P < 0.01$; Figure C.3d) and leaf litter (LR = 861.623, $P < 0.001$; Figure C.3f), but there was no longer any observed difference for microclimates inside tree holes (LR = 1.359, $P = 0.244$; Figure C.3e).

Overall, there is some evidence that thermal buffering from warming and cooling is slightly enhanced for microclimates in logged forest compared to primary forest. However, the size of these effects was so small that they are unlikely to have much biological relevance.

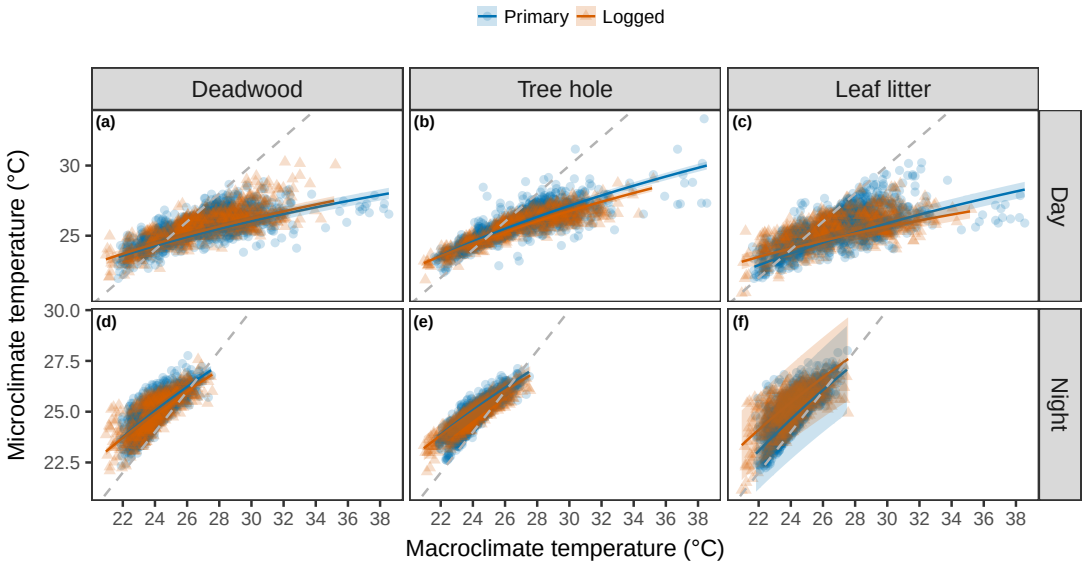

Figure C.3: Comparison of the relationship between microclimate temperature and macroclimate temperature within primary forest (blue circles) and logged forest (orange triangles), during the day (top row) and night (bottom row), and for three microhabitats: deadwood (left column), tree holes (centre column) and leaf litter (right column). The grey dashed line indicates zero temperature buffering, where the microclimate temperature is equal to the macroclimate temperature. Shaded bands are 95% confidence intervals.

C.6 Supplementary figures

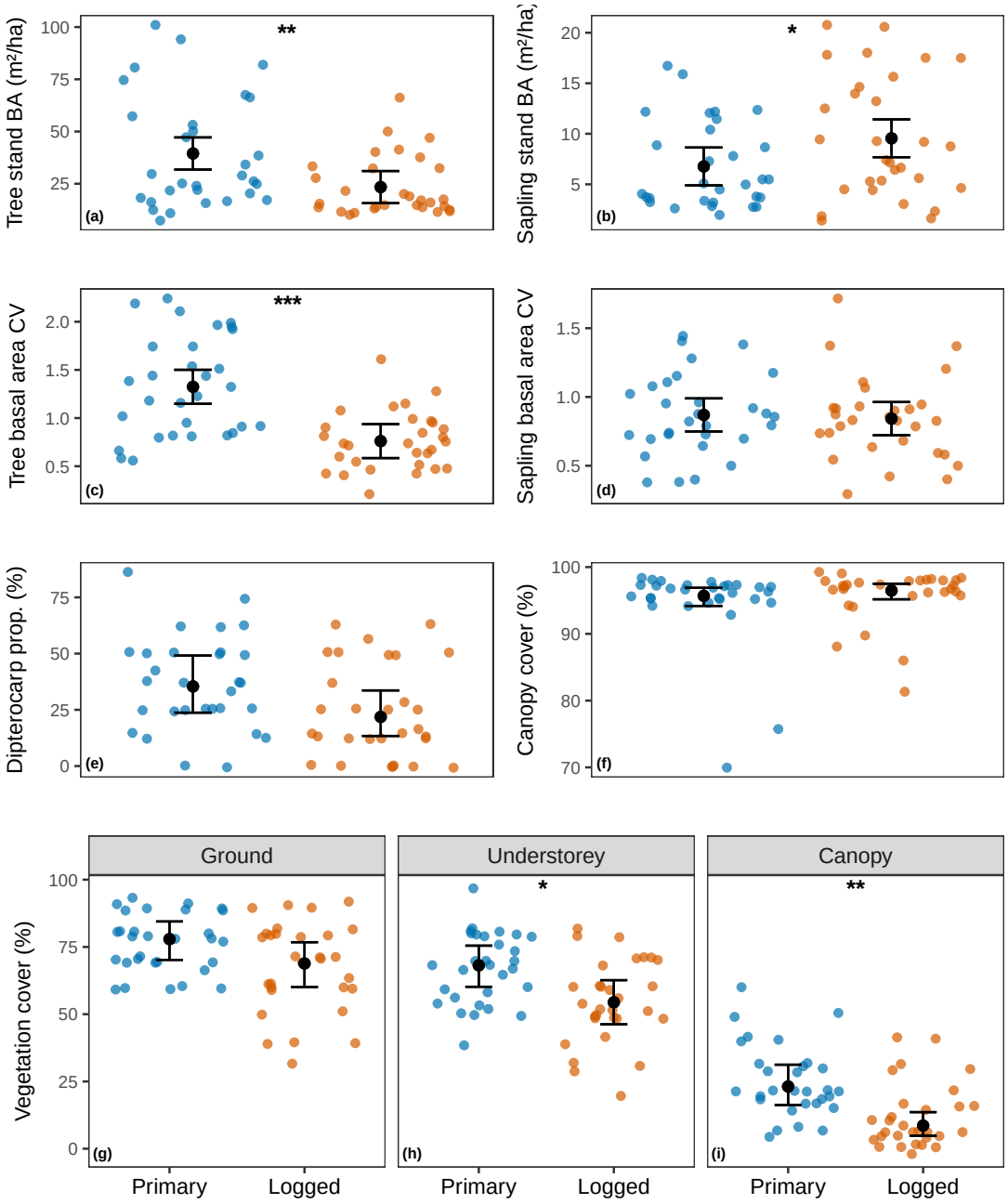

Figure C.4: Comparison between primary forest (blue) and logged forest (orange) for the nine forest structure measures: the stand basal area of trees (a) and saplings (b); the coefficient of variation for tree basal area (c) and sapling basal area (d); the proportion of trees that were in the family Dipterocarpaceae (e); the percentage canopy cover (f); and visual estimates of percentage vegetation at 1.5 m above ground (g), 15 m above ground (h) and > 15 m above ground (i). Statistically significant differences are indicated by asterisks: 0.01 < P < 0.05 (*); 0.001 < P < 0.01 (**) and P < 0.0001 (***). Error bars are 95% confidence intervals.

Appendix D

Supporting information for Chapter 5

D.1 Supplementary analyses for different patch parameters

D.1.1 Methods

Following McGuire et al. (2016) we excluded forest patches less than 10 km^2. This was based on the assumption that excessively small patches are incapable of sustaining populations for long enough to enable range shifts through differential fitness at the leading and trailing edge of a species' range. However, the critical patch size to enable such demographic processes to occur will depend on the species in question, and indeed some species may shift their ranges via within-generation movement of migrating individuals. We tested the influence of minimum patch size by repeating the analyses for patch sizes of 1, 5, 10, 25 and 100 km^2. Note that a minimum size of 1 km^2 corresponds to no exclusions, since this is the resolution of the layers used. To speed up iteration over the different parameters we used a subset of the main data, which excluded land masses less than 10 km^2 and those with a temperature range less than the predicted temperature change under climate warming, since range shifts are unlikely to be sufficient responses to climate change in these land masses.

D.1.2 Results and Discussion

Current climate connectivity was captured by median climate connectivity in 2012, and the proportion of forested area that failed to achieve successful climate connectivity (≥ 0) in 2012. Median climate connectivity differed by realm for all patch sizes assessed ($P < 0.001$; Figure D.1a), and was below zero in all cases except where minimum patch size was 1 km^2. This suggests that for species capable of surviving and reproducing in patch sizes of 1 km^2

or less, current forest cover is sufficiently well-connected along climate gradients that these species should, on average, be able to shift their range within existing forest cover to avoid climate warming. For species requiring a larger critical patch size, tropical forest cover in all biogeographic realms was, on average, insufficient to facilitate such range shifts. For all patch sizes, median climate connectivity was generally lowest in the Neotropics, followed by the Afrotropics, Indomalaya, Australasia and Oceania (precise ranking depended on the minimum patch size applied; Figure D.1a).

The percentage of forest area with unsuccessful climate connectivity (< 0) in the year 2012 varied by biogeographic realm for all minimum patch sizes ($P < 0.001$). Precise ranking varied by minimum patch size (Figure D.1b), but generally the Afrotropics and Indomalaya had the highest proportion of forest failing to connect to future climate analogues, while the Neotropics and Australasia had the lowest. We suggest that low average values of climate connectivity in the Neotropics are somewhat compensated for by the large size of forest patches that do achieve successful climate connectivity. Although the proportion of successfully connected tropical forest was generally more than half of total forest area, a substantial portion of forest failed to achieve climate connectivity and the situation was worse for a larger minimum patch size and when including all land masses in the tropics (see Chapter 5).

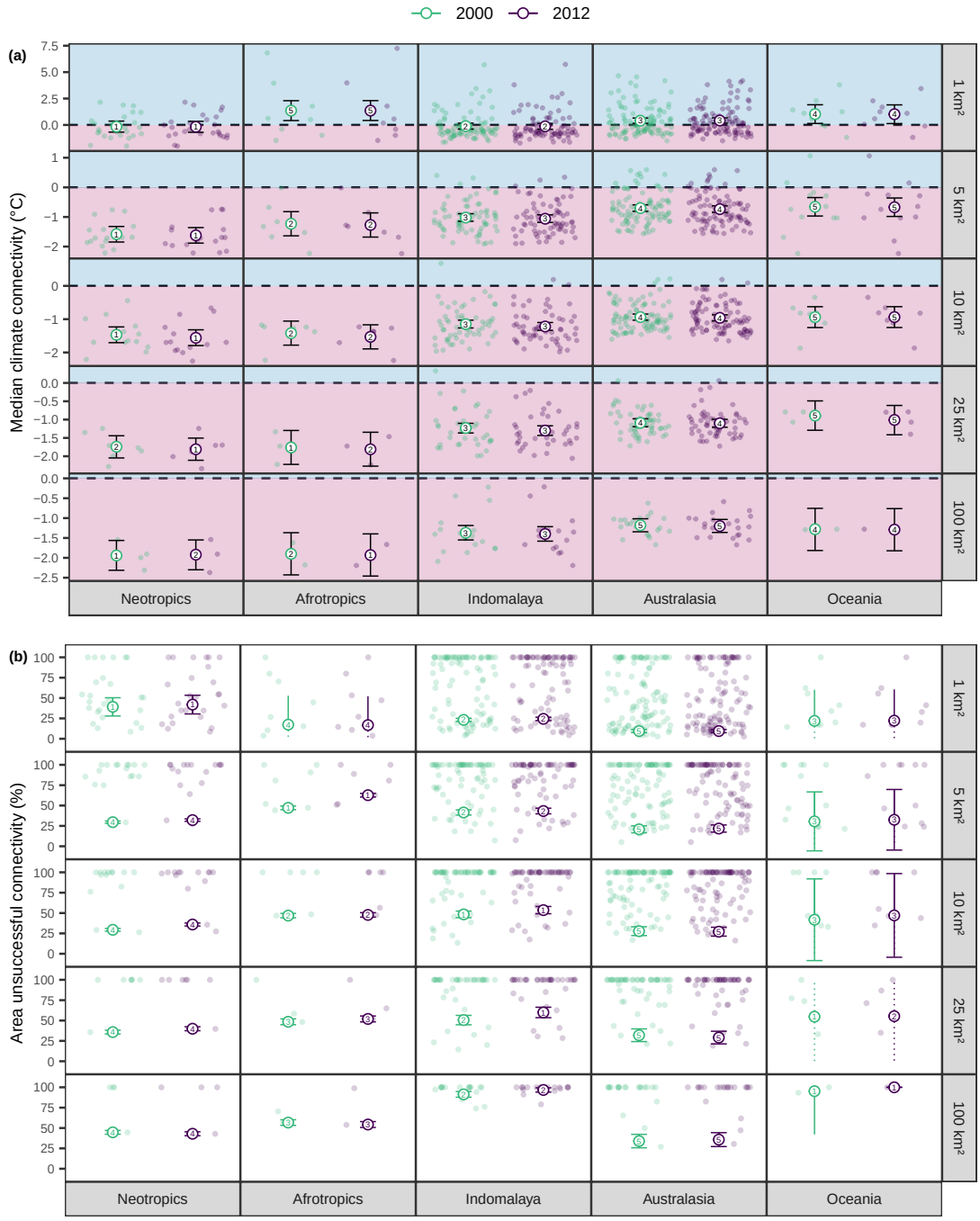

Figure D.1: Climate connectivity in the year 2000 (green) and 2012 (purple), for different values of minimum patch size (rows). Panel (a) shows results for median climate connectivity, with the dashed line indicating zero climate connectivity, at and above which successful climate connectivity is achieved. Panel (b) shows results for the proportion of total forested area that fails to achieve successful climate connectivity. Hollow circles are model-predicted values with 95% confidence intervals. The small number in the centre indicates rank: 1 corresponds to the realm and dataset with the worst climate connectivity, through to 5 for the best. Raw data are plotted in the background as semi-transparent, filled points. Confidence intervals in panel (b) are plotted with dotted lines where they extend beyond 0 or 100%.

From 2000 to 2012 we found that median climate connectivity did not change regardless of the minimum patch size applied ($P > 0.05$; Figure D.1a), and this was true regardless of biogeographic realm ($P > 0.05$; Figure D.1a). The change in proportion of unsuccessfully connected forest was, however, more complicated. For extremes of minimum patch size – either 1 km^2 of 100 km^2 – there was no effect of year ($P > 0.05$; Figure D.1b). In the former case, it may be that any effect of year is masked by the greater amount of noise associated with an abundance of 1 km^2 patches. In the latter case it is likely that so few 100 km^2 patches were present at all that statistical power is lost, as well as the fact that patches of this size are likely to be more robust to relatively small changes in forest cover. For all other patch sizes, the proportion of successfully connected forest decreased from 2000 to 2012 ($P < 0.01$; Figure D.1b). Only for a minimum patch size of 5 km^2 was this relationship affected by realm ($F = 10.9$, $P < 0.001$; Figure D.1b), with a stronger loss of climate connectivity over time for the Afrotropics than in other realms.

Loss of climate connectivity was strongly driven by loss of tree cover, regardless of minimum patch size ($P < 0.001$; Figure D.2). The proportion of forest area losing connectivity differed by realm for all minimum patch sizes ($P < 0.001$; Figure D.2), and was generally highest in Indomalaya, the Neotropics and the Afrotropics. In most cases climate connectivity was lost at an accelerating rate as the area of forest loss increased. It is likely that forest patches become smaller and increasingly isolated as more forest area is lost, to the point where vital connections are severed and climate connectivity is degraded. For minimum patch size of 100 km^2 there was a hump-shaped relationship with tree cover loss, which could be an artefact of there being fewer datapoints for this dataset at high values of tree cover loss.

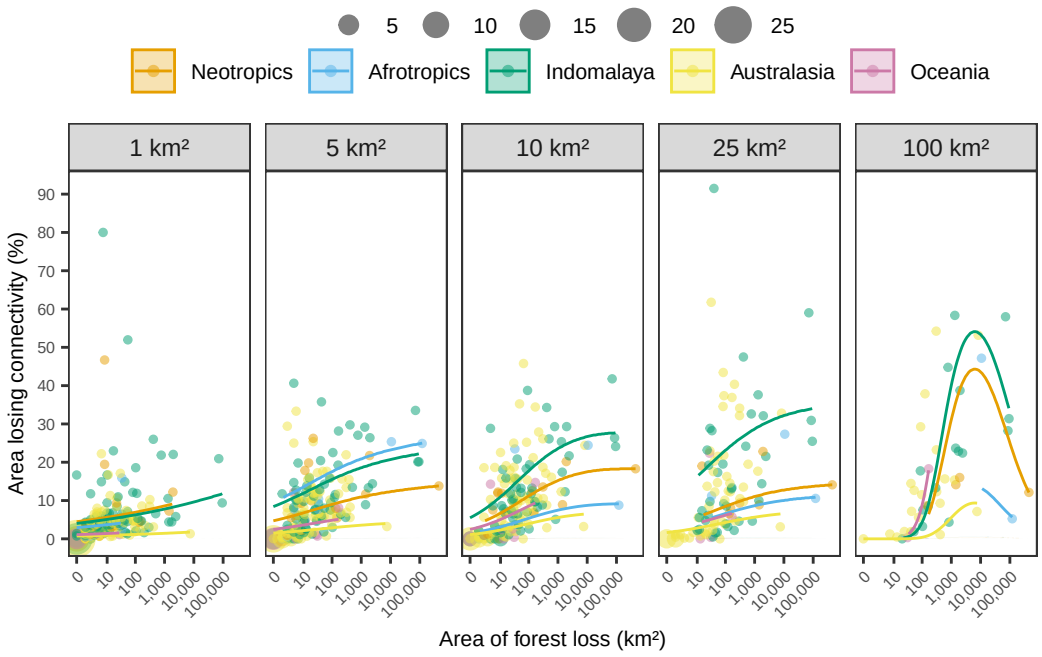

Figure D.2: The proportion of total forested area in each land mass that lost climate connectivity between 2000 and 2012, with increasing area of forest loss and across different biogeographic realms (orange = Neotropics, blue = Afrotropics, green = Indomalaya, yellow = Australasia and pink = Oceania). Points correspond to raw data, with point size indicating the number of observations at that location. Fitted lines derive from model predictions with 95% confidence intervals.

D.2 Supplementary analyses without tree plantations

D.2.1 Methods

The tree cover layers from Hansen et al. (2013) do not currently distinguish between natural forests and tree plantations. However, boundary polygons for tree plantations are available for seven countries: Brazil, Cambodia, Colombia, Indonesia, Liberia, Malaysia, and Peru (Transparent World, 2015). We therefore re-ran our analyses (see Chapter 5: 'Methods') for these seven countries only, with and without cells inside tree plantations. We buffered country polygons by 100 km to prevent artificial truncation of climate gradients (cf. McGuire et al., 2016). Statistical models were analogous to those in Chapter 5, except that biogeographic realm was not included as an explanatory variable because of the smaller and more uneven sample sizes in this subset of the data.

D.2.2 Results and Discussion

Median climate connectivity in 2012 was -1.17°C including cells in tree plantations, versus -1.2°C excluding tree plantations. Median climate connectivity did not differ by year in either case ($P > 0.05$; Figure D.3a). Thus, regardless of the year or inclusion of tree plantations, typical tropical forest fails to connect patches to future analogous climates.

The percentage of forest that failed to achieve successful climate connectivity in 2012 was consistent regardless of whether tree plantations were included (37.6% if including plantations versus 41% excluding plantations), although the trends over time did differ. If cells inside plantations were included, there was a slight decrease (-2.9%) from 2000 to 2012 in the percentage of forest that was unsuccessfully connected ($F = 4.72$, $P < 0.05$; Figure D.3b). The opposite was true when cells inside plantations were excluded ($F = 28.1$, $P < 0.001$; Figure D.3b), with the proportion of unsuccessfully connected forest increasing by 8.6% from 2000 to 2012. The discrepancy between datasets in the effect of year is very likely driven by increasing tree cover inside tree plantations.

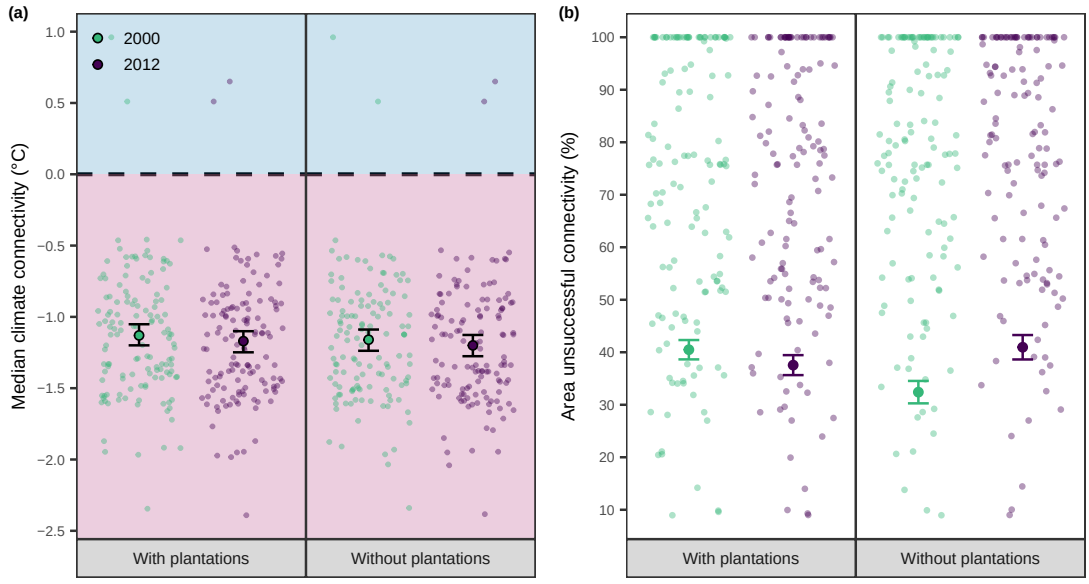

Figure D.3: Climate connectivity in the year 2000 (green) and 2012 (purple), including or excluding cells that fall inside tree plantations. Panel (a) shows results for median climate connectivity, with the dashed line indicating zero climate connectivity, at and above which successful climate connectivity is achieved. Panel (b) shows results for the proportion of total forested area that fails to achieve successful climate connectivity. Solid points are model-predicted values with 95% confidence intervals. Raw data are plotted in the background as semi-transparent points.

From 2000 to 2012, loss of climate connectivity increased with increasing loss of forest area. This was true whether including tree plantations ($F = 96.4$, $P < 0.001$; Figure D.4) or excluding tree plantations ($F = 41.5$, $P < 0.001$; Figure D.4). The relationship for both datasets was weaker than in the full model (see Chapter 5), and when including plantations the relationship appeared to invert for very high loss of forest area. These results may be caused by the smaller sample size and truncation of climate gradients (e.g. from the Amazon to parts of the Andes) when focusing only on countries with tree plantation data. It is also possible that very high loss of forest area is concentrated in places which have already lost climate connectivity, and therefore have little left to lose.

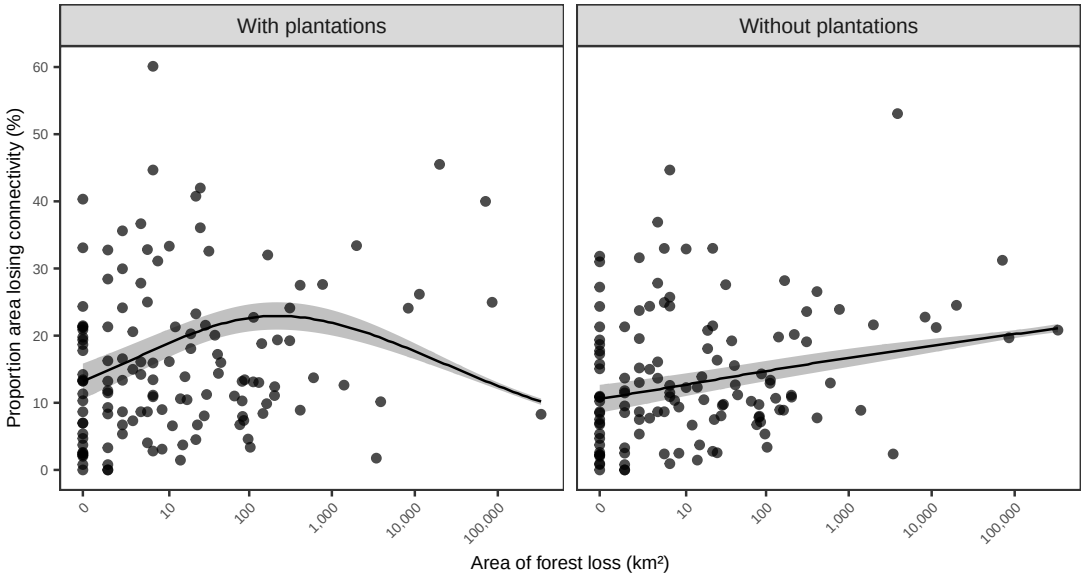

Figure D.4: The proportion of total forested area in each land mass that lost climate connectivity between 2000 and 2012 with increasing area of forest loss, including or excluding cells inside tree plantations. Points correspond to raw data. Fitted lines derive from model predictions with 95% confidence intervals.

D.3 Supplementary analyses for different RCP scenarios

D.3.1 Methods

In Chapter 5 we used Representative Concentration Pathway (RCP) 8.5 to derive Mean Annual Temperature in the year 2070. This is the most severe ('business-as-usual') IPCC scenario (IPCC, 2013), which has thus far been the best predictor of observed climate change (Sanford et al., 2014). However, it is possible that by 2070 stronger mitigating action is taken. We therefore repeated our analyses using RCP2.6, which is the least severe warming scenario. All methods were identical to those in Chapter 5, changing only the layer used for future temperature.

D.3.2 Results and Discussion

For both RCP scenarios, median climate connectivity differed between realms ($P < 0.001$; Figure D.5a), being highest in the Neotropics, Afrotropics and Indomalaya and lowest in Australasia and Oceania. Median climate connectivity was below zero for both scenarios, but closer to zero for RCP2.6 than RCP8.5. The implication is that forest patches across the tropics will generally fail to facilitate species range shifts to the extent that species could completely avoid climate warming, but with mitigation the amount of warming experienced would be less.

The proportion of forest area that failed to achieve successful climate connectivity (≥ 0) in the year 2012 was influenced by biogeographic realm in both RCP scenarios ($P < 0.001$; Figure D.5b). All realms were less successfully connected using RCP8.5 (percentage area that was unsuccessful ranged from 42-71% in RCP8.5 vs. 19-36% in RCP2.6) and the ranking of different realms was also different depending on the RCP scenario. In both scenarios, Indomalaya and Oceania were among the least successfully connected and Australasia the best. The Afrotropics, however, had the lowest proportion of connected forest in 2012 under RCP2.6, but the second highest under RCP8.5. The Neotropics had the second highest proportion of connected forest in 2012 under RCP2.6, versus the second lowest for RCP8.5. Overall, these results suggest that despite the low average climate connectivity in both scenarios of future warming, strong mitigation like that assumed under RCP2.6 could maintain high climate connectivity in large forest patches.

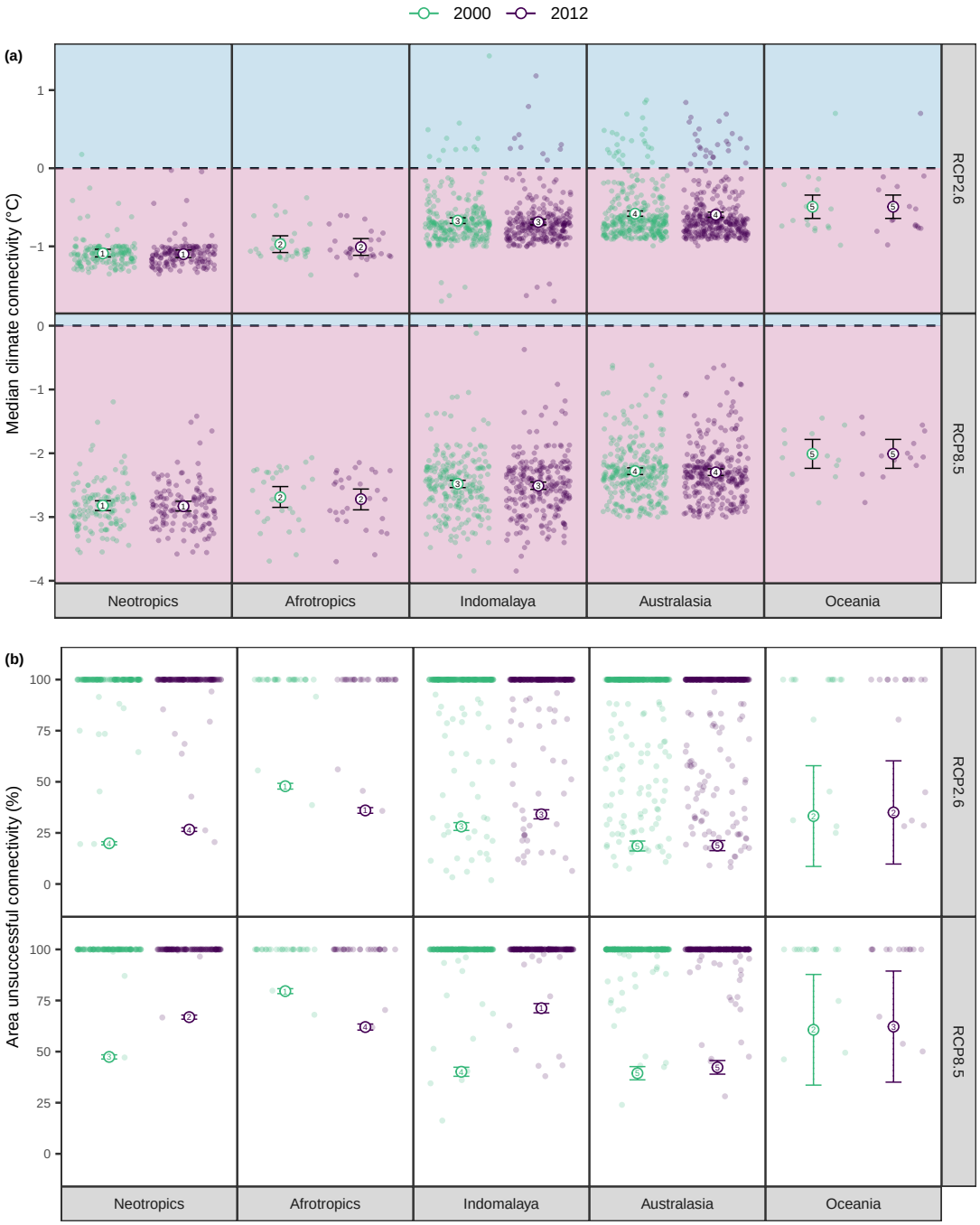

Figure D.5: Climate connectivity in the year 2000 (green) and 2012 (purple), for RCP2.6 (least severe warming scenario) and RCP8.5 (most severe warming scenario). Panel (a) shows results for median climate connectivity, with the dashed line indicating zero climate connectivity, at and above which successful climate connectivity is achieved. Panel (b) shows results for the proportion of total forested area that fails to achieve successful climate connectivity. Hollow circles are model-predicted values with 95% confidence intervals. The small number in the centre indicates rank: 1 corresponds to the smallest y value for that realm and dataset, through to 5 for the highest value. Raw data are plotted in the background as semi-transparent, filled points. Confidence intervals in panel (b) are plotted with dotted lines where they extend beyond 0 or 100%.

For both RCP scenarios we found that median climate connectivity did not change between 2000 and 2012 ($P > 0.05$), and this was consistent across biogeographic realms ($P > 0.05$; Figure D.5b). In contrast, the proportion of forest area that failed to achieve successful climate connectivity was generally higher in 2012 than 2000, for both RCP2.6 ($F = 6.38$, $P < 0.05$; Figure D.5b) and RCP8.5 ($F = 193$, $P < 0.001$; Figure D.5b). Under both scenarios this pattern depended on the biogeographic realm ($P < 0.001$), with the biggest losses in the Neotropics and Indomalaya compared to a decrease in the Afrotropics (Figure D.5b).

The proportion of forest experiencing a decrease in climate connectivity from 2000 to 2012 was influenced by both the area of forest loss ($P < 0.001$) and biogeographic realm ($P < 0.001$; Figure D.6), in both RCP scenarios. Indomalaya and the Neotropics experienced substantial loss of climate connectivity in both scenarios, while the magnitude of change varied between scenarios for the Afrotropics, Oceania and Australasia (Figure D.6). In both scenarios the relationship between connectivity loss and forest loss is non-linear, however under RCP2.6 the steepness of this relationship decreases for very high values of forest loss, while it increases under RCP8.5. This discrepancy should be interpreted with caution since there are only a small number of datapoints at the upper end of the relationship, but the implication is that there is a greater propensity for climate connectivity loss to accelerate under a business-as-usual compared to a strong mitigation scenario.

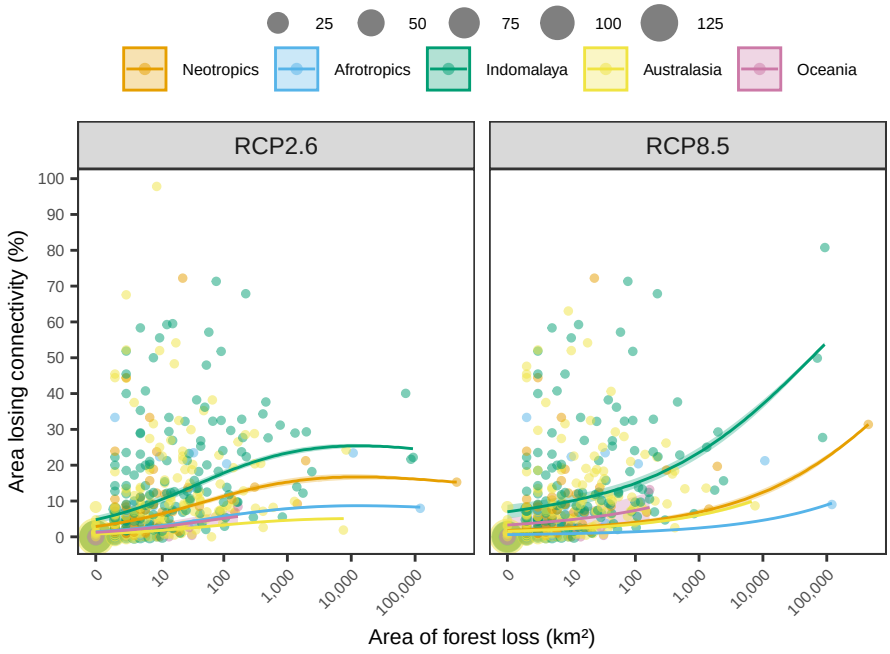

Figure D.6: The proportion of total forested area in each land mass that lost climate connectivity between 2000 and 2012, with increasing area of forest loss and across different biogeographic realms (orange = Neotropics, blue = Afrotropics, green = Indomalaya, yellow = Australasia and pink = Oceania). Points correspond to raw data, with point size indicating the number of observations at that location. Fitted lines derive from model predictions with 95% confidence intervals.

D.4 Worked example of climate connectivity calculation

The following text provides a step-by-step calculation of climate connectivity in the Brazilian states of Rondônia and Mato Grosso.

D.4.1 Step 1: Creating forest patches

Climate connectivity is calculated using climate-partitioned patches of natural habitat (McGuire et al., 2016). In this study natural habitat refers to tropical forest, derived from Hansen et al. (2013) for the years 2000 and 2012. For the year 2000, cells were classed as forested if they had > 50% tree cover (Figure D.7a; Hansen et al., 2013). For the year 2012, cells were classed as forest based on forest loss and forest gain, relative to forest cover in 2000 (Figure D.7b). If a cell experienced forest loss, it had gone from a forested to non-forested state between 2000 and 2012 and was classed as non-forest. If a cell had experienced forest gain, it had gone from a non-forested to forested state between 2000 and 2012; providing there had been no concomitant loss, the cell was classed as forest. All subsequent steps were applied separately to forest cover in 2000 and 2012.

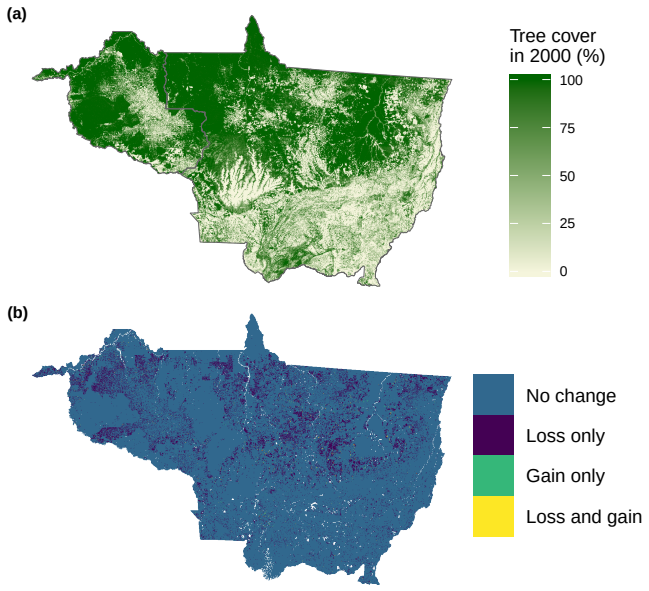

Figure D.7: Tree cover in the year 2000 (a) ranges from low (beige) to high (dark green). Tree cover change from 2000 to 2012 (b) includes: no change (blue), forest loss (purple), forest gain (green) or both loss and gain (yellow). Both layers derive from Hansen et al. (2013), and are used to classify cells into either forest or non-forest in the years 2000 and 2012.

We used Mean Annual Temperature (MAT) as our climate variable, which is the first bioclimatic variable of the WorldClim database (Version 1.4; Hijmans et al., 2005). All layers (forest cover and climate data) were projected into the World Cylindrical Equal

Area projection and re-sampled to 1 km^2 resolution. Current climate (~1950-2000) was assigned to forested cells, and rounded to increments of 0.5°C. Adjacent cells with the same temperature were assigned to the same patch (Figure D.8). Patches less than 10 km^2 in area were removed, and patches within 2 km of each other were assigned to the same patch. Once forest patches had been determined we re-calculated current temperature (so it was no longer rounded to increments of 0.5°C), and calculated future temperature for each patch in the year 2070 (2061-2080) using data from the HadGEM2-AO general circulation model (IPCC, 2013) and Representative Concentration Pathway (RCP) 8.5, which is the most severe ('business-as-usual') IPCC scenario.

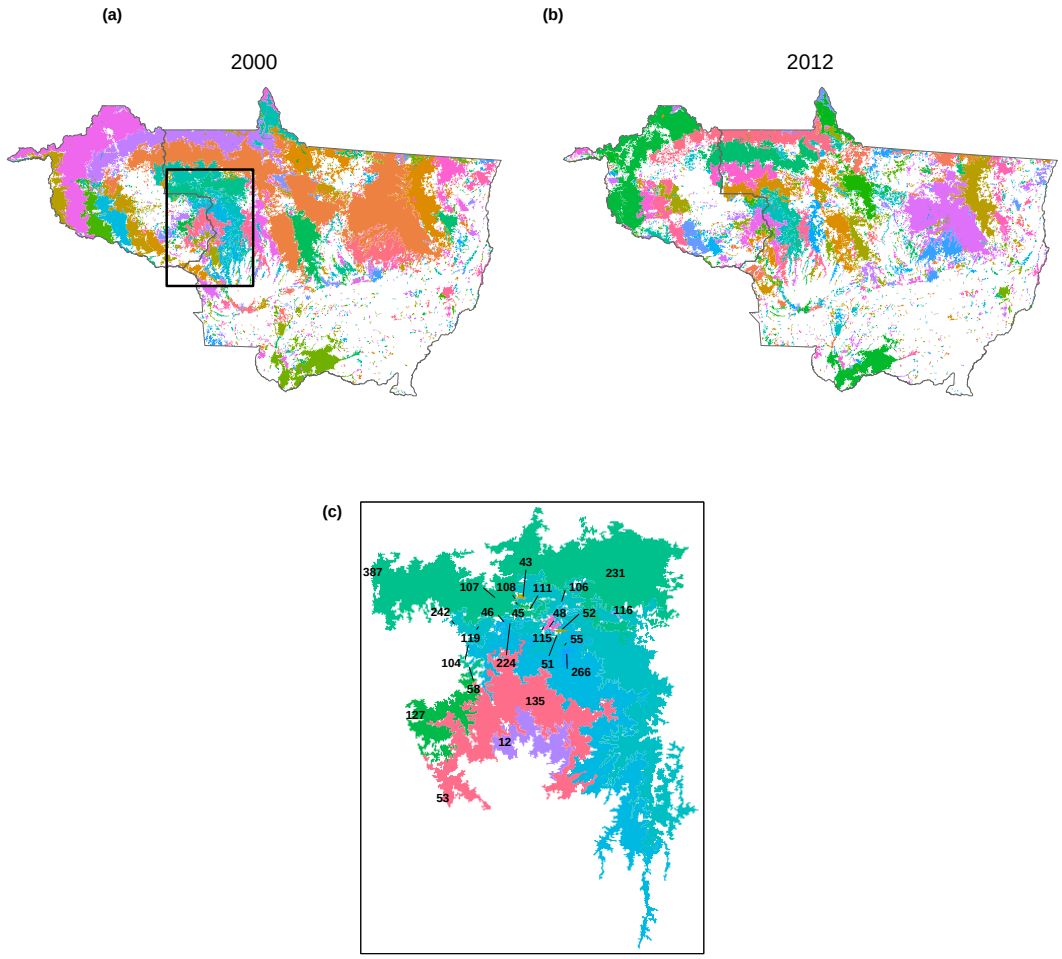

Figure D.8: Forest patches in 2000 (a) and 2012 (b). Black inset (c) corresponds to magnified view of the subset of patches used below to calculate climate connectivity. Shading indicates unique patches and numbers correspond to patch identities, a sample of which can be found in Table D.1.

D.4.2 Step 2: Identifying destination patches

Climate connectivity for a given patch depends on the difference between the current temperature of that patch, and the future temperature of the coolest patch that can be reached by traversing a gradient of hotter to cooler adjacent patches (McGuire et al., 2016). The aim of this next step, therefore, was to determine the coolest destination patch for each origin patch.

(a)

patch1	patch2	temp1	temp2
12	53	22.0	22.5
43	108	22.7	22.9
43	224	22.7	23.5
43	387	22.7	24.0
45	111	22.6	22.9
45	224	22.6	23.5

(b)

origin	dest	origin_temp	dest_temp
53	12	22.5	22.0
108	43	22.9	22.7
224	43	23.5	22.7
387	43	24.0	22.7
111	45	22.9	22.6
224	45	23.5	22.6

Table D.1: Dataframe of patch neighbours before (a) and after (b) sorting neighbours into either the hotter origin patch or cooler destination patch.

We first identified, for each pair of neighbouring patches, which of the two was the hotter 'origin' patch and which was the cooler 'destination' patch (Table D.1). In the code snippets below, `nbr` refers to a dataframe of patch neighbours, and `temp_dat` is a dataframe of the current and future temperature for all patches.

```
nbr$origin <- NA
nbr$dest <- NA
nbr$origin_temp <- NA
nbr$dest_temp <- NA

for (i in 1:nrow(nbr)){
    # If temp1 is more than temp2, patch1 is the origin and
    # patch 2 is the destination
    if(nbr$temp1[i] > nbr$temp2[i]){
        nbr$origin[i] <- nbr$patch1[i]
        nbr$origin_temp[i] <- nbr$temp1[i]
        nbr$dest[i] <-nbr$patch2[i]
        nbr$dest_temp[i] <- nbr$temp2[i]
    # If temp2 is more than temp1, patch2 is the origin and
    # patch 1 is the destination
    }else{
        nbr$origin[i]<- nbr$patch2[i]
```

```
        nbr$origin_temp[i] <- nbr$temp2[i]
        nbr$dest[i]<-nbr$patch1[i]
        nbr$dest_temp[i] <- nbr$temp1[i]
    }
}
```

Most patches have multiple neighbours, so we next identified *all* the neighbours for each origin patch (assigned to: `connections`). For example, we can see below that origin patch 135 has only one neighbour: patch 53. Patch 231 has no neighbours, and patch 224 has many.

```
connections <-
    sapply(1:nrow(temp_dat), function(x){
        nbr$dest[nbr$origin == temp_dat[x,"patch"]]
    })
names(connections) <- temp_dat$patch
# Look at a subset of patch connections:
connections[20:22]
```

```
## $`135`
## [1] 53
##
## $`224`
##  [1]  43  45  48  51  52  53 104 106 108 111 115 116
##
## $`231`
## integer(0)
```

To determine the final, coolest destination patch that can be reached from each origin patch, we traced the path according to which of the immediate neighbours was the coolest. This step was done by iterating over unique patch temperatures (`uniquetemps`), from cooler to hotter.

```
uniquetemps <- sort(unique(temp_dat$temp))
uniquetemps
```

```
##  [1] 22.0 22.5 22.6 22.7 22.8 22.9 23.0 23.1 23.3 23.5 23.6 24.0
```

We created variables in `temp_dat` to populate with the temperature and patch identity of the final destination patch for each origin patch, and created a copy of this dataframe called `running`. The dataframe `running` is updated with each iteration.

```
# Set up output columns
temp_dat$dest <- NA
temp_dat$dest_temp <- NA
temp_dat$inter_patch <- NA

# Copy the original dataframe
running <- temp_dat[, c("patch", "temp")]
```

In each iteration through unique temperatures (from cooler to warmer) we identified:

- The origin patches that corresponded to that temperature;
- The coolest neighbour of each origin patch;

And subsequently we:

- Populated the empty columns in our original dataframe with the patch identity and temperature of the final destination patch of the coolest neighbour;
- Updated the `running` dataframe, to track the pathway from each origin patch to its final destination patch (which may or may not be an immediate neighbour).

The iterations below were run in a loop, but for illustrative purposes we will iterate over each unique temperature manually.

D.4.3 Iteration 1

We begin by defining the focal unique temperature of this iteration. In this case, it's the first (i.e. coolest) value from our previously defined vector of unique temperatures, `uniquetemps`.

```
this_temp <- uniquetemps[1]
this_temp
```

```
## [1] 22
```

Next we define the indices of all patches that are 22°C (`inds`).

```
inds <- which(running[,"temp"] == this_temp)
running[inds, "patch"]
```

```
## [1] 12
```

Patch number 12 is the only patch at this temperature. Now we need to see if patch 12 has any associated destination patches:

```
length(connections[[inds]]) > 0
```

```
## [1] FALSE
```

No, therefore the final destination patch and the final destination temperature are the same as the origin: patch 12, temperature 22°C. The reason that we use the `running` dataframe (a copy of the original `temp_dat` dataframe) to retrieve the temperature and identity of the destination patch will become clear in later iterations (i.e. Iteration 5).

```
temp_dat$dest[inds]<- running[inds, "patch"]
temp_dat$dest_temp[inds]<- this_temp
```

Let's look at the row in our dataframe that we have just populated:

```
temp_dat[inds,]
```

```
##   patch temp ftemp dest dest_temp inter_patch
## 1    12   22    25   12        22          NA
```

Note that because the origin and destination patch are the same, there are no intermediate patches and so the value for `inter_patch` remains NA.

D.4.4 Iteration 2

Moving onto the next unique temperature. This iteration is more complicated because the origin patch *does* have one or more neighbouring destination patches.

```
this_temp <- uniquetemps[2]
this_temp
```

```
## [1] 22.5
```

Again we define the indices of all patches that have this temperature (22.5°C).

```
inds <- which(running[,"temp"] == this_temp)
running[inds, "patch"]
```

```
## [1] 53 58
```

This time both patch 53 and patch 58 have the temperature that we're interested in. We start with patch 53 (index 1 in the vector `inds`).

Are there any associated destination patches?

```
length(connections[[inds[1]]]) > 0
```

```
## [1] TRUE
```

Yes. We define the indices of the destination patches as well (`dest_inds`).

```
dest_inds <- which(temp_dat$patch %in%  connections[[inds[1]]])
```

There may be multiple destination patches, so we need to identify the minimum temperature across all of them (`t`), as well as the index of the patch (or patches) that correspond to this minimum temperature (`min_ind`).

```
t <- min(running[dest_inds, "temp"])
t
```

```
## [1] 22
```

```
min_ind <- which(running[dest_inds, "temp"] == t)
```

Is there more than one destination patch that has this minimum temperature (22°C)?

```
length(min_ind) > 1
```

```
## [1] FALSE
```

No, so `min_ind` is the index of the destination patch that we're interested in. If there were more than one destination patch with the same minimum temperature, the first would be used arbitrarily.

Which patch does this index correspond to?

```
temp_dat$patch[min_ind]
```

```
## [1] 12
```

Patch 12. This is the final destination patch for patch 53. We assign the final temperature (22°C) and the identity of the final destination patch (12) to the associated origin patch (53) in our original dataframe, `temp_dat`.

```
temp_dat$dest_temp[inds[1]] <- t
temp_dat$dest[inds[1]] <- running$patch[min_ind]
```

We must also update the `running` dataframe so that patch 53 acquires the temperature and identity of patch 12. This step is vital for constructing more complicated pathways. In this

example, since the final destination of patch 53 is patch 12, any origin patches in subsequent iterations whose neighbouring destination is patch 53 (see Iteration 5) will be assigned the final destination temperature and identity of patch 12, *not* patch 53.

```
running$temp[inds[1]] <- t
running$patch[inds[1]] <- running$patch[min_ind]
```

Finally, we capture intermediate patches that are traversed from origin to destination. The path from patch 53 to patch 12 cannot have intermediate patches because patch 12 is its own destination (there were no neighbouring patches that were cooler; see Iteration 1).

```
inter_patch <- temp_dat[min_ind, "inter_patch"]
is.na(inter_patch)
```

```
## [1] TRUE
```

We assign the final destination patch as the only intermediate patch. This is not strictly necessary since we have already recorded patch 12 as part of the path because it is the destination. However, this step highlights the fact that in this iteration the destination patch is not the same as the origin patch.

```
temp_dat$inter_patch[inds[1]] <- temp_dat[min_ind, "patch"]
```

We can now check the row for patch 53 in `temp_dat` and in the `running` dataframe. Note how in the `running` dataframe the row associated with patch 53 now has the identity and temperature of patch 12 instead.

```
temp_dat[inds[1],]
```

```
##   patch temp ftemp dest dest_temp inter_patch
## 8    53 22.5  25.6   12        22          12
```

```
running[inds[1],]
```

```
##   patch temp
## 8    12   22
```

Remembering that there were two origin patches corresponding to the focal temperature of this iteration (22.5°C), we must now repeat the above process for patch 58 (index 2 in the vector `inds`).

Does patch 58 have any neighbouring destination patches?

```
length(connections[[inds[2]]]) > 0
```

```
## [1] FALSE
```

No. As with Iteration 1, we assign the final destination temperature and patch identity to be the same as the origin.

```
temp_dat$dest[inds[2]]<- running[inds[2], "patch"]
temp_dat$dest_temp[inds[2]]<- this_temp
temp_dat[inds[2],]
```

```
##    patch temp ftemp dest dest_temp inter_patch
## 10    58 22.5  25.5   58      22.5          NA
```

D.4.5 Iteration 5

We will now skip ahead to the fifth unique temperature, which illustrates the importance of updating the `running` dataframe in each iteration and using this to assign the temperature and identity of the final destination patch.

```
this_temp <- uniquetemps[5]
this_temp
```

```
## [1] 22.8
```

```
inds <- which(running[,"temp"] == this_temp)
running[inds, "patch"]
```

```
## [1] 135
```

Patch 135 is the only origin patch that is 22.8°C. Does it have any neighbouring destination patches?

```
length(connections[[inds[1]]]) > 0
```

```
## [1] TRUE
```

```
dest_inds <- which(temp_dat$patch %in%  connections[[inds[1]]])
```

Yes. Of the one or more neighbouring destination patches, what is the minimum temperature and what is the index of the corresponding patch?

```
t <- min(running[dest_inds, "temp"])
t
```

```
## [1] 22
```

```
min_ind <- dest_inds[which(running[dest_inds, "temp"] == t)]
```

Is there more than one destination patch at this minimum temperature (22°C)?

```
length(min_ind) > 1
```

```
## [1] FALSE
```

```
temp_dat$patch[min_ind]
```

```
## [1] 53
```

No. Patch 53 is the destination for patch 135. At this point, note that patch 53 was encountered in Iteration 2, and is itself connected to patch 12. As such, the row corresponding to the index of patch 53 actually has the temperature and identity of patch 12:

```
running[min_ind,]
```

```
##   patch temp
## 8    12   22
```

Because the final destination temperature and patch identity are retrieved from the `running` dataframe, we assign the final destination identity and temperature as patch 12, 22°C.

```
temp_dat$dest_temp[inds[1]] <- t
temp_dat$dest[inds[1]] <- running$patch[min_ind]
```

We again update the `running` dataframe. In subsequent iterations any origin patch whose coolest neighbour is patch 135 will also be assigned the final destination temperature and identity of patch 12.

```
running$temp[inds[1]] <- t
running$patch[inds[1]] <- running$patch[min_ind]
```

Lastly, we define the intermediate patches.

```
inter_patch <- temp_dat[min_ind, "inter_patch"]
is.na(inter_patch)
```

```
## [1] FALSE
```

In this case, of course, there *is* an intermediate patch between the origin and the destination – patch 53. We paste this patch together with the final destination to construct the full pathway from origin to destination.

```
temp_dat$inter_patch[inds[1]] <-
    paste(temp_dat[min_ind, "patch"],
          inter_patch[!(is.na(inter_patch))],
          sep = ";")
```

Let's inspect the rows that we have just populated:

```
temp_dat[inds[1],]
```

```
##    patch temp ftemp dest dest_temp inter_patch
## 20   135 22.8  25.9   12        22       53;12
```

```
running[inds[1],]
```

```
##    patch temp
## 20    12   22
```

D.4.6 Step 3: Calculating climate connectivity

At this point we know the current and future temperature of all patches (Step 1), and the identity and current temperature of their final destination patches (Step 2). Combining this information we can easily assign to each origin patch the future temperature of its destination patch:

```
temp_dat$dest_ftemp <-
    vapply(1:nrow(temp_dat), function(x){
        dest <- temp_dat$dest[x]
        dest_ftemp <- temp_dat$ftemp[temp_dat$patch == dest]
        return(dest_ftemp)
    }, FUN.VALUE = numeric(1))
```

Finally, we calculate climate connectivity. Conceptually, climate connectivity is the maximum temperature difference that can be achieved by traversing a gradient of hotter to cooler adjacent patches. Mathematically, this is calculated as the current temperature of the origin patch minus the future temperature of the destination patch. If this value is zero or positive

then climate connectivity is successful – organisms could potentially reach a forest patch that, under climate change, is the same as or cooler than where they currently are.

```
temp_dat$clim_conn <- temp_dat$temp - temp_dat$dest_ftemp
```

Final results can be seen in Figure D.9 and Table D.2. Table D.3 demonstrates what the `running` dataframe looks like after having updated for each iteration.

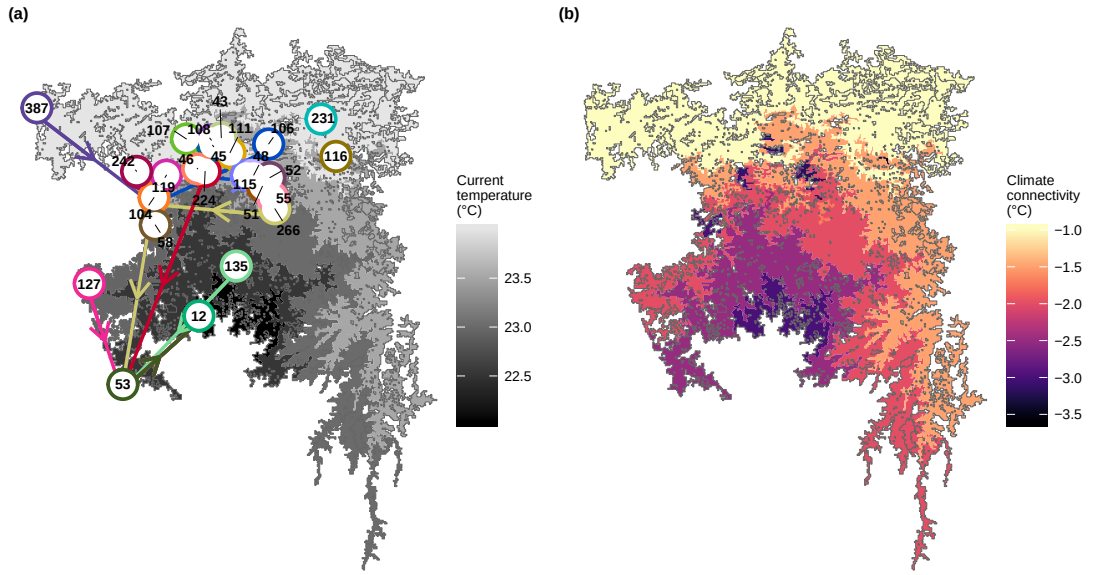

Figure D.9: Pathways from origin to destination patches (a) and climate connectivity across all patches (b). In panel (a), patch shading corresponds to current mean annual temperature (°C), from cooler (black) to hotter (light grey). Circles indicate patch centroids, the numbers inside correspond to the patch identity (as in Tables D.1, D.2 and D.3) and the arrows between indicate the direction of travel from hotter to cooler patches. In panel (b), patch shading corresponds to climate connectivity (°C), measured as the current temperature of the origin patch minus the future temperature of the destination patch. All values here are negative, indicating that existing forest cover would fail to facilitate range shifts to an analogous future climate.

patch	temp	ftemp	dest	dest_temp	inter_patch	dest_ftemp	clim_conn
12	22.0	25.0	12	22.0	NA	25.0	-3.0
43	22.7	26.0	43	22.7	NA	26.0	-3.3
45	22.6	25.8	45	22.6	NA	25.8	-3.2
46	22.6	25.7	46	22.6	NA	25.7	-3.1
48	22.6	25.8	48	22.6	NA	25.8	-3.2
51	22.7	25.8	51	22.7	NA	25.8	-3.1
52	22.6	25.8	52	22.6	NA	25.8	-3.2
53	22.5	25.6	12	22.0	12	25.0	-2.5
55	22.6	25.8	55	22.6	NA	25.8	-3.2
58	22.5	25.5	58	22.5	NA	25.5	-3.0
104	23.0	26.1	12	22.0	53;12	25.0	-2.0
106	23.1	26.2	12	22.0	104;53;12	25.0	-1.9
107	22.9	26.5	107	22.9	NA	26.5	-3.6
108	22.9	26.1	43	22.7	43	26.0	-3.1
111	22.9	26.0	45	22.6	45	25.8	-2.9
115	23.0	26.1	48	22.6	48	25.8	-2.8
116	23.1	26.5	116	23.1	NA	26.5	-3.4
119	23.0	26.1	119	23.0	NA	26.1	-3.1
127	23.0	25.9	12	22.0	53;12	25.0	-2.0
135	22.8	25.9	12	22.0	53;12	25.0	-2.2
224	23.5	26.6	12	22.0	53;12	25.0	-1.5
231	23.6	26.9	231	23.6	NA	26.9	-3.3
242	23.5	26.5	12	22.0	104;53;12	25.0	-1.5
266	23.3	26.4	12	22.0	104;53;12	25.0	-1.7
387	24.0	27.1	12	22.0	104;53;12	25.0	-1.0

Table D.2: The results dataframe with final destination patches, final temperatures and climate connectivity for each origin patch.

patch	temp
12	22.0
43	22.7
45	22.6
46	22.6
48	22.6
51	22.7
52	22.6
12	22.0
55	22.6
58	22.5
12	22.0
12	22.0
107	22.9
43	22.7
45	22.6
48	22.6
116	23.1
119	23.0
12	22.0
12	22.0
12	22.0
231	23.6
12	22.0
12	22.0
12	22.0

Table D.3: The `running` dataframe, after updating with each iteration through unique temperatures. Note the repeated appearance of patch 12, which is a common final destination patch.

D.5 Supplementary Figures

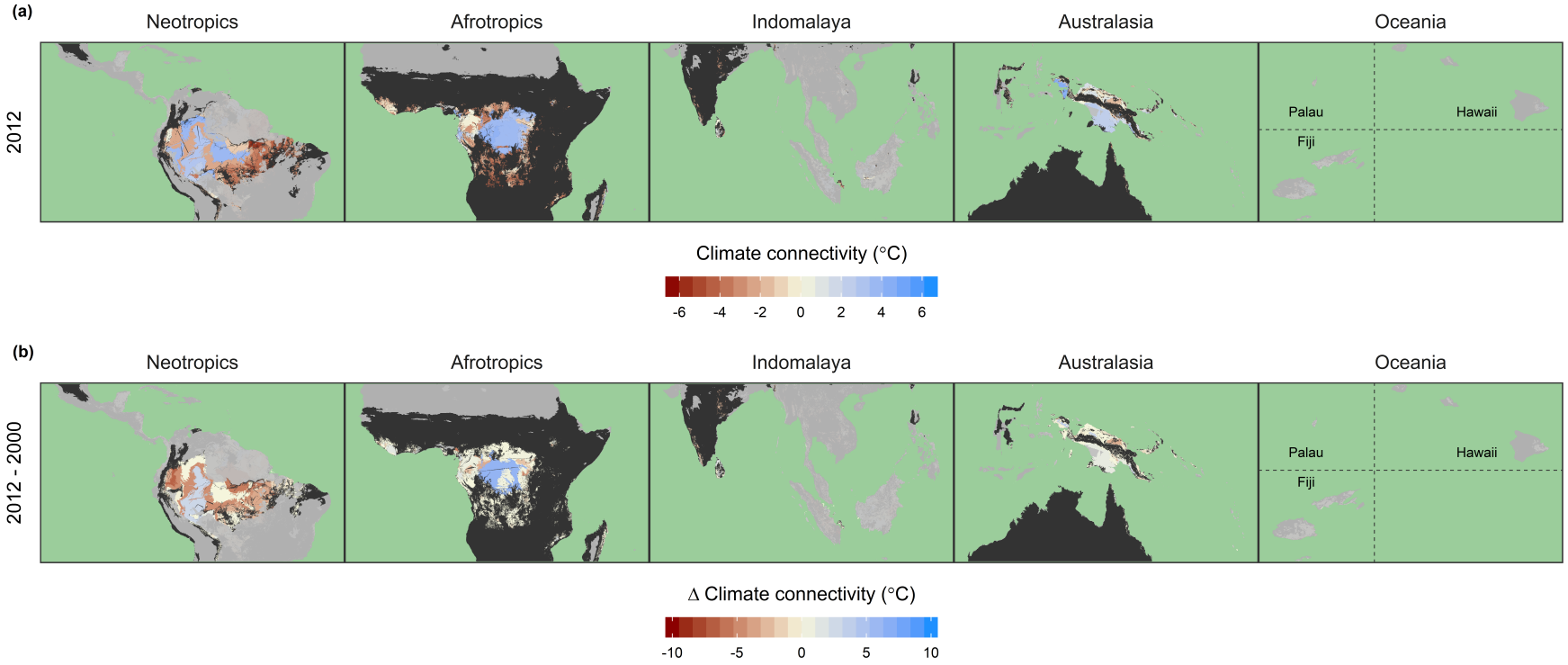

Figure D.10: Climate connectivity in 2012 (a) and change in climate connectivity from 2000 to 2012 (b) overlaid with areas of high climate vulnerability for mammals derived from Pacifici et al. (2018) (regions outside of these areas are masked in grey). We defined high vulnerability areas as those where more than 50% of mammal species had a negative predicted response to climate change. As in Chapter 5 (Figure 5.1), positive values (blue) indicate successful climate connectivity in panel (a), or a gain of connectivity in panel (b). Negative values (red) indicate unsuccessful climate connectivity in panel (a), or a loss of connectivity in panel (b). To aid visualisation we have shifted land masses in Oceania.

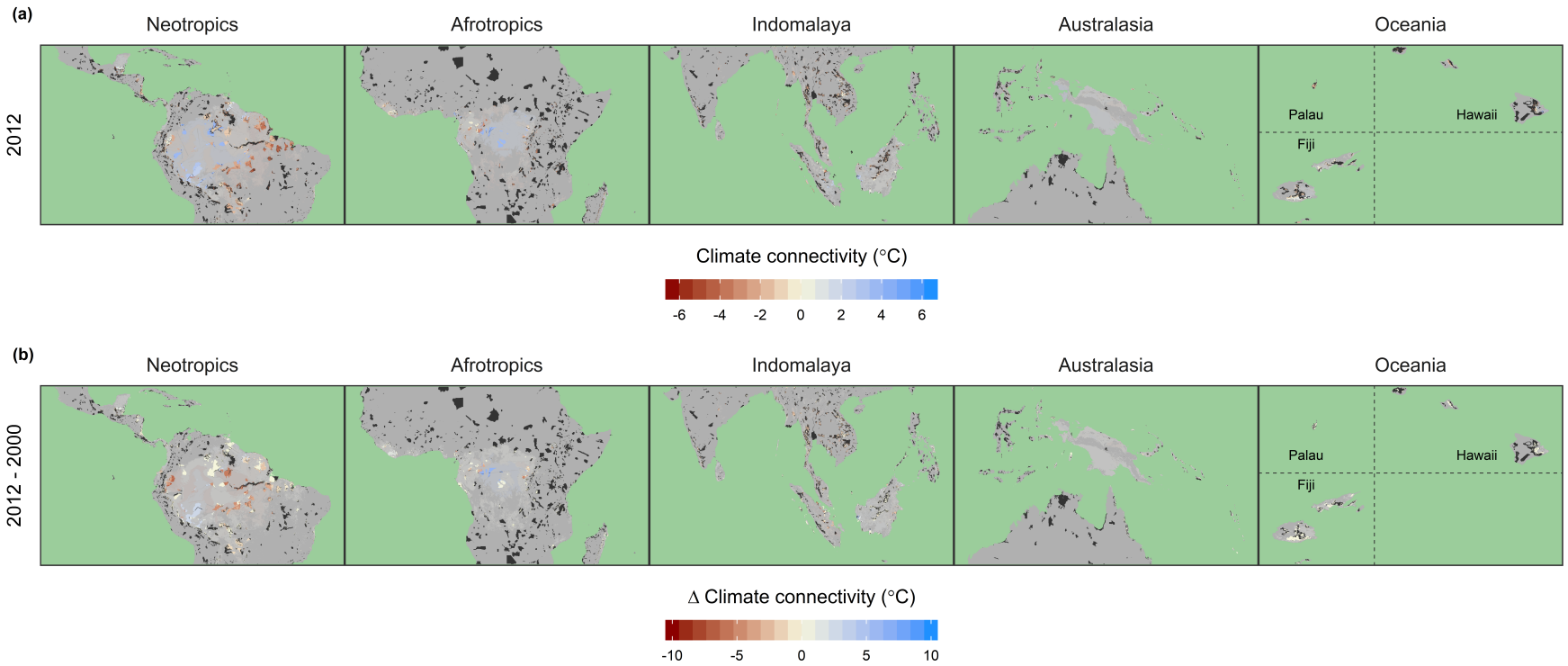

Figure D.11: Climate connectivity in 2012 (a) and change in climate connectivity from 2000 to 2012 (b) overlaid with Key Biodiversity Areas from BirdLife International (regions outside of these areas are masked in grey). As in Chapter 5 (Figure 5.1), positive values (blue) indicate successful climate connectivity in panel (a), or a gain of connectivity in panel (b). Negative values (red) indicate unsuccessful climate connectivity in panel (a), or a loss of connectivity in panel (b). To aid visualisation we have shifted land masses in Oceania.

Bibliography

Adachi, M., Bekku, Y. S., Rashidah, W., Okuda, T., and Koizumi, H. (2006). Differences in soil respiration between different tropical ecosystems. *Applied Soil Ecology*, 34(2–3):258–265.

Agrawal, A., Cashore, B., Hardin, R., Shepherd, G., Benson, C., and Miller, D. (2013). Economic contributions of forests. In *Background Paper 1. United Nations Forum on Forests 10th Session, Istanbul, Turkey*. Available at http://www.un.org/esa/forests/pdf/session_documents/unff10/EcoContrForests.pdf.

Aide, T. M., Clark, M. L., Grau, H. R., López-Carr, D., Levy, M. A., Redo, D., Bonilla-Moheno, M., Riner, G., Andrade-Núñez, M. J., and Muñiz, M. (2013). Deforestation and Reforestation of Latin America and the Caribbean (2001–2010). *Biotropica*, 45(2):262–271.

Asner, G. P., Keller, M., Pereira, Rodrigo, J., Zweede, J. C., and Silva, J. N. M. (2004). Canopy Damage and Recovery After Selective Logging in Amazonia: Field and Satellite Studies. *Ecological Applications*, 14(sp4):280–298.

Asner, G. P., Rudel, T. K., Aide, T. M., Defries, R., and Emerson, R. (2009). A contemporary assessment of change in humid tropical forests. *Conservation Biology*, 23(6):1386–1395.

Badejo, M. A. (1990). Seasonal abundance of soil mites (*Acarina*) in two contrasting environments. *Biotropica*, 22(4):382–390.

Badejo, M. A., De Aquino, A. M., De-Polli, H., and Correia, M. E. F. (2004). Response of soil mites to organic cultivation in an ultisol in southeast Brazil. *Experimental & Applied Acarology*, 34(3-4):345–364.

Bagchi, R., Hole, D. G., Butchart, S. H. M., Collingham, Y. C., Fishpool, L. D., Plumptre, A. J., Owiunji, I., Mugabe, H., and Willis, S. G. (2018). Forecasting potential routes for movement of endemic birds among important sites for biodiversity in the Albertine Rift under projected climate change. *Ecography*, 41(2):401–413.

Baillie, J., Hilton-Taylor, C., and Stuart, S. N. (2004). *2004 IUCN Red List of Threatened Species. A Global Species Assessment*. IUCN, Gland, Switzerland and Cambridge, United Kingdom.

Ball, I. R., Lindenmayer, D. B., and Possingham, H. P. (1999). A tree hollow dynamics simulation model. *Forest Ecology and Management*, 123(2–3):179–194.

Balmford, A., Bruner, A., Cooper, P., Costanza, R., Farber, S., Green, R. E., Jenkins, M., Jefferiss, P., Jessamy, V., and Madden, J. (2002). Economic reasons for conserving wild nature. *Science*, 297(5583):950–953.

Barlow, J., França, F., Gardner, T. A., Hicks, C. C., Lennox, G. D., Berenguer, E., Castello, L., Economo, E. P., Ferreira, J., Guénard, B., Leal, C. G., Isaac, V., Lees, A. C., Parr, C. L., Wilson, S. K., Young, P. J., and Graham, N. A. J. (2018). The future of hyperdiverse tropical ecosystems. *Nature*, 559(7715):517–526.

Barlow, J., Lennox, G. D., Ferreira, J., Berenguer, E., Lees, A. C., Nally, R. M., Thomson, J. R., Ferraz, S. F. d. B., Louzada, J., Oliveira, V. H. F., Parry, L., Ribeiro de Castro Solar, R., Vieira, I. C. G., Aragão, L. E. O. C., Begotti, R. A., Braga, R. F., Cardoso, T. M., Jr, R. C. d. O., Souza Jr, C. M., Moura, N. G., Nunes, S. S., Siqueira, J. V., Pardini, R., Silveira, J. M., Vaz-de Mello, F. Z., Veiga, R. C. S., Venturieri, A., and Gardner, T. A. (2016). Anthropogenic disturbance in tropical forests can double biodiversity loss from deforestation. *Nature*, 535(7610):144–147.

Barnosky, A. D., Matzke, N., Tomiya, S., Wogan, G. O. U., Swartz, B., Quental, T. B., Marshall, C., McGuire, J. L., Lindsey, E. L., Maguire, K. C., Mersey, B., and Ferrer, E. A. (2011). Has the Earth's sixth mass extinction already arrived? *Nature*, 471(7336):51–57.

Bates, D., Mächler, M., Bolker, B., and Walker, S. (2015). Fitting Linear Mixed-Effects Models Using lme4. *Journal of Statistical Software*, 67(1):1–48.

Berry, N. J., Phillips, O. L., Ong, R. C., and Hamer, K. C. (2008). Impacts of selective logging on tree diversity across a rainforest landscape: the importance of spatial scale. *Landscape Ecology*, 23(8):915–929.

Betts, M. G., Wolf, C., Ripple, W. J., Phalan, B., Millers, K. A., Duarte, A., Butchart, S. H. M., and Levi, T. (2017). Global forest loss disproportionately erodes biodiversity in intact landscapes. *Nature*, 547(7664):441–444.

Bivand, R. and Piras, G. (2015). Comparing implementations of estimation methods for spatial econometrics. *Journal of Statistical Software, Articles*, 63(18):1–36.

Blakely, T. J. and Didham, R. K. (2008). Tree holes in a mixed broad-leaf–podocarp rain forest, New Zealand. *New Zealand Journal of Ecology*, 32(2):197–208.

Bradshaw, W. E. and Holzapfel, C. M. (2006). Evolutionary Response to Rapid Climate Change. *Science*, 312(5779):1477–1478.

Bramer, I., Anderson, B. J., Bennie, J., Bladon, A. J., De Frenne, P., Hemming, D., Hill, R. A., Kearney, M. R., Körner, C., Korstjens, A. H., Lenoir, J., Maclean, I. M. D., Marsh, C. D., Morecroft, M. D., Ohlemüller, R., Slater, H. D., Suggitt, A. J., Zellweger, F., and Gillingham, P. K. (2018). Chapter Three - Advances in Monitoring and Modelling Climate at Ecologically Relevant Scales. In Bohan, D. A., Dumbrell, A. J., Woodward, G., and Jackson, M., editors, *Advances in Ecological Research*, volume 58 of *Next Generation Biomonitoring: Part 1*, pages 101–161. Academic Press.

Brito-Morales, I., García Molinos, J., Schoeman, D. S., Burrows, M. T., Poloczanska, E. S., Brown, C. J., Ferrier, S., Harwood, T. D., Klein, C. J., McDonald-Madden, E., Moore, P. J., Pandolfi, J. M., Watson, J. E., Wenger, A. S., and Richardson, A. J. (2018). Climate Velocity Can Inform Conservation in a Warming World. *Trends in Ecology & Evolution*, 33(6):441–457.

Brodie, J. F., Giordano, A. J., Zipkin, E. F., Bernard, H., Mohd-Azlan, J., and Ambu, L. (2015). Correlation and persistence of hunting and logging impacts on tropical rainforest mammals. *Conservation Biology*, 29(1):110–121.

Brook, B. W., Sodhi, N. S., and Bradshaw, C. J. A. (2008). Synergies among extinction drivers under global change. *Trends in Ecology & Evolution*, 23(8):453–460.

Brook, B. W., Sodhi, N. S., and Ng, P. K. L. (2003). Catastrophic extinctions follow deforestation in Singapore. *Nature*, 424(6947):420–426.

Butchart, S. H. M., Walpole, M., Collen, B., Strien, A. v., Scharlemann, J. P. W., Almond, R. E. A., Baillie, J. E. M., Bomhard, B., Brown, C., Bruno, J., Carpenter, K. E., Carr, G. M., Chanson, J., Chenery, A. M., Csirke, J., Davidson, N. C., Dentener, F., Foster, M., Galli, A., Galloway, J. N., Genovesi, P., Gregory, R. D., Hockings, M., Kapos, V., Lamarque, J.-F., Leverington, F., Loh, J., McGeoch, M. A., McRae, L., Minasyan, A., Morcillo, M. H., Oldfield, T. E. E., Pauly, D., Quader, S., Revenga, C., Sauer, J. R., Skolnik, B., Spear, D., Stanwell-Smith, D., Stuart, S. N., Symes, A., Tierney, M., Tyrrell, T. D., Vié, J.-C., and Watson, R. (2010). Global Biodiversity: Indicators of Recent Declines. *Science*, 328(5982):1164–1168.

Caillon, R., Suppo, C., Casas, J., Arthur Woods, H., and Pincebourde, S. (2014). Warming decreases thermal heterogeneity of leaf surfaces: implications for behavioural thermoregulation by arthropods. *Functional Ecology*, 28(6):1449–1458.

Campos, C. (2006). Response of soil surface CO_2-C flux to land use changes in a tropical cloud forest (Mexico). *Forest Ecology and Management*, 234(1–3):305–312.

Carlson, B. S., Koerner, S. E., Medjibe, V. P., White, L. J. T., and Poulsen, J. R. (2017). Deadwood stocks increase with selective logging and large tree frequency in Gabon. *Global Change Biology*, 23(4):1648–1660.

CBD (2010). Strategic plan for biodiversity 2011–2020 and the Aichi targets. Available at: https://www.cbd.int/doc/strategic-plan/2011-2020/Aichi-Targets-EN.pdf.

Chen, I.-C., Hill, J. K., Ohlemüller, R., Roy, D. B., and Thomas, C. D. (2011). Rapid Range Shifts of Species Associated with High Levels of Climate Warming. *Science*, 333(6045):1024–1026.

Chen, I.-C., Shiu, H.-J., Benedick, S., Holloway, J. D., Chey, V. K., Barlow, H. S., Hill, J. K., and Thomas, C. D. (2009). Elevation increases in moth assemblages over 42 years on a tropical mountain. *Proceedings of the National Academy of Sciences*, 106(5):1479–1483.

Chen, J., Franklin, J. F., and Spies, T. A. (1995). Growing-season microclimatic gradients from clearcut edges into old-growth douglas-fir forests. *Ecological Applications*, 5(1):74–86.

Chou, C., Chiang, J. C. H., Lan, C.-W., Chung, C.-H., Liao, Y.-C., and Lee, C.-J. (2013). Increase in the range between wet and dry season precipitation. *Nature Geoscience*, 6(4):263–267.

Chou, C. and Lan, C.-W. (2012). Changes in the annual range of precipitation under global warming. *Journal of Climate*, 25(1):222–235.

Christidis, N., Stott, P. A., Hegerl, G. C., and Betts, R. A. (2013). The role of land use change in the recent warming of daily extreme temperatures. *Geophysical Research Letters*, 40(3):589–594.

Collas, L., Green, R. E., Ross, A., Wastell, J. H., and Balmford, A. (2017). Urban development, land sharing and land sparing: the importance of considering restoration. *Journal of Applied Ecology*, 54(6):1865–1873.

Colwell, R. K., Brehm, G., Cardelús, C. L., Gilman, A. C., and Longino, J. T. (2008). Global warming, elevational range shifts, and lowland biotic attrition in the wet tropics. *Science*, 322(5899):258–261.

Corlett, R. T. (2011). Impacts of warming on tropical lowland rainforests. *Trends in Ecology & Evolution*, 26(11):606–613.

Corlett, R. T. (2012). Climate change in the tropics: The end of the world as we know it? *Biological Conservation*, 151(1):22 – 25.

Cosgrove, A. J., McWhorter, T. J., and Maron, M. (2018). Consequences of impediments to animal movements at different scales: A conceptual framework and review. *Diversity and Distributions*, 24(4):448–459.

Costanza, R., d'Arge, R., Groot, R. d., Farber, S., Grasso, M., Hannon, B., Limburg, K., Naeem, S., O'Neill, R. V., Paruelo, J., Raskin, R. G., Sutton, P., and Belt, M. v. d. (1997). The value of the world's ecosystem services and natural capital. *Nature*, 387(6630):253–260.

Davin, E. L. and de Noblet-Ducoudré, N. (2010). Climatic impact of global-scale deforestation: radiative versus nonradiative processes. *Journal of Climate*, 23(1):97–112.

Deutsch, C. A., Tewksbury, J. J., Huey, R. B., Sheldon, K. S., Ghalambor, C. K., Haak, D. C., and Martin, P. R. (2008). Impacts of climate warming on terrestrial ectotherms across latitude. *Proceedings of the National Academy of Sciences*, 105(18):6668–6672.

du Plessis, K. L., Martin, R. O., Hockey, P. A. R., Cunningham, S. J., and Ridley, A. R. (2012). The costs of keeping cool in a warming world: implications of high temperatures for foraging, thermoregulation and body condition of an arid-zone bird. *Global Change Biology*, 18(10):3063–3070.

Dubreuil, V., Debortoli, N., Funatsu, B., Nédélec, V., and Durieux, L. (2011). Impact of land-cover change in the Southern Amazonia climate: a case study for the region of Alta Floresta, Mato Grosso, Brazil. *Environmental Monitoring and Assessment*, 184(2):877–891.

Duellman, W. E. and Trueb, L. (1986). *Biology of Amphibians*. McGraw-Hill, New York, NY, USA.

Early, R. and Sax, D. F. (2011). Analysis of climate paths reveals potential limitations on species range shifts. *Ecology Letters*, 14(11):1125–1133.

Edwards, D. P., Gilroy, J. J., Thomas, G. H., Uribe, C. A. M., and Haugaasen, T. (2015). Land-Sparing Agriculture Best Protects Avian Phylogenetic Diversity. *Current Biology*, 25(18):2384–2391.

Edwards, D. P., Gilroy, J. J., Woodcock, P., Edwards, F. A., Larsen, T. H., Andrews, D. J. R., Derhé, M. A., Docherty, T. D. S., Hsu, W. W., Mitchell, S. L., Ota, T., Williams, L. J., Laurance, W. F., Hamer, K. C., and Wilcove, D. S. (2014a). Land-sharing versus land-sparing logging: reconciling timber extraction with biodiversity conservation. *Global Change Biology*, 20(1):183–191.

Edwards, D. P., Larsen, T. H., Docherty, T. D. S., Ansell, F. A., Hsu, W. W., Derhé, M. A., Hamer, K. C., and Wilcove, D. S. (2011). Degraded lands worth protecting: the biological importance of Southeast Asia's repeatedly logged forests. *Proceedings of the Royal Society B: Biological Sciences*, 278:82–90.

Edwards, D. P. and Laurance, W. F. (2013). Biodiversity Despite Selective Logging. *Science*, 339(6120):646–647.

Edwards, D. P., Magrach, A., Woodcock, P., Ji, Y., Lim, N. T.-L., Edwards, F. A., Larsen, T. H., Hsu, W. W., Benedick, S., Khen, C. V., Chung, A. Y. C., Reynolds, G., Fisher, B., Laurance, W. F., Wilcove, D. S., Hamer, K. C., and Yu, D. W. (2014b). Selective-logging

and oil palm: multitaxon impacts, biodiversity indicators, and trade-offs for conservation planning. *Ecological Applications*, 24(8):2029–2049.

Edwards, D. P., Tobias, J. A., Sheil, D., Meijaard, E., and Laurance, W. F. (2014c). Maintaining ecosystem function and services in logged tropical forests. *Trends in Ecology & Evolution*, 29(9):511–520.

Elsen, P. R., Monahan, W. B., and Merenlender, A. M. (2018). Global patterns of protection of elevational gradients in mountain ranges. *Proceedings of the National Academy of Sciences*, 115(23):6004–6009.

Elsen, P. R. and Tingley, M. W. (2015). Global mountain topography and the fate of montane species under climate change. *Nature Climate Change*, 5(8):772–776.

ESRI (2011). ArcGIS Desktop: Release 10.

Ewers, R. M. and Banks-Leite, C. (2013). Fragmentation Impairs the Microclimate Buffering Effect of Tropical Forests. *PLOS ONE*, 8(3):e58093.

Ewers, R. M., Boyle, M. J. W., Gleave, R. A., Plowman, N. S., Benedick, S., Bernard, H., Bishop, T. R., Bakhtiar, E. Y., Chey, V. K., Chung, A. Y. C., Davies, R. G., Edwards, D. P., Eggleton, P., Fayle, T. M., Hardwick, S. R., Homathevi, R., Kitching, R. L., Khoo, M. S., Luke, S. H., March, J. J., Nilus, R., Pfeifer, M., Rao, S. V., Sharp, A. C., Snaddon, J. L., Stork, N. E., Struebig, M. J., Wearn, O. R., Yusah, K. M., and Turner, E. C. (2015). Logging cuts the functional importance of invertebrates in tropical rainforest. *Nature Communications*, 6:6836.

Faye, E., Rebaudo, F., Yánez-Cajo, D., Cauvy-Fraunié, S., and Dangles, O. (2016). A toolbox for studying thermal heterogeneity across spatial scales: from unmanned aerial vehicle imagery to landscape metrics. *Methods in Ecology and Evolution*, 7(4):437–446.

Fick, S. E. and Hijmans, R. J. (2017). WorldClim 2: New 1-km spatial resolution climate surfaces for global land areas. *International Journal of Climatology*, 37(12):4302–4315.

Findell, K. L., Shevliakova, E., Milly, P. C. D., and Stouffer, R. J. (2007). Modeled impact of anthropogenic land cover change on climate. *Journal of Climate*, 20(14):3621–3634.

Fisher, B., Edwards, D. P., Larsen, T. H., Ansell, F. A., Hsu, W. W., Roberts, C. S., and Wilcove, D. S. (2011). Cost-effective conservation: calculating biodiversity and logging trade-offs in Southeast Asia. *Conservation Letters*, 4(6):443–450.

FLIR (2016). User's manual FLIR Exx series. Available at: http://flir.custhelp.com/app/account/fl_download_manuals.

Foley, J. A., DeFries, R., Asner, G. P., Barford, C., Bonan, G., Carpenter, S. R., Chapin, F. S., Coe, M. T., Daily, G. C., Gibbs, H. K., Helkowski, J. H., Holloway, T., Howard, E. A., Kucharik, C. J., Monfreda, C., Patz, J. A., Prentice, I. C., Ramankutty, N., and Snyder, P. K. (2005). Global consequences of land use. *Science*, 309(5734):570–574.

Foley, J. A., Ramankutty, N., Brauman, K. A., Cassidy, E. S., Gerber, J. S., Johnston, M., Mueller, N. D., O'Connell, C., Ray, D. K., and West, P. C. (2011). Solutions for a cultivated planet. *Nature*, 478(7369):337–342.

Foster, W. A., Snaddon, J. L., Turner, E. C., Fayle, T. M., Cockerill, T. D., Ellwood, M. D. F., Broad, G. R., Chung, A. Y. C., Eggleton, P., Khen, C. V., and Yusah, K. M. (2011). Establishing the evidence base for maintaining biodiversity and ecosystem function in the oil palm landscapes of South East Asia. *Philosophical Transactions of the Royal Society B: Biological Sciences*, 366(1582):3277–3291.

França, F., Louzada, J., Korasaki, V., Griffiths, H., Silveira, J. M., and Barlow, J. (2016). Do space-for-time assessments underestimate the impacts of logging on tropical biodiversity? An Amazonian case study using dung beetles. *Journal of Applied Ecology*, 53(4):1098–1105.

Freeman, B. G. and Class Freeman, A. M. (2014). Rapid upslope shifts in New Guinean birds illustrate strong distributional responses of tropical montane species to global warming. *Proceedings of the National Academy of Sciences*, 111(12):4490–4494.

Frenne, P. D. and Verheyen, K. (2016). Weather stations lack forest data. *Science*, 351(6270):234–234.

Furukawa, Y., Inubushi, K., Ali, M., Itang, A. M., and Tsuruta, H. (2005). Effect of changing groundwater levels caused by land-use changes on greenhouse gas fluxes from tropical peat lands. *Nutrient Cycling in Agroecosystems*, 71(1):81–91.

Getis, A. and Ord, J. K. (1996). Local spatial statistics: an overview. In Longley, P. and Batty, M., editors, *Spatial analysis: modelling in a GIS environment*, chapter 14, pages 261–277. GeoInformation International, Cambridge, United Kingdom.

Gibbs, H. K., Ruesch, A. S., Achard, F., Clayton, M. K., Holmgren, P., Ramankutty, N., and Foley, J. A. (2010). Tropical forests were the primary sources of new agricultural land in the 1980s and 1990s. *Proceedings of the National Academy of Sciences*, 107(38):16732–16737.

Gibson, L., Lee, T. M., Koh, L. P., Brook, B. W., Gardner, T. A., Barlow, J., Peres, C. A., Bradshaw, C. J. A., Laurance, W. F., Lovejoy, T. E., and Sodhi, N. S. (2011). Primary forests are irreplaceable for sustaining tropical biodiversity. *Nature*, 478(7369):378–381.

Gillies, C. S. and Clair, C. C. S. (2008). Riparian corridors enhance movement of a forest specialist bird in fragmented tropical forest. *Proceedings of the National Academy of Sciences*, 105(50):19774–19779.

Gillingham, P. (2010). *The relative importance of microclimate and land use to biodiversity*. PhD thesis, University of York, Department of Biology. Available at: http://etheses.whiterose.ac.uk/1210/.

Godfray, H. C. J., Beddington, J. R., Crute, I. R., Haddad, L., Lawrence, D., Muir, J. F., Pretty, J., Robinson, S., Thomas, S. M., and Toulmin, C. (2010). Food Security: The Challenge of Feeding 9 Billion People. *Science*, 327(5967):812–818.

González del Pliego, P. (n.d.). Unpublished data. Provided directly by the author (pgonzalezdelpliego@gmail.com).

González del Pliego, P., Scheffers, B. R., Basham, E. W., Woodcock, P., Wheeler, C., Gilroy, J. J., Medina Uribe, C. A., Haugaasen, T., Freckleton, R. P., and Edwards, D. P. (2016). Thermally buffered microhabitats recovery in tropical secondary forests following land abandonment. *Biological Conservation*, 201:385–395.

González-Di Pierro, A. M., Benítez-Malvido, J., Méndez-Toribio, M., Zermeño, I., Arroyo-Rodríguez, V., Stoner, K. E., and Estrada, A. (2011). Effects of the physical environment and primate gut passage on the early establishment of *Ampelocera hottlei* Standley in rain forest fragments. *Biotropica*, 43(4):459–466.

Goode, L. K. (n.d.). Unpublished data. Provided directly by the author (goodelaurel@gmail.com).

Goode, L. K. and Allen, M. F. (2009). Seed germination conditions and implications for establishment of an epiphyte, *Aechmea bracteata* (Bromeliaceae). *Plant Ecology*, 204(2):179–188.

Greenwood, O., Mossman, H. L., Suggitt, A. J., Curtis, R. J., and Maclean, I. M. D. (2016). REVIEW: Using in situ management to conserve biodiversity under climate change. *Journal of Applied Ecology*, 53(3):885–894.

Gunderson, A. R. and Leal, M. (2016). A conceptual framework for understanding thermal constraints on ectotherm activity with implications for predicting responses to global change. *Ecology Letters*, 19(2):111–120.

Haddad, N. M., Brudvig, L. A., Clobert, J., Davies, K. F., Gonzalez, A., Holt, R. D., Lovejoy, T. E., Sexton, J. O., Austin, M. P., Collins, C. D., Cook, W. M., Damschen, E. I., Ewers, R. M., Foster, B. L., Jenkins, C. N., King, A. J., Laurance, W. F., Levey, D. J., Margules, C. R., Melbourne, B. A., Nicholls, A. O., Orrock, J. L., Song, D.-X., and Townshend, J. R. (2015).

Habitat fragmentation and its lasting impact on Earth's ecosystems. *Science Advances*, 1(2):e1500052.

Hamer, K. C., Hill, J. K., Benedick, S., Mustaffa, N., Sherratt, T. N., Maryati, M., and K., C. V. (2003). Ecology of butterflies in natural and selectively logged forests of northern Borneo: the importance of habitat heterogeneity. *Journal of Applied Ecology*, 40(1):150–162.

Hannah, L., Flint, L., Syphard, A. D., Moritz, M. A., Buckley, L. B., and McCullough, I. M. (2014). Fine-grain modeling of species' response to climate change: holdouts, stepping-stones, and microrefugia. *Trends in Ecology & Evolution*, 29(7):390–397.

Hansen, M. C., Potapov, P. V., Moore, R., Hancher, M., Turubanova, S. A., Tyukavina, A., Thau, D., Stehman, S. V., Goetz, S. J., Loveland, T. R., Kommareddy, A., Egorov, A., Chini, L., Justice, C. O., and Townshend, J. R. G. (2013). High-resolution global maps of 21st-century forest cover change. *Science*, 342(6160):850–853. Data available at: http://earthenginepartners.appspot.com/science-2013-global-forest.

Hansen, M. C., Stehman, S. V., Potapov, P. V., Loveland, T. R., Townshend, J. R. G., DeFries, R. S., Pittman, K. W., Arunarwati, B., Stolle, F., Steininger, M. K., Carroll, M., and DiMiceli, C. (2008). Humid tropical forest clearing from 2000 to 2005 quantified by using multitemporal and multiresolution remotely sensed data. *Proceedings of the National Academy of Sciences*, 105(27):9439–9444.

Hardwick, S. and Orme, D. (2016). Aboveground microclimate at SAFE 2013 - 2015. Available at: https://doi.org/10.5281/zenodo.46183.

Hardwick, S. R., Toumi, R., Pfeifer, M., Turner, E. C., Nilus, R., and Ewers, R. M. (2015). The relationship between leaf area index and microclimate in tropical forest and oil palm plantation: Forest disturbance drives changes in microclimate. *Agricultural and Forest Meteorology*, 201:187–195.

Hassall, M., Edwards, D. P., Carmenta, R., Derhé, M. A., and Moss, A. (2010). Predicting the effect of climate change on aggregation behaviour in four species of terrestrial isopods. *Behaviour*, 147(2):151–164.

He, H. S., DeZonia, B. E., and Mladenoff, D. J. (2000). An aggregation index (AI) to quantify spatial patterns of landscapes. *Landscape Ecology*, 15(7):591–601.

Hijmans, R. J., Cameron, S. E., Parra, J. L., Jones, P. G., and Jarvis, A. (2005). Very high resolution interpolated climate surfaces for global land areas. *International Journal of Climatology*, 25(15):1965–1978.

Hijmans, R. J. and Graham, C. H. (2006). The ability of climate envelope models to predict the effect of climate change on species distributions. *Global Change Biology*, 12(12):2272–2281.

Hill, J. K., Thomas, C. D., Fox, R., Telfer, M. G., Willis, S. G., Asher, J., and Huntley, B. (2002). Responses of butterflies to twentieth century climate warming: implications for future ranges. *Proceedings of the Royal Society B: Biological Sciences*, 269(1505):2163–2171.

Hill, J. K., Thomas, C. D., and Lewis, O. T. (1999). Flight morphology in fragmented populations of a rare British butterfly, Hesperia comma. *Biological Conservation*, 87(3):277–283.

Hirsch, T. and Secretariat of the Convention on Biological Diversity (2010). *Global Biodiversity Outlook 3.* Secretariat of the Convention on Biological Diversity, Montreal, Quebec, Canada.

Hoffmann, A. A., Chown, S. L., and Clusella-Trullas, S. (2013). Upper thermal limits in terrestrial ectotherms: how constrained are they? *Functional Ecology*, 27(4):934–949.

Hoffmann, A. A. and Sgrò, C. M. (2011). Climate change and evolutionary adaptation. *Nature*, 470(7335):479–485.

Holl, K. D. (1999). Factors limiting tropical rain forest regeneration in abandoned pasture: seed rain, seed germination, microclimate, and soil. *Biotropica*, 31(2):229–242.

Hérault, B., Beauchêne, J., Muller, F., Wagner, F., Baraloto, C., Blanc, L., and Martin, J.-M. (2010). Modeling decay rates of dead wood in a neotropical forest. *Oecologia*, 164(1):243–251.

Hurtt, G. C., Chini, L. P., Frolking, S., Betts, R. A., Feddema, J., Fischer, G., Fisk, J. P., Hibbard, K., Houghton, R. A., Janetos, A., Jones, C. D., Kindermann, G., Kinoshita, T., Goldewijk, K. K., Riahi, K., Shevliakova, E., Smith, S., Stehfest, E., Thomson, A., Thornton, P., Vuuren, D. P. v., and Wang, Y. P. (2011). Harmonization of land-use scenarios for the period 1500–2100: 600 years of global gridded annual land-use transitions, wood harvest, and resulting secondary lands. *Climatic Change*, 109(1-2):117–161.

Ibanez, T., Hély, C., and Gaucherel, C. (2013). Sharp transitions in microclimatic conditions between savanna and forest in New Caledonia: Insights into the vulnerability of forest edges to fire. *Austral Ecology*, 38(6):680–687.

IPCC (2013). *Climate Change 2013: The Physical Science Basis. Contribution of Working Group I to the Fifth Assessment Report of the Intergovernmental Panel on Climate Change*. Cambridge University Press, Cambridge, United Kingdom and New York, NY, USA.

Isaac, J. L., De Gabriel, J. L., and Goodman, B. A. (2008). Microclimate of daytime den sites in a tropical possum: implications for the conservation of tropical arboreal marsupials. *Animal Conservation*, 11(4):281–287.

Jarvis, A., Reuter, H., Nelson, A., and E., G. (2008). Hole-filled SRTM for the globe Version 4, available from the CGIAR-CSI SRTM 90m Database (http://srtm.csi.cgiar.org/).

Jenkins, C. N., Pimm, S. L., and Joppa, L. N. (2013). Global patterns of terrestrial vertebrate diversity and conservation. *Proceedings of the National Academy of Sciences*, 110(28):E2602–E2610.

Joppa, L. N., Roberts, D. L., Myers, N., and Pimm, S. L. (2011). Biodiversity hotspots house most undiscovered plant species. *Proceedings of the National Academy of Sciences*, 108(32):13171–13176.

Jucker, T., Bongalov, B., Burslem, D. F. R. P., Nilus, R., Dalponte, M., Lewis, S. L., Phillips, O. L., Qie, L., and Coomes, D. A. (2018). Topography shapes the structure, composition and function of tropical forest landscapes. *Ecology Letters*, 21(7):989–1000.

Kaspari, M., Clay, N. A., Lucas, J., Yanoviak, S. P., and Kay, A. (2015). Thermal adaptation generates a diversity of thermal limits in a rainforest ant community. *Global Change Biology*, 21(3):1092–1102.

Kearney, M., Shine, R., and Porter, W. P. (2009). The potential for behavioral thermoregulation to buffer "cold-blooded" animals against climate warming. *Proceedings of the National Academy of Sciences*, 106(10):3835–3840.

Kearney, M. R. and Porter, W. P. (2017). NicheMapR – an R package for biophysical modelling: the microclimate model. *Ecography*, 40(5):664–674.

Khaliq, I., Hof, C., Prinzinger, R., Böhning-Gaese, K., and Pfenninger, M. (2014). Global variation in thermal tolerances and vulnerability of endotherms to climate change. *Proceedings of the Royal Society of London B: Biological Sciences*, 281(1789):20141097.

King, J. R., Andersen, A. N., and Cutter, A. D. (1998). Ants as bioindicators of habitat disturbance: validation of the functional group model for Australia's humid tropics. *Biodiversity & Conservation*, 7(12):1627–1638.

Kingsolver, J. G. (2009). The well-temperatured biologist. *The American Naturalist*, 174(6):755–768.

Klein, A.-M., Steffan-Dewenter, I., and Tscharntke, T. (2002). Predator–prey ratios on cocoa along a land-use gradient in Indonesia. *Biodiversity & Conservation*, 11(4):683–693.

Kumar, R. and Shahabuddin, G. (2005). Effects of biomass extraction on vegetation structure, diversity and composition of forests in Sariska Tiger Reserve, India. *Environmental Conservation*, 32(3):248–259.

Laurance, W. F., Clements, G. R., Sloan, S., O'Connell, C. S., Mueller, N. D., Goosem, M., Venter, O., Edwards, D. P., Phalan, B., Balmford, A., Van Der Ree, R., and Arrea, I. B. (2014). A global strategy for road building. *Nature*, 513(7517):229–232.

Laurance, W. F., Goosem, M., and Laurance, S. G. W. (2009). Impacts of roads and linear clearings on tropical forests. *Trends in Ecology & Evolution*, 24(12):659–669.

Lawler, J. J., Ruesch, A. S., Olden, J. D., and McRae, B. H. (2013). Projected climate-driven faunal movement routes. *Ecology Letters*, 16(8):1014–1022.

Lawrence, D. and Vandecar, K. (2015). Effects of tropical deforestation on climate and agriculture. *Nature Climate Change*, 5(1):27–36.

Lebrija-Trejos, E., Pérez-García, E. A., Meave, J. A., Poorter, L., and Bongers, F. (2011). Environmental changes during secondary succession in a tropical dry forest in Mexico. *Journal of Tropical Ecology*, 27(05):477–489.

Lees, A. C. and Peres, C. A. (2008). Conservation Value of Remnant Riparian Forest Corridors of Varying Quality for Amazonian Birds and Mammals. *Conservation Biology*, 22(2):439–449.

Lemmon, P. E. (1956). A spherical densiometer for estimating forest overstory density. *Forest Science*, 2(4):314–320.

Lewis, S. L., Edwards, D. P., and Galbraith, D. (2015). Increasing human dominance of tropical forests. *Science*, 349(6250):827–832.

Li, Y., Zhao, M., Motesharrei, S., Mu, Q., Kalnay, E., and Li, S. (2015). Local cooling and warming effects of forests based on satellite observations. *Nature Communications*, 6:6603.

Lindenmayer, D. B., Cunningham, R. B., Pope, M. L., Gibbons, P., and Donnelly, C. F. (2000). Cavity sizes and types in Australian eucalypts from wet and dry forest types–a simple of rule of thumb for estimating size and number of cavities. *Forest Ecology and Management*, 137(1–3):139–150.

Littlefield, C. E., McRae, B. H., Michalak, J. L., Lawler, J. J., and Carroll, C. (2017). Connecting today's climates to future climate analogs to facilitate movement of species under climate change. *Conservation Biology*, 31(6):1397–1408.

Liu, Z. G. and Zou, X. M. (2002). Exotic earthworms accelerate plant litter decomposition in a Puerto Rican pasture and a wet forest. *Ecological Applications*, 12(5):1406–1417.

Loarie, S. R., Duffy, P. B., Hamilton, H., Asner, G. P., Field, C. B., and Ackerly, D. D. (2009). The velocity of climate change. *Nature*, 462(7276):1052–1055.

Lucey, J. M. and Hill, J. K. (2012). Spillover of Insects from Rain Forest into Adjacent Oil Palm Plantations. *Biotropica*, 44(3):368–377.

Luskin, M. S. and Potts, M. D. (2011). Microclimate and habitat heterogeneity through the oil palm lifecycle. *Basic and Applied Ecology*, 12(6):540–551.

Maclean, I. M. D., Hopkins, J. J., Bennie, J., Lawson, C. R., and Wilson, R. J. (2015). Microclimates buffer the responses of plant communities to climate change. *Global Ecology and Biogeography*, 24(11):1340–1350.

Maclean, I. M. D., Suggitt, A. J., Wilson, R. J., Duffy, J. P., and Bennie, J. J. (2017). Fine-scale climate change: modelling spatial variation in biologically meaningful rates of warming. *Global Change Biology*, 23(1):256–268.

Mantyka-pringle, C. S., Martin, T. G., and Rhodes, J. R. (2012). Interactions between climate and habitat loss effects on biodiversity: a systematic review and meta-analysis. *Global Change Biology*, 18(4):1239–1252.

Mason, T. H., Stephens, P. A., Apollonio, M., and Willis, S. G. (2014). Predicting potential responses to future climate in an alpine ungulate: interspecific interactions exceed climate effects. *Global Change Biology*, 20(12):3872–3882.

Maxwell, S. L., Fuller, R. A., Brooks, T. M., and Watson, J. E. M. (2016). Biodiversity: The ravages of guns, nets and bulldozers. *Nature News*, 536(7615):143.

McAlpine, C. A., Johnson, A., Salazar, A., Syktus, J. I., Wilson, K., Meijaard, E., Seabrook, L. M., Dargusch, P., Nordin, H., and Sheil, D. (2018). Forest loss and Borneo's climate. *Environmental Research Letters*.

McGarigal, K., Cushman, S. A., and Ene, E. (2012). FRAGSTATS v4: Spatial pattern analysis program for categorical and continuous maps. Computer software program produced by the authors at the University of Massachusetts, Amherst. Available at: http://www.umass.edu/landeco/research/fragstats/fragstats.html.

McGuire, J. L., Lawler, J. J., McRae, B. H., and Theobald, D. M. (2016). Achieving climate connectivity in a fragmented landscape. *Proceedings of the National Academy of Sciences*, 113(26):7195–7200.

McLaughlin, B. C., Ackerly, D. D., Klos, P. Z., Natali, J., Dawson, T. E., and Thompson, S. E. (2017). Hydrologic refugia, plants, and climate change. *Global Change Biology*, 23(8):2941–2961.

Millennium Ecosystem Assessment (2005). *Ecosystems and Human Well-being: Biodiversity Synthesis*. World Resources Institute, Washington, DC, USA.

Mitchell, A. L., Rosenqvist, A., and Mora, B. (2017). Current remote sensing approaches to monitoring forest degradation in support of countries measurement, reporting and verification (MRV) systems for REDD+. *Carbon Balance and Management*, 12(1):9.

Mittermeier, R. A., Mittermeier, C. G., Brooks, T. M., Pilgrim, J. D., Konstant, W. R., Fonseca, G. A. B. d., and Kormos, C. (2003). Wilderness and biodiversity conservation. *Proceedings of the National Academy of Sciences*, 100(18):10309–10313.

Moore, R. P., Robinson, W. D., Lovette, I. J., and Robinson, T. R. (2008). Experimental evidence for extreme dispersal limitation in tropical forest birds. *Ecology Letters*, 11(9):960–968.

Mora, C., Frazier, A. G., Longman, R. J., Dacks, R. S., Walton, M. M., Tong, E. J., Sanchez, J. J., Kaiser, L. R., Stender, Y. O., Anderson, J. M., Ambrosino, C. M., Fernandez-Silva, I., Giuseffi, L. M., and Giambelluca, T. W. (2013). The projected timing of climate departure from recent variability. *Nature*, 502(7470):183–187.

Murcia, C. (1995). Edge effects in fragmented forests: implications for conservation. *Trends in Ecology & Evolution*, 10(2):58–62.

Myers, N., Mittermeier, R. A., Mittermeier, C. G., Da Fonseca, G. A. B., and Kent, J. (2000). Biodiversity hotspots for conservation priorities. *Nature*, 403:853–858.

Nadeau, C. P., Urban, M. C., and Bridle, J. R. (2017). Coarse climate change projections for species living in a fine-scaled world. *Global Change Biology*, 23(1):12–24.

Negrete-Yankelevich, S., Fragoso, C., Newton, A. C., and Heal, O. W. (2007). Successional changes in soil, litter and macroinvertebrate parameters following selective logging in a Mexican Cloud Forest. *Applied Soil Ecology*, 35(2):340–355.

Newbold, T., Hudson, L. N., Hill, S. L. L., Contu, S., Lysenko, I., Senior, R. A., Börger, L., Bennett, D. J., Choimes, A., Collen, B., Day, J., De Palma, A., Díaz, S., Echeverria-Londoño, S., Edgar, M. J., Feldman, A., Garon, M., Harrison, M. L. K., Alhusseini, T., Ingram, D. J., Itescu, Y., Kattge, J., Kemp, V., Kirkpatrick, L., Kleyer, M., Correia, D. L. P., Martin, C. D., Meiri, S., Novosolov, M., Pan, Y., Phillips, H. R. P., Purves, D. W., Robinson, A., Simpson, J., Tuck, S. L., Weiher, E., White, H. J., Ewers, R. M., Mace, G. M., Scharlemann, J. P. W., and Purvis, A. (2015). Global effects of land use on local terrestrial biodiversity. *Nature*, 520(7545):45–50.

NOAA (n.d.). Solar Calculations. Available at: https://www.esrl.noaa.gov/gmd/grad/solcalc/calcdetails.html.

NOAA Climate Prediction Center (2015). Available at: http://www.cpc.noaa.gov/products/analysis_monitoring/ensostuff/ensoyears.shtml.

Nuñez, T. A., Lawler, J. J., Mcrae, B. H., Pierce, D. J., Krosby, M. B., Kavanagh, D. M., Singleton, P. H., and Tewksbury, J. J. (2013). Connectivity Planning to Address Climate Change. *Conservation Biology*, 27(2):407–416.

Nussey, D. H., Postma, E., Gienapp, P., and Visser, M. E. (2005). Selection on Heritable Phenotypic Plasticity in a Wild Bird Population. *Science*, 310(5746):304–306.

O'Connor, M. I., Selig, E. R., Pinsky, M. L., and Altermatt, F. (2012). Toward a conceptual synthesis for climate change responses. *Global Ecology and Biogeography*, 21(7):693–703.

Oke, T. R. (1987). *Boundary layer climates*. Methuen, London, United Kingdom, 2nd edition.

Okuda, T., Suzuki, M., Adachi, N., Quah, E. S., Hussein, N. A., and Manokaran, N. (2003). Effect of selective logging on canopy and stand structure and tree species composition in a lowland dipterocarp forest in peninsular Malaysia. *Forest Ecology and Management*, 175(1–3):297–320.

Oliver, T. H., Isaac, N. J. B., August, T. A., Woodcock, B. A., Roy, D. B., and Bullock, J. M. (2015). Declining resilience of ecosystem functions under biodiversity loss. *Nature Communications*, 6:10122.

Oliver, T. H. and Morecroft, M. D. (2014). Interactions between climate change and land use change on biodiversity: attribution problems, risks, and opportunities. *Wiley Interdisciplinary Reviews: Climate Change*, 5(3):317–335.

Opdam, P. and Wascher, D. (2004). Climate change meets habitat fragmentation: linking landscape and biogeographical scale levels in research and conservation. *Biological Conservation*, 117(3):285–297.

Pacifici, M., Visconti, P., and Rondinini, C. (2018). A framework for the identification of hotspots of climate change risk for mammals. *Global Change Biology*, 24(4):1626–1636.

Parmesan, C. (2006). Ecological and Evolutionary Responses to Recent Climate Change. *Annual Review of Ecology, Evolution, and Systematics*, 37(1):637–669.

Parmesan, C., Ryrholm, N., Stefanescu, C., Hill, J. K., Thomas, C. D., Descimon, H., Huntley, B., Kaila, L., Kullberg, J., Tammaru, T., Tennent, W. J., Thomas, J. A., and Warren, M. (1999). Poleward shifts in geographical ranges of butterfly species associated with regional warming. *Nature*, 399(6736):579–583.

Parsons, S. A., Shoo, L. P., and Williams, S. E. (2009). Volume measurements for quicker determination of forest litter standing crop. *Journal of Tropical Ecology*, 25(06):665–669.

Pfeifer, M., Lefebvre, V., Peres, C. A., Banks-Leite, C., Wearn, O. R., Marsh, C. J., Butchart, S. H. M., Arroyo-Rodríguez, V., Barlow, J., Cerezo, A., Cisneros, L., D'Cruze, N., Faria, D., Hadley, A., Harris, S. M., Klingbeil, B. T., Kormann, U., Lens, L., Medina-Rangel, G. F., Morante-Filho, J. C., Olivier, P., Peters, S. L., Pidgeon, A., Ribeiro, D. B., Scherber, C., Schneider-Maunoury, L., Struebig, M., Urbina-Cardona, N., Watling, J. I., Willig, M. R., Wood, E. M., and Ewers, R. M. (2017). Creation of forest edges has a global impact on forest vertebrates. *Nature*, 551(7679):187–191.

Phalan, B., Onial, M., Balmford, A., and Green, R. E. (2011). Reconciling Food Production and Biodiversity Conservation: Land Sharing and Land Sparing Compared. *Science*, 333(6047):1289–1291.

Pielke, R. A., Pitman, A., Niyogi, D., Mahmood, R., McAlpine, C., Hossain, F., Goldewijk, K. K., Nair, U., Betts, R., Fall, S., Reichstein, M., Kabat, P., and de Noblet, N. (2011). Land use/land cover changes and climate: modeling analysis and observational evidence. *Wiley Interdisciplinary Reviews: Climate Change*, 2(6):828–850.

Pimm, S. L., Russell, G. J., Gittleman, J. L., and Brooks, T. M. (1995). The Future of Biodiversity. *Science*, 269(5222):347–350.

Pinheiro, J., Bates, D., DebRoy, S., Sarkar, D., and R Core Team (2017). nlme: Linear and Nonlinear Mixed Effects Models. Available at: https://CRAN.R-project.org/package=nlme.

Potter, K. A., Arthur Woods, H., and Pincebourde, S. (2013). Microclimatic challenges in global change biology. *Global Change Biology*, 19(10):2932–2939.

Putz, F. E., Sist, P., Fredericksen, T., and Dykstra, D. (2008). Reduced-impact logging: Challenges and opportunities. *Forest Ecology and Management*, 256(7):1427–1433.

Putz, F. E., Zuidema, P. A., Synnott, T., Peña-Claros, M., Pinard, M. A., Sheil, D., Vanclay, J. K., Sist, P., Gourlet-Fleury, S., Griscom, B., Palmer, J., and Zagt, R. (2012). Sustaining conservation values in selectively logged tropical forests: the attained and the attainable. *Conservation Letters*, 5(4):296–303.

Puurtinen, M., Elo, M., Jalasvuori, M., Kahilainen, A., Ketola, T., Kotiaho, J. S., Mönkkönen, M., and Pentikäinen, O. T. (2016). Temperature-dependent mutational robustness can explain faster molecular evolution at warm temperatures, affecting speciation rate and global patterns of species diversity. *Ecography*, 39(11):1025–1033.

R Core Team (2017). R: A Language and Environment for Statistical Computing. Available at: https://www.R-project.org/.

R Core Team (2018). R: A Language and Environment for Statistical Computing. Available at: https://www.R-project.org/.

Ramdani, F., Moffiet, T., and Hino, M. (2014). Local surface temperature change due to expansion of oil palm plantation in Indonesia. *Climatic Change*, 123(2):189–200.

Raxworthy, C. J., Pearson, R. G., Rabibisoa, N., Rakotondrazafy, A. M., Ramanamanjato, J.-B., Raselimanana, A. P., Wu, S., Nussbaum, R. A., and Stone, D. A. (2008). Extinction vulnerability of tropical montane endemism from warming and upslope displacement: a preliminary appraisal for the highest massif in Madagascar. *Global Change Biology*, 14(8):1703–1720.

Reynolds, G., Payne, J., Sinun, W., Mosigil, G., and Walsh, R. P. D. (2011). Changes in forest land use and management in Sabah, Malaysian Borneo, 1990–2010, with a focus on the Danum Valley region. *Philosophical Transactions of the Royal Society B: Biological Sciences*, 366(1582):3168–3176.

Rockström, J., Steffen, W., Noone, K., Persson, s., Chapin, F. S., Lambin, E. F., Lenton, T. M., Scheffer, M., Folke, C., Schellnhuber, H. J., Nykvist, B., de Wit, C. A., Hughes, T., van der Leeuw, S., Rodhe, H., Sörlin, S., Snyder, P. K., Costanza, R., Svedin, U., Falkenmark, M., Karlberg, L., Corell, R. W., Fabry, V. J., Hansen, J., Walker, B., Liverman, D., Richardson, K., Crutzen, P., and Foley, J. A. (2009). A safe operating space for humanity. *Nature*, 461(7263):472–475.

Sala, O. E., Chapin, F. S., Iii, Armesto, J. J., Berlow, E., Bloomfield, J., Dirzo, R., Huber-Sanwald, E., Huenneke, L. F., Jackson, R. B., Kinzig, A., Leemans, R., Lodge, D. M., Mooney, H. A., Oesterheld, M., Poff, N. L., Sykes, M. T., Walker, B. H., Walker, M., and Wall, D. H. (2000). Global biodiversity scenarios for the year 2100. *Science*, 287(5459):1770–1774.

Sanchez-Azofeifa, A., Guzmán, J. A., Campos, C. A., Castro, S., Garcia-Millan, V., Nightingale, J., and Rankine, C. (2017). Twenty-first century remote sensing technologies are revolutionizing the study of tropical forests. *Biotropica*, 49(5):604–619.

Saner, P., Lim, R., Burla, B., Ong, R. C., Scherer-Lorenzen, M., and Hector, A. (2009). Reduced soil respiration in gaps in logged lowland dipterocarp forests. *Forest Ecology and Management*, 258(9):2007–2012.

Sanford, T., Frumhoff, P. C., Luers, A., and Gulledge, J. (2014). The climate policy narrative for a dangerously warming world. *Nature Climate Change*, 4(3):164–166.

Santos, B. A. (2011). *La interacción de Heliconia con sus insectos herbívoros y hongos patógenos foliares en selvas tropicales fragmentadas*. PhD thesis, Universidad Nacional Autónoma de México, Centro de Investigaciones en Ecosistemas.

Santos, B. A. and Benítez-Malvido, J. (2012). Insect herbivory and leaf disease in natural and human disturbed habitats: lessons from early-successional *Heliconia* herbs. *Biotropica*, 44(1):53–62.

Scheffers, B. R., Edwards, D. P., Diesmos, A., Williams, S. E., and Evans, T. A. (2014a). Microhabitats reduce animal's exposure to climate extremes. *Global Change Biology*, 20(2):495–503.

Scheffers, B. R., Edwards, D. P., Macdonald, S. L., Senior, R. A., Andriamahohatra, L. R., Roslan, N., Rogers, A. M., Haugaasen, T., Wright, P., and Williams, S. E. (2017a). Extreme thermal heterogeneity in structurally complex tropical rain forests. *Biotropica*, 49(1):35–44.

Scheffers, B. R., Evans, T. A., Williams, S. E., and Edwards, D. P. (2014b). Microhabitats in the tropics buffer temperature in a globally coherent manner. *Biology Letters*, 10(12):20140819.

Scheffers, B. R., Joppa, L. N., Pimm, S. L., and Laurance, W. F. (2012). What we know and don't know about Earth's missing biodiversity. *Trends in Ecology & Evolution*, 27(9):501–510.

Scheffers, B. R., Phillips, B. L., Laurance, W. F., Sodhi, N. S., Diesmos, A., and Williams, S. E. (2013). Increasing arboreality with altitude: a novel biogeographic dimension. *Proceedings of the Royal Society of London B: Biological Sciences*, 280(1770):20131581.

Scheffers, B. R., Shoo, L., Phillips, B., Macdonald, S. L., Anderson, A., VanDerWal, J., Storlie, C., Gourret, A., Williams, S. E., and Algar, A. (2017b). Vertical (arboreality) and horizontal (dispersal) movement increase the resilience of vertebrates to climatic instability. *Global Ecology and Biogeography*, 26(7):787–798.

Scheffers, B. R. and Williams, S. E. (2018). Tropical mountain passes are out of reach – but not for arboreal species. *Frontiers in Ecology and the Environment*, 16(2):101–108.

Schloss, C. A., Nuñez, T. A., and Lawler, J. J. (2012). Dispersal will limit ability of mammals to track climate change in the Western Hemisphere. *Proceedings of the National Academy of Sciences*, 109(22):8606–8611.

Schnitzer, S. A., Parren, M. P. E., and Bongers, F. (2004). Recruitment of lianas into logging gaps and the effects of pre-harvest climber cutting in a lowland forest in Cameroon. *Forest Ecology and Management*, 190(1):87–98.

Schumaker, N. H. (1996). Using Landscape Indices to Predict Habitat Connectivity. *Ecology*, 77(4):1210–1225.

Scriven, S. A., Hodgson, J. A., McClean, C. J., and Hill, J. K. (2015). Protected areas in Borneo may fail to conserve tropical forest biodiversity under climate change. *Biological Conservation*, 184:414–423.

Sears, M. W., Angilletta, M. J., Schuler, M. S., Borchert, J., Dilliplane, K. F., Stegman, M., Rusch, T. W., and Mitchell, W. A. (2016). Configuration of the thermal landscape determines thermoregulatory performance of ectotherms. *Proceedings of the National Academy of Sciences*, 113(38):10595–10600.

Sears, M. W., Raskin, E., and Angilletta, M. J. (2011). The world is not flat: defining relevant thermal landscapes in the context of climate change. *Integrative and Comparative Biology*, 51(5):666–675.

Senior, R. A., Hill, J. K., Benedick, S., and Edwards, D. P. (2018). Tropical forests are thermally buffered despite intensive selective logging. *Global Change Biology*, 24(3):1267–1278.

Senior, R. A., Hill, J. K., and Edwards, D. P. (in prep 2018a). A framework for quantifying fine-scale thermal heterogeneity using thermography. Manuscript in preparation.

Senior, R. A., Hill, J. K., and Edwards, D. P. (in prep 2018b). Global loss of climate connectivity in tropical forests. Manuscript in preparation.

Senior, R. A., Hill, J. K., González del Pliego, P., Goode, L. K., and Edwards, D. P. (2017). A pantropical analysis of the impacts of forest degradation and conversion on local temperature. *Ecology and Evolution*, 7(19):7897–7908.

Shi, H., Wen, Z., Paull, D., and Guo, M. (2016). A framework for quantifying the thermal buffering effect of microhabitats. *Biological Conservation*, 204:175–180.

Shoo, L. P., Storlie, C., Williams, Y. M., and Williams, S. E. (2010). Potential for mountaintop boulder fields to buffer species against extreme heat stress under climate change. *International Journal of Biometeorology*, 54(4):475–478.

Sirami, C., Caplat, P., Popy, S., Clamens, A., Arlettaz, R., Jiguet, F., Brotons, L., and Martin, J.-L. (2017). Impacts of global change on species distributions: obstacles and solutions to integrate climate and land use. *Global Ecology and Biogeography*, 26(4):385–394.

Snyder, P. K., Foley, J. A., Hitchman, M. H., and Delire, C. (2004). Analyzing the effects of complete tropical forest removal on the regional climate using a detailed three-dimensional energy budget: An application to Africa. *Journal of Geophysical Research: Atmospheres*, 109(D21):D21102.

Snyder, W. C., Wan, Z., Zhang, Y., and Feng, Y.-Z. (1998). Classification-based emissivity for land surface temperature measurement from space. *International Journal of Remote Sensing*, 19(14):2753–2774.

Socolar, J. B., Epanchin, P. N., Beissinger, S. R., and Tingley, M. W. (2017). Phenological shifts conserve thermal niches in north american birds and reshape expectations

for climate-driven range shifts. *Proceedings of the National Academy of Sciences*, 114(49):12976–12981.

Sodhi, N. S., Koh, L. P., Brook, B. W., and Ng, P. K. L. (2004). Southeast Asian biodiversity: an impending disaster. *Trends in Ecology & Evolution*, 19(12):654–660.

Sonnleitner, M., Dullinger, S., Wanek, W., and Zechmeister, H. (2009). Microclimatic patterns correlate with the distribution of epiphyllous bryophytes in a tropical lowland rain forest in Costa Rica. *Journal of Tropical Ecology*, 25(03):321–330.

Spooner, F. E. B., Pearson, R. G., and Freeman, R. (2018). Rapid warming is associated with population decline among terrestrial birds and mammals globally. *Global Change Biology*, 00:1–11. Advance online publication. doi: https://doi.org/10.1111/gcb.14361.

Stewart, J. R., Lister, A. M., Barnes, I., and Dalén, L. (2010). Refugia revisited: individualistic responses of species in space and time. *Proceedings of the Royal Society of London B: Biological Sciences*, 277(1682):661–671.

Suggitt, A. J., Gillingham, P. K., Hill, J. K., Huntley, B., Kunin, W. E., Roy, D. B., and Thomas, C. D. (2011). Habitat microclimates drive fine-scale variation in extreme temperatures. *Oikos*, 120(1):1–8.

Suggitt, A. J., Wilson, R. J., Isaac, N. J. B., Beale, C. M., Auffret, A. G., August, T., Bennie, J. J., Crick, H. Q. P., Duffield, S., Fox, R., Hopkins, J. J., Macgregor, N. A., Morecroft, M. D., Walker, K. J., and Maclean, I. M. D. (2018). Extinction risk from climate change is reduced by microclimatic buffering. *Nature Climate Change*, 8(8):713–717.

Sunday, J. M., Bates, A. E., Kearney, M. R., Colwell, R. K., Dulvy, N. K., Longino, J. T., and Huey, R. B. (2014). Thermal-safety margins and the necessity of thermoregulatory behavior across latitude and elevation. *Proceedings of the National Academy of Sciences of the United States of America*, 111(15):5610–5615.

Tattersall, G. J. (2017). Thermimage: Thermal Image Analysis. Available at: https://CRAN.R-project.org/package=Thermimage.

Taubert, F., Fischer, R., Groeneveld, J., Lehmann, S., Müller, M. S., Rödig, E., Wiegand, T., and Huth, A. (2018). Global patterns of tropical forest fragmentation. *Nature*, 554(7693):519–522.

Tewksbury, J. J., Huey, R. B., and Deutsch, C. A. (2008). Putting the heat on tropical animals. *Science*, 320(5881):1296–1297.

Thomas, C. D., Bodsworth, E. J., Wilson, R. J., Simmons, A. D., Davies, Z. G., Musche, M., and Conradt, L. (2001). Ecological and evolutionary processes at expanding range margins. *Nature*, 411(6837):577–581.

Thomas, C. D., Cameron, A., Green, R. E., Bakkenes, M., Beaumont, L. J., Collingham, Y. C., Erasmus, B. F. N., de Siqueira, M. F., Grainger, A., Hannah, L., Hughes, L., Huntley, B., van Jaarsveld, A. S., Midgley, G. F., Miles, L., Ortega-Huerta, M. A., Townsend Peterson, A., Phillips, O. L., and Williams, S. E. (2004). Extinction risk from climate change. *Nature*, 427(6970):145–148.

Thomas, C. D. and Lennon, J. J. (1999). Birds extend their ranges northwards. *Nature*, 399(6733):213–213.

Tilman, D., Balzer, C., Hill, J., and Befort, B. L. (2011). Global food demand and the sustainable intensification of agriculture. *Proceedings of the National Academy of Sciences*, 108(50):20260–20264.

Titeux, N., Henle, K., Mihoub, J.-B., Regos, A., Geijzendorffer, I. R., Cramer, W., Verburg, P. H., and Brotons, L. (2017). Global scenarios for biodiversity need to better integrate climate and land use change. *Diversity and Distributions*, 23(11):1231–1234.

Transparent World (2015). Tree plantations. Available at: www.globalforestwatch.org.

Tucker, M. A., Böhning-Gaese, K., Fagan, W. F., Fryxell, J. M., Moorter, B. V., Alberts, S. C., Ali, A. H., Allen, A. M., Attias, N., Avgar, T., Bartlam-Brooks, H., Bayarbaatar, B., Belant, J. L., Bertassoni, A., Beyer, D., Bidner, L., Beest, F. M. v., Blake, S., Blaum, N., Bracis, C., Brown, D., Bruyn, P. J. N. d., Cagnacci, F., Calabrese, J. M., Camilo-Alves, C., Chamaillé-Jammes, S., Chiaradia, A., Davidson, S. C., Dennis, T., DeStefano, S., Diefenbach, D., Douglas-Hamilton, I., Fennessy, J., Fichtel, C., Fiedler, W., Fischer, C., Fischhoff, I., Fleming, C. H., Ford, A. T., Fritz, S. A., Gehr, B., Goheen, J. R., Gurarie, E., Hebblewhite, M., Heurich, M., Hewison, A. J. M., Hof, C., Hurme, E., Isbell, L. A., Janssen, R., Jeltsch, F., Kaczensky, P., Kane, A., Kappeler, P. M., Kauffman, M., Kays, R., Kimuyu, D., Koch, F., Kranstauber, B., LaPoint, S., Leimgruber, P., Linnell, J. D. C., López-López, P., Markham, A. C., Mattisson, J., Medici, E. P., Mellone, U., Merrill, E., Mourão, G. d. M., Morato, R. G., Morellet, N., Morrison, T. A., Díaz-Muñoz, S. L., Mysterud, A., Nandintsetseg, D., Nathan, R., Niamir, A., Odden, J., O'Hara, R. B., Oliveira-Santos, L. G. R., Olson, K. A., Patterson, B. D., Paula, R. C. d., Pedrotti, L., Reineking, B., Rimmler, M., Rogers, T. L., Rolandsen, C. M., Rosenberry, C. S., Rubenstein, D. I., Safi, K., Saïd, S., Sapir, N., Sawyer, H., Schmidt, N. M., Selva, N., Sergiel, A., Shiilegdamba, E., Silva, J. P., Singh, N., Solberg, E. J., Spiegel, O., Strand, O., Sundaresan, S., Ullmann, W., Voigt, U., Wall, J., Wattles, D., Wikelski, M., Wilmers, C. C., Wilson, J. W., Wittemyer, G., Zięba, F., Zwijacz-Kozica, T., and Mueller, T. (2018). Moving in the Anthropocene: Global reductions in terrestrial mammalian movements. *Science*, 359(6374):466–469.

Tuff, K. T., Tuff, T., and Davies, K. F. (2016). A framework for integrating thermal biology into fragmentation research. *Ecology Letters*, 19(4):361–374.

United Nations Development Programme (2018). Human Development Reports. Available at: http://hdr.undp.org/en/countries.

Van Houtan, K. S., Pimm, S. L., Halley, J. M., Bierregaard, R. O., and Lovejoy, T. E. (2007). Dispersal of Amazonian birds in continuous and fragmented forest. *Ecology Letters*, 10(3):219–229.

VanDerWal, J., Falconi, L., Januchowski, S., Shoo, L., and Storlie, C. (2014). SDMTools: Species distribution modelling tools: Tools for processing data associated with species distribution modelling exercises. R package version 1.1-221. Available at: https://CRAN.R-project.org/package=SDMTools.

Waddell, K. L. (2002). Sampling coarse woody debris for multiple attributes in extensive resource inventories. *Ecological Indicators*, 1(3):139–153.

Walsh, R. P. D. and Newbery, D. M. (1999). The ecoclimatology of Danum, Sabah, in the context of the world's rainforest regions, with particular reference to dry periods and their impact. *Philosophical Transactions of the Royal Society of London B: Biological Sciences*, 354(1391):1869–1883.

Walther, G. R., Post, E., Convey, P., Menzel, A., Parmesan, C., Beebee, T. J. C., Fromentin, J. M., Hoegh-Guldberg, O., and Bairlein, F. (2002). Ecological responses to recent climate change. *Nature*, 416(6879):389–395.

Wangluk, S., Boonyawat, S., Diloksumpun, S., and Tongdeenok, P. (2013). Role of soil temperature and moisture on soil respiration in a teak plantation and mixed deciduous forest in Thailand. *Journal of Tropical Forest Science*, 25:339–349.

Warton, D. I. and Hui, F. K. C. (2011). The arcsine is asinine: the analysis of proportions in ecology. *Ecology*, 92(1):3–10.

Watson, J. E. M., Shanahan, D. F., Di Marco, M., Allan, J., Laurance, W. F., Sanderson, E. W., Mackey, B., and Venter, O. (2016). Catastrophic Declines in Wilderness Areas Undermine Global Environment Targets. *Current Biology*, 26(21):2929–2934.

Werner, C., Zheng, X., Tang, J., Xie, B., Liu, C., Kiese, R., and Butterbach-Bahl, K. (2006). N_2O, CH_4 and CO_2 emissions from seasonal tropical rainforests and a rubber plantation in Southwest China. *Plant and Soil*, 289(1-2):335–353.

Wiens, J. A. and Bachelet, D. (2010). Matching the multiple scales of conservation with the multiple scales of climate change. *Conservation Biology*, 24(1):51–62.

Williams, S. E., Shoo, L. P., Isaac, J. L., Hoffmann, A. A., and Langham, G. (2008). Towards an Integrated Framework for Assessing the Vulnerability of Species to Climate Change. *PLOS Biology*, 6(12):e325.

Willis, S. G., Foden, W., Baker, D. J., Belle, E., Burgess, N. D., Carr, J. A., Doswald, N., Garcia, R. A., Hartley, A., Hof, C., Newbold, T., Rahbek, C., Smith, R. J., Visconti, P., Young, B. E., and Butchart, S. H. M. (2015). Integrating climate change vulnerability assessments from species distribution models and trait-based approaches. *Biological Conservation*, 190:167–178.

Willis, S. G., Hill, J. K., Thomas, C. D., Roy, D. B., Fox, R., Blakeley, D. S., and Huntley, B. (2009). Assisted colonization in a changing climate: a test-study using two U.K. butterflies. *Conservation Letters*, 2(1):46–52.

Wood, S. and Scheipl, F. (2017). gamm4: Generalized additive mixed models using 'mgcv' and 'lme4'. R package version 0.2-5. Available at: https://CRAN.R-project.org/package=gamm4.

Wood, S. N. (2017). *Generalized Additive Models: An Introduction with R*. CRC press, Boca Raton, FL, USA, 2nd edition.

Wood, T. E. and Lawrence, D. (2008). No short-term change in soil properties following four-fold litter addition in a Costa Rican rain forest. *Plant and Soil*, 307(1-2):113–122.

Yashiro, Y., Kadir, W. R., Okuda, T., and Koizumi, H. (2008). The effects of logging on soil greenhouse gas (CO_2, CH_4, N_2O) flux in a tropical rain forest, Peninsular Malaysia. *Agricultural and Forest Meteorology*, 148(5):799–806.

Yeong, K. L., Reynolds, G., and Hill, J. K. (2016). Leaf litter decomposition rates in degraded and fragmented tropical rain forests of Borneo. *Biotropica*, 48(4):443–452.

Zuur, A. F. (2009). *Mixed Effects Models and Extensions in Ecology with R*. Statistics for biology and health. Springer, New York, NY, USA.